MyCOE/SERVIR Himalayas Fellowship Program

UNDERSTANDING THE ISSUES INVOLVED IN URBAN LANDSLIDE VULNERABILITY IN CHITTAGONG METROPOLITAN AREA, BANGLADESH

Submitted by-

YIASER ARAFAT RUBEL

Student Fellow

Department of Civil Engineering

Bangladesh University of Engineering and Technology (BUET)

Dhaka-1000, Bangladesh

Email: arafatbdbuet@gmail.com

&

BAYES AHMED

Mentor

Institute for Risk and Disaster Reduction (IRDR)

University College London (UCL)

Gower Street, London WC1E 6BT, United Kingdom

Email: bayesahmed@gmail.com

December, 2013

ABSTRACT

Chittagong Metropolitan Area (CMA) is highly vulnerable to landslide hazard, with an increasing trend of frequency and damage. The major recent landslide events were related to extreme rainfall intensities having short period of time. All the major landslide events occurred as a much higher rainfall amount compared to the monthly average. Moreover rapid urbanization, increased population density, improper landuse, alterations in the hilly regions by illegally cutting the hills, indiscriminate deforestation and agricultural practices are aggravating the landslide vulnerability in CMA.

It is therefore essential to produce the future landslide susceptibility maps for CMA so that appropriate landslide mitigation strategies can be developed to help combat the impacts of climate change. In this research Geographic Information System (GIS) and Remote Sensing (RS) based Weighted Linear Combination (WLC), Logistic Regression (LR) and Multiple Regressions (MR) models were used to scientifically assess the landslide susceptible areas. Later the performances of the models were compared using Relative Operating Characteristic (ROC) method. The area under ROC curves (AUC) is indicating that the WLC_1, WLC_2, WLC_3, LR and MR models had AUC values of 0.839, 0.911, 0.885, 0.767 and 0.967, respectively. The verification results showed satisfactory agreement between the susceptibility maps and the existing data on the 20 landslide locations.

In the second stage of this research, soil samples from 17 different landslide vulnerable areas were collected to analyse different properties of soil related to shear strength. It is known as Atterberg Limit/ Soil Consistency Test. Liquid Limit, Flow Index, Plastic Limit, Liquidity Index, Shrinkage Limit; Linear Shrinkage and Plasticity Index parameters were tested in laboratory. In all cases, it is found that the locations are highly vulnerable to landslides.

At the end of this research, some recommendations like- understanding the human adaptation to landslide risks, the processes and mechanism of landslides in CMA; developing a Web-GIS based early warning system, implementation of the existing master plan, creating awareness among the local people, increasing cooperation among different public/ private/ autonomous/ NGOs organizations and generating facilities for proper evacuation system in crisis moment etc. were stated.

The authors believe that the outcome of this research shall help the endangered local communities, urban planners and engineers to reduce losses caused by the future landslides in CMA by means of prevention, mitigation and avoidance.

ACKNOWLEDGEMENTS

First of all, I would like to thank AAG, USAID, NASA, ICIMOD and other organizations for taking such a great initiative named MyCOE/SERVIR Himalayas fellowship program for inspiring youths to solve climate change induced problems by using geospatial technologies.

I am really glad to have a very friendly, helpful and dedicated mentor like Mr. Bayes Ahmed without whom I would definitely not be able to finish my research work with such good outcomes. His knowledge, experience and innovative ideas have given new dimension in my research work which might be helpful in solving some complex urban disaster related problems. Thank to all other mentors and fellow mates from different countries for sharing their knowledge in the capacity building workshop which helped me in developing my research work. They also encouraged me to work in this project passionately.

My gratitude goes to our beloved professor Dr. Richard A Marston, other staffs of ICIMOD and AAG for their informative lectures in the time of skill developing workshop held in Kathmandu, Nepal as a part of the MyCOE/SERVIR Fellowship program. I am very also thankful to Mr. Basanta Shrestha and Mr. Kabir Uddin of ICIMOD for providing us with the detailed land cover map of Chittagong Hill Tract (CHT) area. I am also very grateful to Dr. Patricia Solic, Astrid Ng and Marcela Zeballos for their support from the beginning of the fellowship period.

I would like to thank the authority of Bangladesh University of Engineering & Technology (BUET) for allowing me to be a part of the fellowship and also giving me the laboratory facilities in performing soil tests in the Civil Engineering Department laboratory. I would also like to thank my fellow university mate, Mr. Muntasir Mamun, Moon for assisting me in conducting field survey and collecting sample soils from the Chittagong Metropolitan Area.

I want to thank the officials of Chittagong Development Authority, especially Planner Md. Abutalha Talukdar for his support during the field survey. Moreover, I am grateful to the local people and communities of landslide vulnerable areas of CMA for their kindness and hospitality.

My special gratitude goes to Dr. Hasan Mahmud, the honorable Environment and Forest Minister of Bangladesh, for his valuable time and suggestions as part of our outreach activities. In the end, I would like to thank the Ministry of Environment and Forest for their consent to implement my research suggestions for reducing landslide risks in hilly regions of Bangladesh.

Yiaser Arafat Rubel

UNDERSTANDING THE ISSUES INVOLVED IN URBAN LANDSLIDE VULNERABILITY IN CHITTAGONG METROPOLITAN AREA, BANGLADESH

AUTHORS DECLARATION

This is to certify that this research work is entirely our own and not of any other person, unless explicitly acknowledged (including citation of published and unpublished sources).

All views and opinions expressed therein remain the sole responsibility of the authors (student fellow and mentor), and do not necessarily represent those of the institutes.

Moreover, it is to declare that the Chapters 1, 2, 3, 4 and 6 are written by Mr. Bayes Ahmed. Conducting field surveying, soil testing and chapter 5 is written by Mr. Yiaser Arafat Rubel.

We want to thank the International Centre for Integrated Mountain Development (ICIMOD), Chittagong Development Authority (CDA), Bangladesh Meteorological Department (BMD), Bangladesh University of Engineering and Technology (BUET), Chittagong University of Engineering and Technology (CUET) and University College London (UCL) for providing necessary data and research logistics.

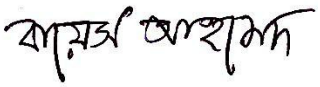

YIASER ARAFAT RUBEL | **BAYES AHMED**

December 30, 2013

Chapter 1

INTRODUCTION

1.1. Background of the Research

1.1.1. Land Cover Change and Landslides

Land use and land cover changes have been recognized as world's one of the most important factors stirring rainfall-triggered landslides [1]. As per the definition by Deepak Chapagai (2011), the term 'Landslide' is used in this research as- the down-slope movement of rock, debris, organic materials or soil under the effects of gravity in which much of the material moves with little internal deformation and also the landform that results from such movement [2]. Mass movement, slope movement, slope failure and mass wasting are some of the frequently used terminologies for landslide [3].

Landslide incidence as a response to land use/ land cover changes has been identified by numerous researchers. Thomas Glade (2002) has showed how landslide can take place because of the change in land use in the context of New Zealand [1]. Mugagga et al. (2011) has also depicted the impacts of land use changes and its implications for the occurrence of landslides in mountainous areas of Eastern Uganda [4]. Moreover, expansion of urban development, deforestation and increased agricultural practices into the hillslope areas are immensely threatened by landslide hazards [5, 6 and 7].

Land cover changes (e.g. deforestation) cause large variations in the hydro-morphological functioning of hillslopes, affecting rainfall partitioning, infiltration characteristics and runoff production. All these factors trigger landslides in hilly areas [8]. Therefore it can be stated that there is a strong and positive correlation between land-use change and landslides.

1.1.2. Climate Change and Landslides

Climate Change, which is now acknowledged as a major threat to the future society and environment, is mainly caused by the increasing concentration of three principal Green House Gases (GHG)- carbon dioxide (CO_2), methane (CH_4) and nitrous oxide (N_2O) [9]. Moreover, land use and land cover (LULC) changes play constitutive role in climate change at global, regional and local scales [10].

It has been stated, in the Global Report on Human Settlements (2011), that climate change is

the outcome of human-induced driving forces (e.g. combustion of fossil fuel and land use change). An important finding of the report is that the proportion of human-induced Green House Gas (GHG) emissions resulting from cities could be between 40 to 70% [11]. Therefore, LULC change (e.g. urbanization) is responsible for releasing GHG to the atmosphere, at global scale, thereby driving global warming [10].

Moreover, the rural-urban migrants and climate refugees, arriving in the already overstressed cities, are often forced to live in endangered places like- unstable hillsides, floodplains, swamp areas, wetlands, low-elevation coastal zones etc. Thus the effects of urbanization and climate change are converging in dangerous ways by threatening peerless negative impacts upon quality of life, economic and social stability. This is how, urban areas, with high population density and infrastructure, are more likely to face the severe impacts of climate change [11].

At this drawback, it is important to understand the impacts of climate change on the urban environment as well. The impacts of climatic changes are as follows [11]:

i. **Increased frequency of heavy precipitation events**
ii. Warmer and more frequent hot days and nights
iii. Fewer colds days and nights
iv. Frequency increase in heat waves
v. Increase of drought affected areas
vi. Increase in intense tropical cyclone activity
vii. Increased incidence of extreme sea level rise

The main concern of this research is 'Heavy Precipitation Events' due to climate change, in specific- 'Landslides'.

Heavy precipitation events are defined as the percentage of days with precipitation that exceeds some fixed or regional threshold compared to an average [12]. It has also been noticed that heavy one or multiple-day precipitation events have increased in most areas of the world in the 20^{th} century. This situation is very alarming and it will continue throughout the 21^{st} century as well [11].

The heavy precipitation events are able to give rise to deep-rooted negative socio-economic consequences through the urban environment, especially through flooding and landslides in developing countries of the world. Land cover changes, precipitation pattern, slope stability, slope angle etc. are the factors influencing landslides vulnerability of an area [11].

Urban expansion and clearing vegetation cover, for constructing infrastructure can lead to soil erosion or soil instability, which can increase the likelihood of landslides. Moreover rapid urbanization and increased population pressure are forcing the urban development continuing towards the marginal and dangerous lands. Therefore, the urban poor are increasingly settling in areas that are unsuitable for residential use and prone to hazardous landslides (e.g. steep hilly slopes). This is how people living in urban areas are becoming more and more vulnerable to landslides [11].

1. 2. Statement of the Problem

Urbanization is one of the most significant human induced global changes worldwide. In the past 200 years, the world population has increased 6 times and the urban population has multiplied 100 times [13]. By the end of the last decade the world reached a milestone when, for the first time in urban history, half of the world's population lived in urban areas. Moreover, the fastest rates of urbanization are currently taking place in the least developed countries, followed by the rest of the developing countries [11].

Like many other cities in the world Chittagong, the port and second largest city of Bangladesh, is also the outcome of spontaneous rapid growth without any prior or systematic planning. Chittagong City has undergone radical changes in its physical form, not only in its vast territorial expansion, but also through internal physical transformations over the last decades.

In the process of urbanization, the physical characteristics of Chittagong are gradually changing as plots and open spaces have been transformed into building areas, certain hilly areas into settlements, low land and water bodies into reclaimed built-up lands etc.

Chittagong is now attracting a huge amount of rural-urban migrants from all over the country due to well-paid job and business opportunities, better educational, health and other daily life facilities [14].

The city population of Chittagong has increased almost quadruplicate in the last three decades. Moreover, the percentage of urban population, in terms of total population, is also increasing gradually (Table 1.1). The present urbanization rate of Chittagong is 41.39% [15]. If this trend continues, then the city population will reach approximately 10.8 million in 2050 (Table 1.1).

Table 1.1. Growth of Chittagong City in Urban Agglomerations (1950-2050)

Year	City Population (Thousands)	Urban Population as a Percentage of the Total Population (%)
1950	289	4.3
1955	323	4.7
1960	360	5.1
1965	503	6.2
1970	723	7.6
1975	1017	9.8
1980	1340	14.9
1985	1655	17.5
1990	2023	19.8
1995	2578	21.7
2000	3308	23.6
2005	4180	25.7
2010	4962	28.1
2015	5680	30.8
2020	6447	33.9
2025	7265	37.4
2030	8085	41.0
2035	8861	44.8
2040	9580	48.7
2045	10231	52.5
2050	10786	56.4

Source: Population Division of the Department of Economic and Social Affairs of the United Nations Secretariat, World Population Prospects: The 2008 Revision and World Urbanization Prospects: The 2009 Revision, http://esa.un.org/wup2009/unup/, Accessed on May 03, 2013.

All these are creating numerous problems like haphazard urbanization, forcing urban-poor to live in dangerous hill-slopes, landslides, water logging, extensive urban poverty, growth of urban slums and squatters, traffic jam, environmental pollution and other socio-economic problems [14].

This rapid urbanization, coupled with the increased intensity and frequency of adverse weather events (e.g. landslides), is causing devastating effects on the country, which also has lower capacities to deal with the consequences of climate change [11]. Particularly in Chittagong, many urban dwellers and their livelihoods, quality of life, property and future prosperity are being continuously threatened by the risks of cyclones, sea-level rise, tidal waves, flooding, landslides, earthquakes and other hazards that climate change is expected to aggravate. These disasters have almost become the day-to-day realities for the poor and vulnerable populations that inhibit many of the most hazardous areas in the city [11].

Chittagong has been hit repeatedly by devastating landslides in recent years (Table 1.2). At least 90 people were killed in a recent landslide in Chittagong on June 26, 2012. The reasons were heavy rainfall and multiple landslides over three consecutive days. The officials reported that at least another 15,000 people were stranded [17].

Table 1.2. Major Landslides in Chittagong City in Recent Years

Date	Location	Rainfall Sequence (Cumulated Rainfall)	Consequences
13 August 1999	Gopaipur, Kotwali Thana, Chittagong	435 mm – 12 days 2 – 13 Aug 1999	10 people killed
24 June 2000	Chittagong University Campus	108 mm – 8 days 17 – 24 June 2000	13 people killed and 20 injured
29 June 2003	Patiya	658 mm – 10 days 20 – 29 June 2003	4 people killed
3 August 2005	Nizam Road Housing Society of the port city's Panchlaish area	25 mm – 2 days 2-3 August 2005	2 people killed and 12 injured
11 June 2007	Mati Jharna Colony of Lalkhan Bazar, Chittagong	610 mm – 8 days 4 – 11 June 2007	128 people killed and 100 injured
10 September 2007	Nabi Nagar in Chittagong	452 mm – 7 days 4 – 10 Sept 2007	2 people killed
18 august 2008	Matijharna in Chittagong	454 mm – 11 days 8 – 18 August 2008	11 people killed and 25 injured
26 June 2012	Chittagong (Lebubagan area and Foys lake surroundings)	889 mm – 8 days 19 – 26 June 2012	90 people killed and 150 injured

Source: Department of Disaster Management, Bangladesh; Bangladesh Network Office for Urban Safety (BNUS) & Asian Disaster Preparedness Center (ADPC), Bangladesh.

Chittagong City is highly vulnerable to landslide hazard, with an increasing trend of frequency and damage. The major recent landslide events were related to extreme rainfall intensities having short period of time. All the major landslide events occurred as a much higher rainfall amount compared to the monthly average [18].

The following figure depicts how this excessive rainfall in a short period of time can put adverse effects on city life (Figure 1.1). These pictures were captured on 4 June 2013 from the center part of Chittagong City. Many parts of the city went under water just after the torrential rain flooded parts of the city. The Chittagong divisional meteorological office recorded 162.8 millimetres of rainfall in that day [19]. This clearly indicates the landslide vulnerability of people living in dangerous hilly slopes (Figure 1.2).

Figure 1.1. Some major roads of Chittagong City Corporation area submerged under water after a day's (4 June 2013) torrential rainfall (162.8mm) [19]

Figure 1.2. Some landslide vulnerable areas of Chittagong City

Source: Field Survey, March, 2013 (Photos taken by Yiaser Arafat Rubel).

The landslides in Chittagong are classified as 'earth slides' since those consist of 80% sand and finer particles. These landslides are shallow in nature as well. It has been stated that the rainfall intensity and duration play very important role in producing these shallow landslides in Chittagong [18].

Because of climate change, Bangladesh is experiencing high intensity of rainfall in recent years which is making the landslide situation worse. Moreover improper landuse, alterations in the hilly regions by illegally cutting the hills, indiscriminate deforestation and agricultural practices are aggravating the landslide vulnerability in Chittagong [20].

If this situation continues then Chittagong would soon become an urban-slum with the least liveable situation for the city dwellers. In this regard, it is much needed to track the land cover changes over-time, analyse socio-economic impacts and project the future landslide vulnerability scenario of Chittagong City.

In addition, there is no strict hill management policy within Chittagong City. This has encouraged many informal settlements along the landslide-prone hillslopes of Chittagong. These settlements are being considered as illegal by the formal authorities, while the settlers demand themselves as legal occupants. This is how; there is acute land tenure conflict among the formal authorities, the settlers and the local communities over the past few decades. This kind of conflict has also weakened the institutional arrangement for reducing the landslide vulnerability in Chittagong [21].

It is therefore essential that the trend of land cover changes (e.g. urbanization) in the hilly areas of Chittagong are assessed so that appropriate landslide mitigation strategies can be developed to help combat the impacts of climate change.

1.3. Aim of the Research

The aim of this research is to understand the issues involved in urban disaster risk based on the case study of recent landslide events in Chittagong City, Bangladesh.

1.4. Objectives of the Research

a) To establish the nature of relationships among land-cover change, climate change and landslide disaster.
b) To produce the predictive landslide susceptibility maps using different methods and modelling techniques.
c) To understand the geotechnical issues related to landslides.
d) To recommend appropriate mitigation and adaptation policies for landslide disaster management within Chittagong Metropolitan Area (CMA).

Chapter 2

STUDY AREA PROFILE

2.1. General Description

Chittagong is the second-largest and main seaport of Bangladesh, situated on the banks of the Karnaphuli River; it is the principle city of Chittagong Division [Figure 2.1 (a, b)] and a major center of commerce and industry in South Asia. The city, under the jurisdiction of the city corporation, has a population of about 2.5 million and is constantly growing [22].

It is also the Commercial Capital City of Bangladesh. The surrounding mountains and rivers make the city attractive. Karnaphuli River falls in Chittagong. The largest land port of the country, "Chittagong Port", situated in Chittagong. That's why Chittagong is the city for export and import. Most of the large industries of Bangladesh are situated in Chittagong. Chittagong is an ideal vacation spot. Its green hills and forests, its broad sandy beaches and its fine cool climate always attract the holiday-makers [22].

Chittagong City is not only the principal city of the district of Chittagong but also the second largest city of Bangladesh. It is situated within 22° 14′ and 22° 24′ 30″ North Latitude and between 91° 46′ and 91° 53′ East Longitude.

2.2. Location of Study Area

Chittagong City is divided into different administrative boundaries like Chittagong Statistical Metropolitan Area (SMA), Chittagong Metropolitan Area (CMA) and Chittagong City Corporation (CCC). The study area for this research is CMA (Figure 2.2). This selected study area covers the biggest urban agglomeration and is the central part of Chittagong District in terms of social and economic aspects [14]. Therefore, this area has huge potentiality to landslide risks in near future based on the current trend of rapid urbanization.

Chittagong Development Authority (CDA) is the statutory planning and development authority for the CMA was created in 1959, in order to ensure the planned and systematic growth of the city. It is today the authority for planning, promoting and developing the CMA. CDA is working under the Ministry of Housing and Public works of the Government [22]. The total area of CMA is approximately 775 square kilometres (Bangladesh Transverse Mercator projection). The extent of CMA is top 495491.250000 m, bottom 445877.187500 m, left 673293.625000 m and right 709824.000000 m (Figure 2.2).

Figure 2.1 (a). Location of Bangladesh

Source: Banglapedia, National Encyclopaedia of Bangladesh, 2013

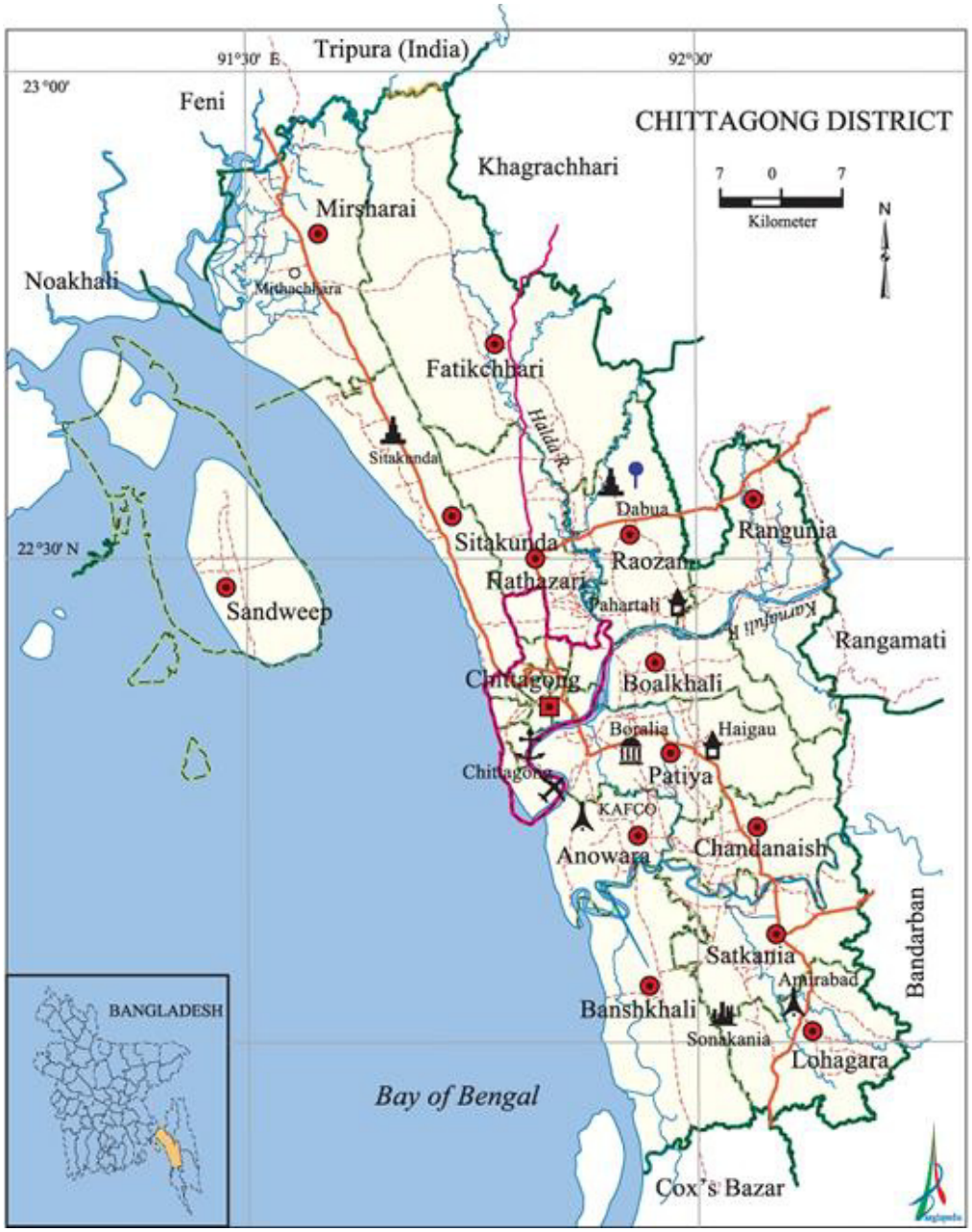

Figure 2.1 (b). Location of Chittagong District

Source: Banglapedia, National Encyclopaedia of Bangladesh, 2013

2.3. Topography

Chittagong is very different in terms of topography, with the exception of Sylhet and northern Dinajpur, from the rest of Bangladesh, being a part of the hilly regions that branch off from the Himalayas. This eastern offshoot of the Himalayas, turning south and southeast, passes through Assam and Tripura State and enters Chittagong across the river Feni. The range loses height as it approaches Chittagong town and breaks up into small hillocks scattered all over the town. This range appears again on the southern bank of the Karnaphuli River and extends from one end of the district to the other. Chandranath or Sitakunda is the highest peak in the district, with an altitude of 1152 feet above mean sea level. Nangarkhana to the north of

Chittagong town is 289 feet high. In the town itself, there is a peak known as Batali Hill, which used to be 280 feet high and was the highest point in the town. There was a light post at the top of Batali Hill for the guidance of vessels far away in the sea. This famous hill, like other beautiful hills and hillocks in the city of Chittagong, is being gradually levelled up and reduced in height for the construction of houses [23].

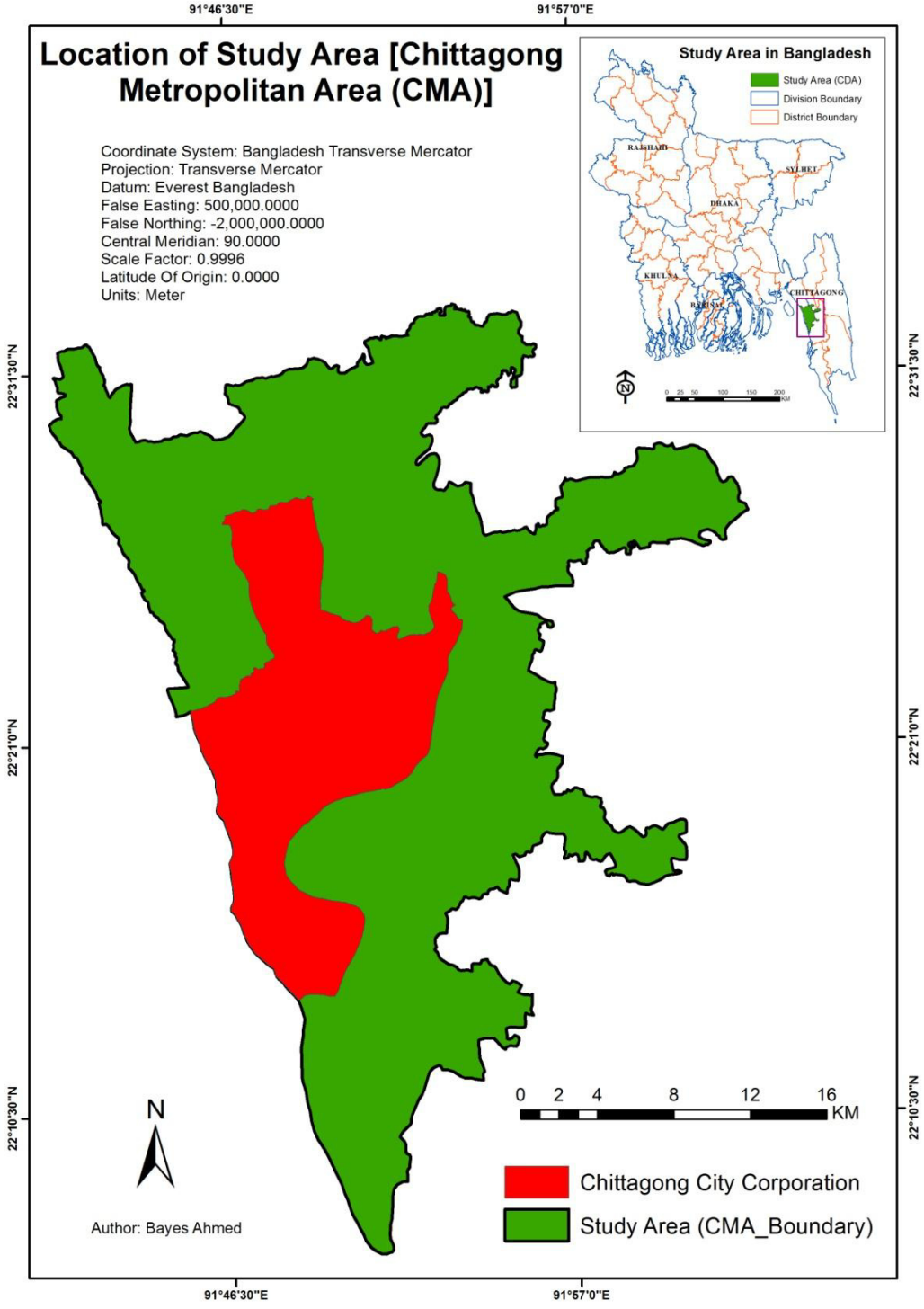

Figure 2.2. Location of the study area (Chittagong Metropolitan Area)

2.4. A Brief Description of Chittagong Hill Tracts (CHT)

The selected study area is a part of Chittagong Hill Tracts (CHT) of Bangladesh (Figure 2.3). Therefore it is important to know about the characteristics of CHT, to understand the causes and geological reasons of landslides in CMA.

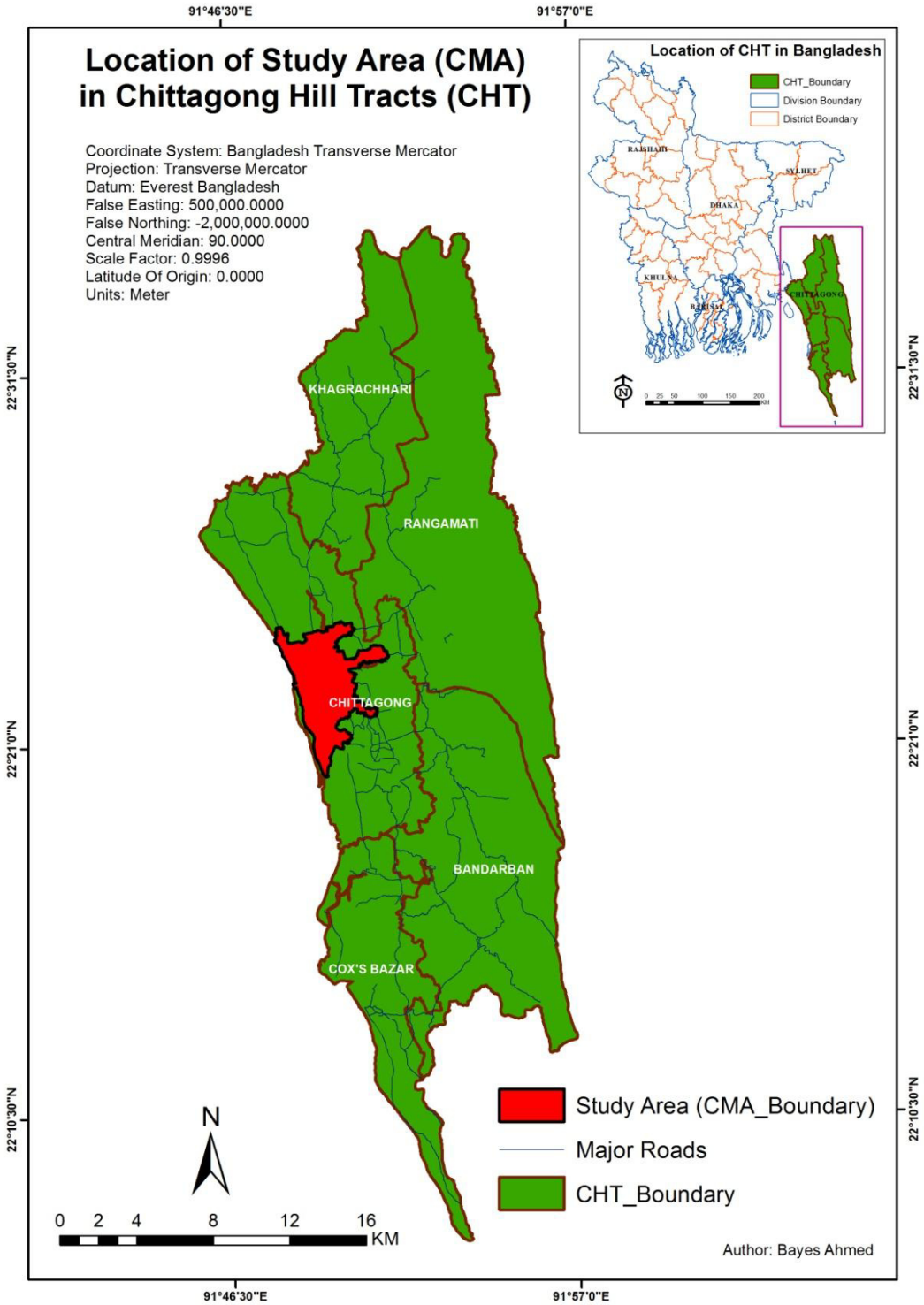

Figure 2.3. Location of Chittagong Metropolitan Area in Chittagong Hill Tracts

2.4.1. Climate

The weather of this region is characterised by tropical monsoon climate with mean annual rainfall nearly 2540 mm in the north and east and 2540 mm to 3810 mm in the south and west. The dry and cool season is from November to March; pre-monsoon season is April-May which is very hot and sunny and the monsoon season is from June to October, which is warm, cloudy and wet [24].

2.4.2. Soil conditions

The hill soils (dystric cambisols) are mainly yellowish brown to reddish brown loams which grade into broken shale or sandstone as well as mottled sand at a variable depth. The soils are very strongly acidic [24].

2.4.3. Vegetation

The hills are unsuitable for cultivation but natural vegetation remains widely. Jhum cultivation (slash and burn technology of agriculture practiced mainly by the people of pre-plough age) is being practised on the hill slopes. Cotton, rice, tea and oilseeds are raised in the valleys between the hills [24].

2.4.4. Physiography

According to the physiography of Bangladesh, the CHT falls under the Northern and Eastern Hill unit and the High Hill or Mountain Ranges sub-unit. At present, all the mountain ranges of the Chittagong Hill Tracts are almost hogback ridges. They rise steeply, thus looking far more impressive than their height would imply. Most of the ranges have scarps in the west, with cliffs and waterfalls. The region is characterised by a huge network of trellis and dendritic drainage consisting of some major rivers draining into the Bay of Bengal [24].

Generally the hill ranges and the river valleys are longitudinally aligned. Four ranges, with an average elevation of over three hundred metres, strike in a north-south direction in the northern part of the hill tract districts. These are Phoromain range (Phoromain, 463m), Dolajeri range (Langtrai, 429m), Bhuachhari (Changpai, 611m) and Barkal range (Thangnang, 735m). South of the Karnaphuli River within the Chittagong Hill Tracts, there are seven main mountain ranges within Bangladesh [24].

2.4.5. Geology

The Chittagong Hill Tracts is originated as a result of the collision between India and Asia. After the break-up of Gondwanaland, Indo-Australian plate together moved towards south-easterly of about 1750 km at a drift rate of 6 cm/yr. Later India broke apart from Australia and started to drift north north-easterly. That is the time when the history began for the Chittagong Hill Tracts [24].

Central Burma or Irrawaddy Basin represents the back-arc basin and Arakan-Yoma folded belt and its western extension up to Chittagong-Tripura hills, a part of which is the Chittagong Hill Tracts, representing the fore-arc basin. The thick sediments deposited in the Irrawaddy Basin during Miocene and Lower Pleistocene time are exposed in the Chittagong and Tripura hills [24].

In the Chittagong Hill Tracts the Upper Tertiary sandy-argillaceous sediments have been folded into a series of long submeridional (NNW-SSE) anticlines and synclines represented in the surface topography by elongated hill ranges and intervening valleys. The folded structures are characterised by en-echelon orientation with an increasing degree of intensity and complexity toward the east. Accordingly, the folded flank is divided into three parallel almost N-S trending zones from west to east as [24]:

(a) The Western Zone is characterised by simple box-like or similar shaped anticlines with steep flanks and gentle crests separated by gentle synclines, viz Matamuhuri anticline, Semutang anticline, etc [24];

(b) The Middle Zone is characterised by more compressed structures, other than just simple box-like folds, with ridge like asymmetric anticlines frequently associated with faults and separated by narrow synclines viz Sitapahar anticline, Bandarban anticline, Gilasari anticline, Patiya anticline, Changohtung anticline, Tulamura anticline, Kaptai syncline, Alikadam syncline, etc [24];

(c) The Eastern Zone is characterised by highly disturbed narrow anticlines with steep clipping flanks and mostly associated with thrust faults, viz Belasari anticline, Subalong syncline, Utanchatra anticline, Barkal anticline, Mowdac anticline, Ratlong anticline, Kasalong syncline, Sangu Valley syncline and few others [24].

To get more ideas on geological issues, please go through Figure 2.4 and Figure 2.5.

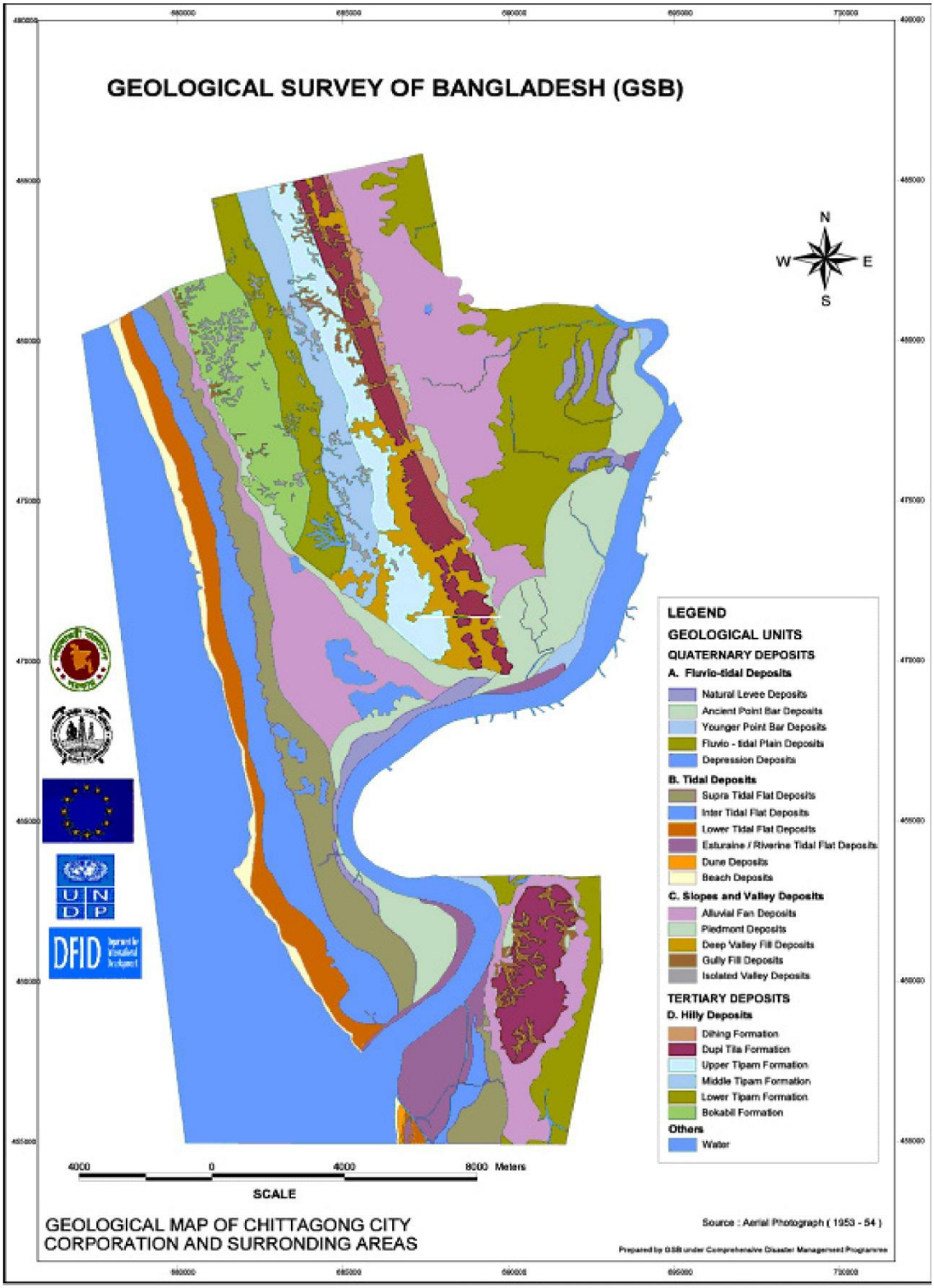

Figure 2.4. Geological map of CCC and its surrounding areas

Source: Geological Survey of Bangladesh (GSB), 2013

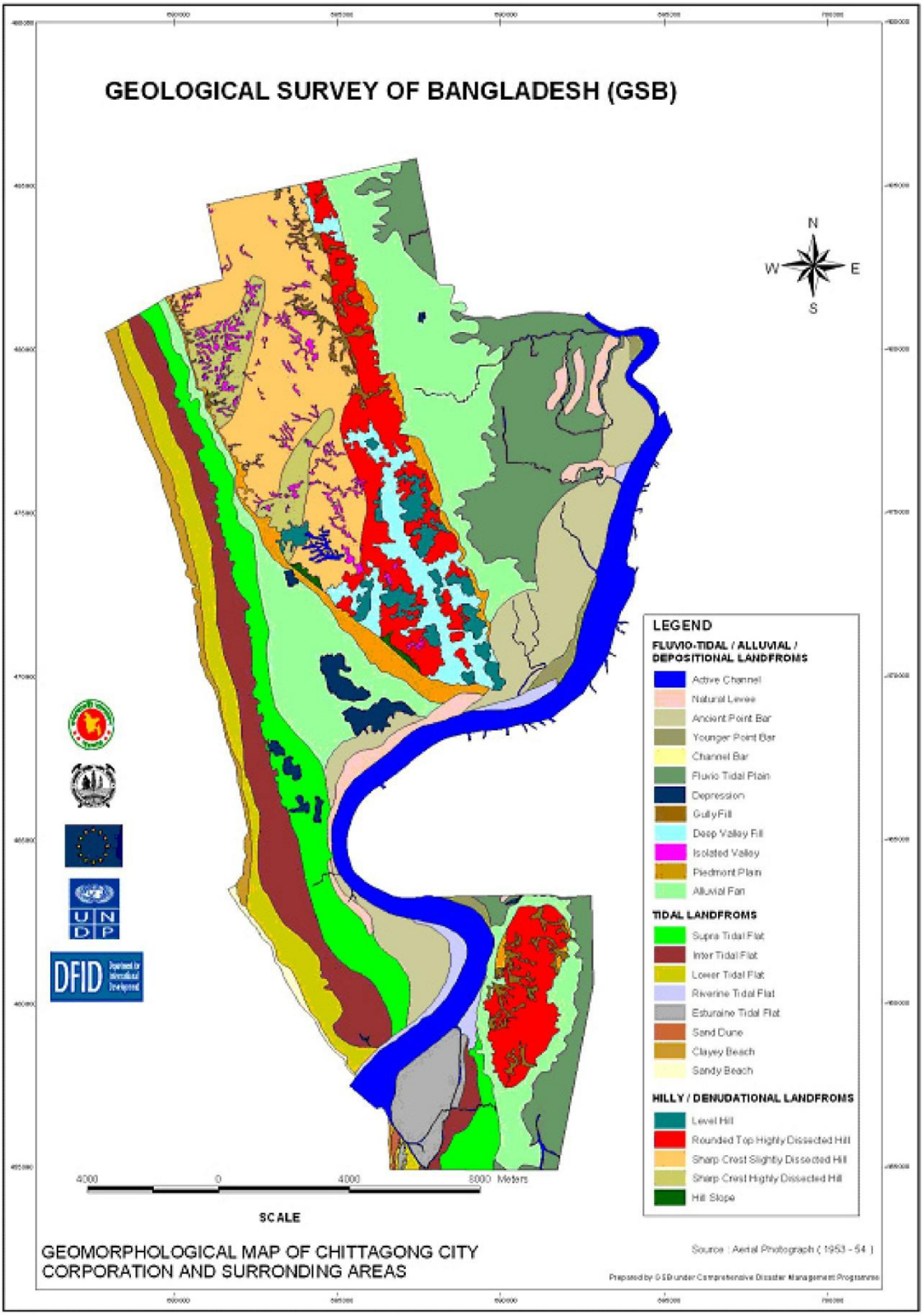

Figure 2.5. Geomorphological map of CCC and its surrounding areas

Source: Geological Survey of Bangladesh (GSB), 2013

Some photos from the field visits are attached in Appendix-I.

Chapter 3

LITERATURE REVIEW AND DATA COLLECTION

3.1. Existing Literary Works

Landslides are one of the most significant natural damaging disasters in hilly environments [25]. Social and economic losses due to landslides can be reduced by the means of effective planning and management [26]. Landslide hazard assessment is generally based on the concept that "the present and the past are keys to the future". This is why; most landslide hazard analyses take into account an up-to-date landslide inventory that represents the fundamental tool for identifying the hillslope instability factors in triggering landslides [27]. However, in spite of improvements in hazard recognition, prediction, mitigation measures, and warning systems, worldwide landslide activity is increasing [28]. This trend is expected to continue for the following reasons in the landslide prone areas [29, 30]:

a) Increased urbanization and illegal hill-cutting
b) Continued deforestation and agricultural activities
c) Increased regional precipitation (heavy rainfall) due to climate change

Various geo-structural as well as causative-factor based approaches have been proposed for landslide susceptibility zoning [31]. But GIS modeling of landslide phenomena has taken precedence in recent time. Geospatial technologies like geographic information system (GIS), global positioning system (GPS) and remote sensing (RS) are useful in the hazard assessment, risk identification, and disaster management for landslides. The GPS is a space-based global navigation satellite system which provides the information of position and time anywhere in the world in all weather conditions [32]. Previous studies showed the application of GPS for mapping and indentifying landslide zones. GIS is used for collection, storage, and analysis of processes where geographic information is involved [32]. The use of GIS for landslide mapping is very common in various studies. Remote sensing is the science in which information is acquired about the surface of earth without physically being in contact with it. RS is also used for monitoring and mapping of landslides in various studies [32].

Mapping the areas that are susceptible to landslides is essential for proper landuse planning and disaster management for a particular locality or region. Throughout the years different techniques and methods have been developed and applied in the literature for landslide susceptibility mapping. Landslide susceptibility maps can be produced using both the quantitative or qualitative approach [33].

Qualitative maps weight each factors affecting the landslides based on the practical experience and expertise of the researcher [33]. Qualitative methods simply portray the hazard zoning in descriptive terms [34]. The qualitative approaches were used by the scientists until the late 1970's [35]. But because of the developments in computer programming and geospatial technologies, qualitative techniques have become very popular in recent decades. Moreover, it incorporates the causes of landslides (instability factors) and probabilistic methods which give much better results than the quantitative methods [35].

Methods to map landslide susceptibility can be classified into four groups, namely landslide inventory based probabilistic, deterministic, heuristic, and statistical techniques [34]. Landslide inventory based probabilistic techniques involve the inventory of landslides, construction of databases, geomorphological analysis, and producing the susceptibility maps based on the collected data [36]. Deterministic techniques (quantitative methods) involve the estimation of quantitative values of stability variables and require the creation of a map that displays the spatial distribution of input data [37, 38]. Heuristic analysis (qualitative method) is based on the intrinsic properties of the geomorphologists to analyse aerial photographs or to conduct field surveying [39].

In this kind of analysis, the susceptibility is established by researchers and the analyst uses expert knowledge to assign weights to a series of parameters for preparing the qualitative map [38]. Statistical analysis is used to analyse factors affecting landslides in areas with environmental conditions similar to those where past landslides have been reported [33]. These methods use sample data based on the relationship between the dependent variable (the presence or absence of landslides), and the independent variables (landslides triggering/causative factors). Through these statistical techniques, quantitative predictions are possible to make for areas where there is no landslides and with similar conditions [38].

Within these techniques, the probabilistic and statistical methods have been most commonly used in recent years. These methods have become more popular, assisted by the geographic information system (GIS) and remote sensing (RS) techniques [27].

The probabilistic (non-deterministic) models like frequency ratio, bivariate analysis, multivariate analysis, and Poisson probability model [40] are more frequently used to determine landslide susceptibility zones [41]. Among the most widely used statistical method is the logistic regression [38]. Many researchers have used different techniques such as heuristic approach [29] and deterministic models [28].

Moreover, GIS based multi criteria decision analysis (MCDA) provides powerful techniques for the analysis and prediction of landslide hazards. These include the analytic hierarchy process (AHP) [42], the weighted linear combination (WLC), the ordered weighted average (OWA) [42] etc.

Most recently, new non-parametric techniques like cellular automata, fuzzy-logic, artificial neural networks (ANN) [43], support vector machines (SVM), and neuro-fuzzy models have been used for landslide modeling [33]. [Please go through Appendix- II, for the detailed structural literature review]

In most cases the researchers have used the following thematic layers for modelling or predicting landslide susceptibility maps [28, 32, 33, 43]:

1) Landslide Inventory
2) Precipitation Data/ Rainfall Intensity Map
3) Land Cover Maps
4) Digital Elevation Model (DEM)
5) Aspect
6) Elevation/ Internal Relief
7) Slope
8) Curvature (Plan & Profile)
9) Geology
10) Geomorphology
11) Soil/ Lithology
12) Lineaments/ Distance from Faults
13) Drainage Density
14) Distance to Road
15) Distance to Stream
16) Topographic Wetness Index (TWI)
17) Normalized Difference Vegetation Index (NDVI)

18) Stream Power Index (SPI)
19) Seismic Data
20) Surrounding Infrastructure (e.g. Buildings)

If the above mentioned 20 thematic layers/ variables are analysed, then it is clear that the land cover maps and precipitation data (rainfall pattern) can be changed markedly over time. Similarly drainage density, distance to road/ stream, TWI, NDVI, SPI and surrounding infrastructure can change in course of time. Therefore, these variables can be considered as 'dynamic variables'. The rest of the layers can be termed as 'persistent variables'.

3.2. Data Collection

For landslide susceptibility mapping (LSM), it is very important to collect necessary data layers. For this research purpose, 9 different GIS layers have been produced for LSM. The details of the data collection technique and ways of preparing the thematic layers are described below:

3.2.1. Land Cover Mapping

Landsat Thematic Mapper (TM) satellite images were used for the land cover mapping (2010) of CHT area. This CHT base map was collected from International Centre for Integrated Mountain Development (ICIMOD), Kathmandu, Nepal. But the procedure for preparing the map is described in brief. Initially four scenes were collected to cover the whole CHT area. TM sensor collects reflected energy in three visible bands (blue = 1, green = 2, and red = 3) and three infrared bands (two NIR = 4, 5 and one middle infrared = 7). The base year for this land cover mapping is selected as 2010.

Among the four scenes, three were acquired using the Global Visualization Viewer (GLOVIS) of United States Geological Survey (USGS) and the one was from GISTDA (Geo-Informatics and Space Technology Development Agency), Thailand. However, thermal band was not used in this particular study. The details of the scenes used are listed in Table 3.1. All the image-dates are of the dry season in Bangladesh.

The land cover classification methodology for this research is based on 'Object Based Image Analysis (OBIA)'. 'OBIA' is also called 'Geographic Object-Based Image Analysis (GEOBIA)'. 'OBIA' is a sub-discipline of geoinformation science devoted to partitioning remote sensing imagery into meaningful image objects, and assessing their characteristics

through spatial, spectral and temporal scale. The fundamental step of any object based image analysis is a segmentation of a scene representing an image into image objects.

Table 3.1. Details of the Landsat 4-5 TM scenes of CHT

Satellite	Sensor	Path	Row	Date (DD/MM/YY)	Source Agency
Landsat 4-5	TM	136	044	08/02/2010	USGS
		136	045	06/12/2009	
		135	045	01/02/2010	GISTDA
		135	046	01/02/2010	

The projection detail of all the raster images (cell size 30m × 30m)/ vector-shapefiles used in this research is as follows:

Projection: Bangladesh_Transverse_Mercator (BTM)

False_Easting: 500000.000000

False_Northing: -2000000.000000

Central_Meridian: 90.000000

Scale_Factor: 0.999600

Latitude_Of_Origin: 0.000000

Linear Unit: Meter (1.000000)

Geographic Coordinate System: GCS_Everest_Bangladesh

Angular Unit: Degree (0.0174532925199433299)

Prime Meridian: Greenwich (0.000000000000000000)

Datum: D_Everest_Bangladesh

Spheroid: Everest_Adjustment_1937

Semimajor Axis: 6377276.344999999700000000

Semiminor Axis: 6356075.413140240100000000

Inverse Flattening: 300.801699999999980000

At first, the acquired Landsat TM images were inserted in ‘eCognition Developer 64 8.7’ software for processing. The ‘‘multi-resolution segmentation’’ algorithm was used which

consecutively merges pixels or existing image objects that essentially identifies single image objects of one pixel in size and merges them with their neighbours, based on relative homogeneity criteria. Multi-resolution segmentations are those groups of similar pixel values which merges the homogeneous areas into larger objects and heterogeneous areas in smaller ones.

During the classification process, information on spectral values of image layers, vegetation indices like the Normalized Difference Vegetation Index (NDVI) and land water mask which were created through band rationing, slope and texture information were used. Image indices are very important during the image classification. Image rationing is a "synthetic image layer" created from the existing bands of a multispectral image. This new layer often provides unique and valuable information not found in any of the other individual bands. Image index is a calculated results or generated product from satellite band/channels. It is help to identify different land cover from mathematical definition.

NDVI: One of the commonly used indices and it is related to vegetation is that healthy vegetation reflects very well in the near infrared part of the spectrum. NDVI index values can range from -1.0 to 1.0. NDVI was calculated using the following formula:

NDVI = (NIR - red) / (NIR + red)

Land and water mask: Land and water mask indices values can range from 0 to 255, but water values typically range between 0 and 50. The land and water mask was created using the formula

Land and water mask: IR/Green*100

The next step is to code these image objects according to their attributes, such as NDVI, Land and water mask, layer value and colour and relative position to other objects using user-defined rules. In this process, selected object that represent patterns were recognize with the help from other sources namely already known Ground truthing information and high resolution Google earth images. Normally similar features observed similar spectral responses and unique with respect to all other image objects.

After that comparison, features using the '2D Feature Space Plot' were used for correlation of two features from the selected image objects. Developing rule sets investigated single image objects and generated land cover map. Image objects have spectral, shape, and hierarchical

characteristics and these features are used as sources of information to define the inclusion-or-exclusion parameters used to classify image objects. Over each scene rules were generated for each land cover class and evaluated for their separation, tested for their visual assessment over Google earth images.

After ascertaining the class separation using segment based approach, classification is performed to get land cover classification map for each scene. Each scene thus prepared again evaluated with available field data and Google earth image over randomly selected points for accuracy assessment. After finalization of classification of each scene, all the scenes were gone through mosaic to obtain land cover map of CHT area (Figure 3.1).

Figure 3.1 consists of 14 land cover classes. But for this research purpose, only 5 broad land cover classes (urban area, semi-urban area, water body, vegetation and bare soil) were chosen by reclassification technique. Later the study area was extracted from the CHT land cover map using the CMA boundary. This is the final land cover map of the study area (Figure 3.2).

3.2.2. Precipitation Map

The daily observed precipitation data were collected from Bangladesh Meteorological Department (1950-2010). Based on the average annual precipitation, the final precipitation map of CMA was prepared using Kriging overlaying technique (Figure 3.3).

3.2.3. Landslide Inventory Map

A total of 20 landslide locations were identified in the study area through field visit (Appendix-III). The latitude and longitude values were collected using a Global Positioning System (GPS) device. Moreover, the Digital Elevation Model (DEM) data were collected from the ASTER GDEM portal. The Advanced Spaceborne Thermal Emission and Reflection Radiometer (ASTER) Global Digital Elevation Model (GDEM) was developed jointly by the Ministry of Economy, Trade, and Industry (METI) of Japan and the United States National Aeronautics and Space Administration (NASA). The ASTER GDEM was contributed by METI and NASA to the Global Earth Observation System of Systems (GEOSS) and is available at no charge to users via electronic download from the Earth Remote Sensing Data Analysis Center (ERSDAC) of Japan and NASA's Land Processes Distributed Active Archive Center (LP DAAC) [47].

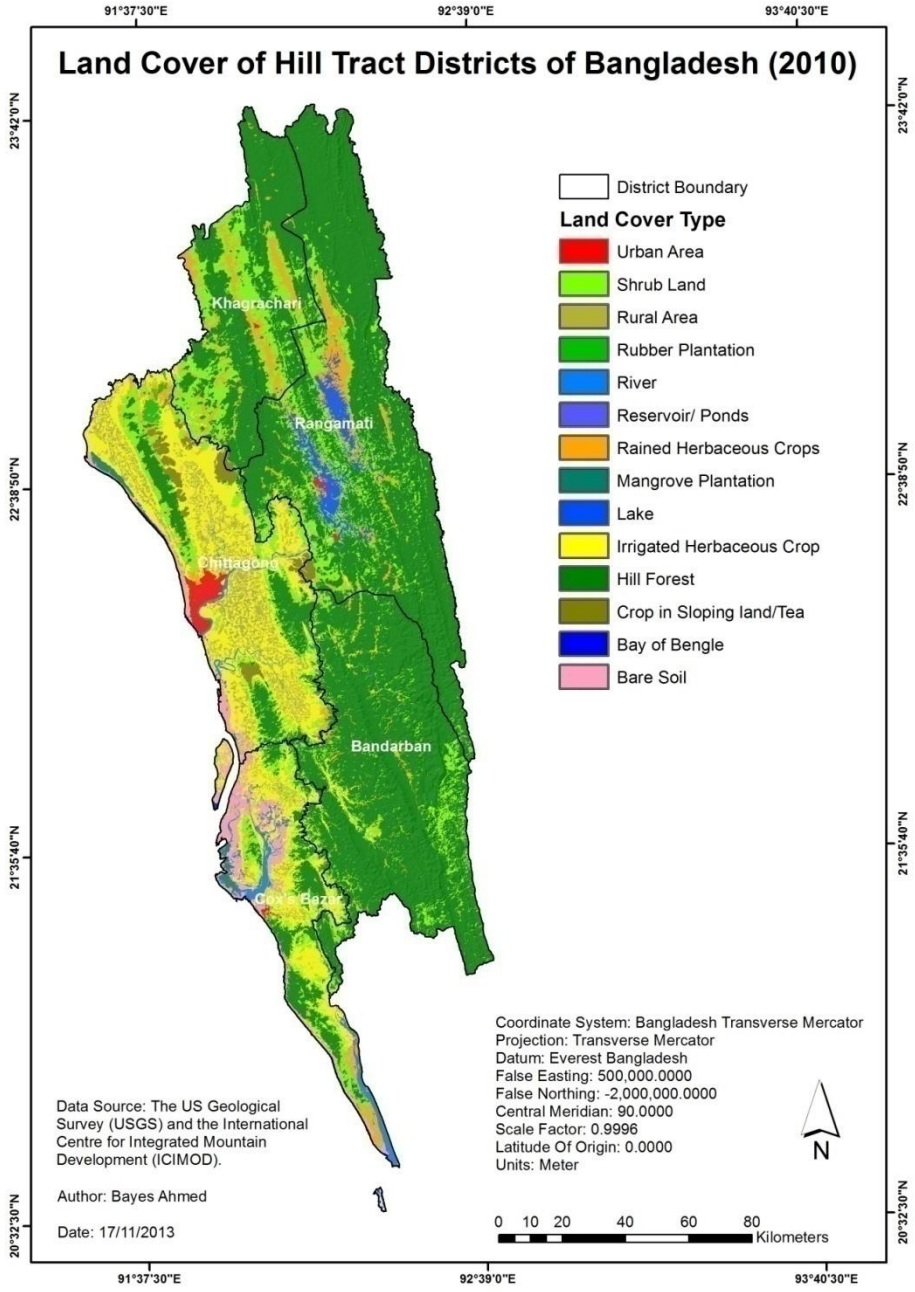

Figure 3.1. Land cover map of Chittagong Hill Tract (CHT) area

The tiles of ASTGTM2_N20E092, ASTGTM2_N22E092, ASTGTM2_N21E092, ASTGTM2_N21E091, ASTGTM2_N22E091, ASTGTM2_N23E091 and ASTGTM2_N23E092 (acquired on 29 November 2013); cover the whole CHT area. The characteristics of the ASTER GDEM are listed in Table 3.2 [47]. Later the DEM map of CMA was extracted from CHT DEM. Finally the observed landslide locations of CMA were represented in Figure 3.4.

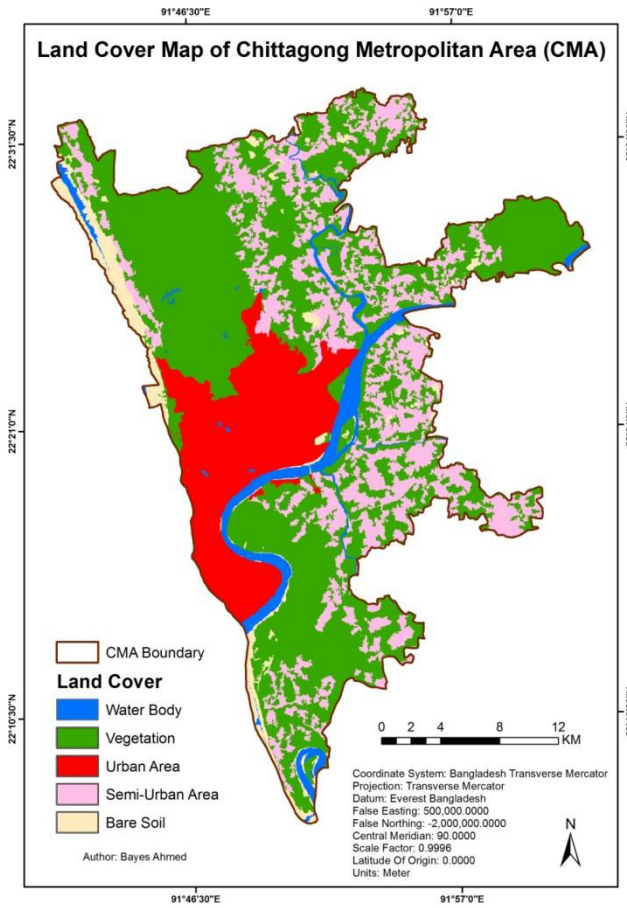

Figure 3.2. Land cover map

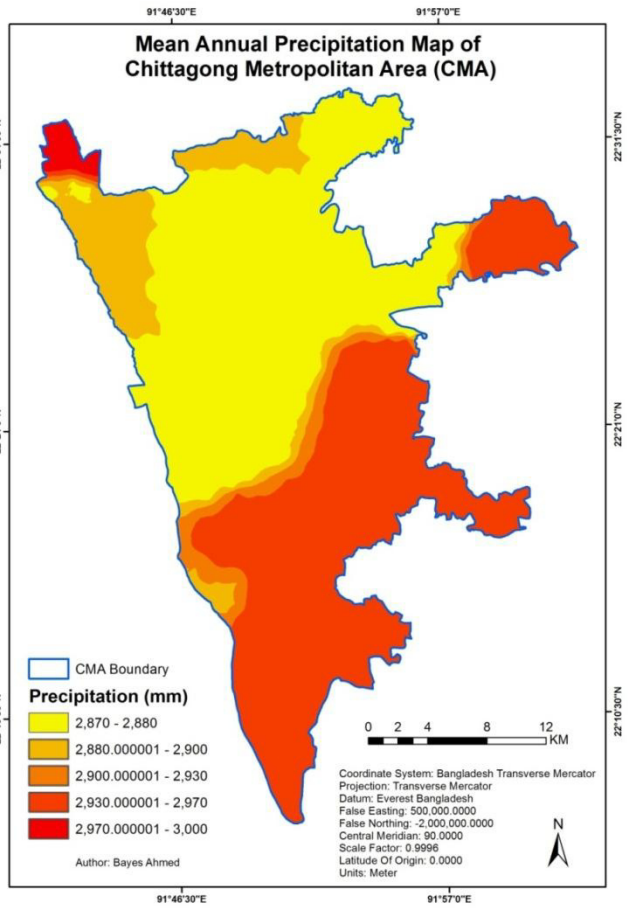

Figure 3.3. Precipitation map

Table 3.2. ASTER GDEM raster image characteristics [47]

Item	Description
Tile Size	3601-by-3601 pixels (1-by-1 degree)
Posting interval	1 arc-second
Geographic coordinates	Geographic latitude and longitude
Output format	GeoTIFF, signed 16 bits
DN values	1m/DN referenced to the WGS84/EGM96 geoid-9999 for void pixels, and 0 for sea water body
Coverage	North 83 degrees to south 83 degrees, 22,600 tiles
Posting interval	30m
DEM accuracy (stdev.)	7~14m

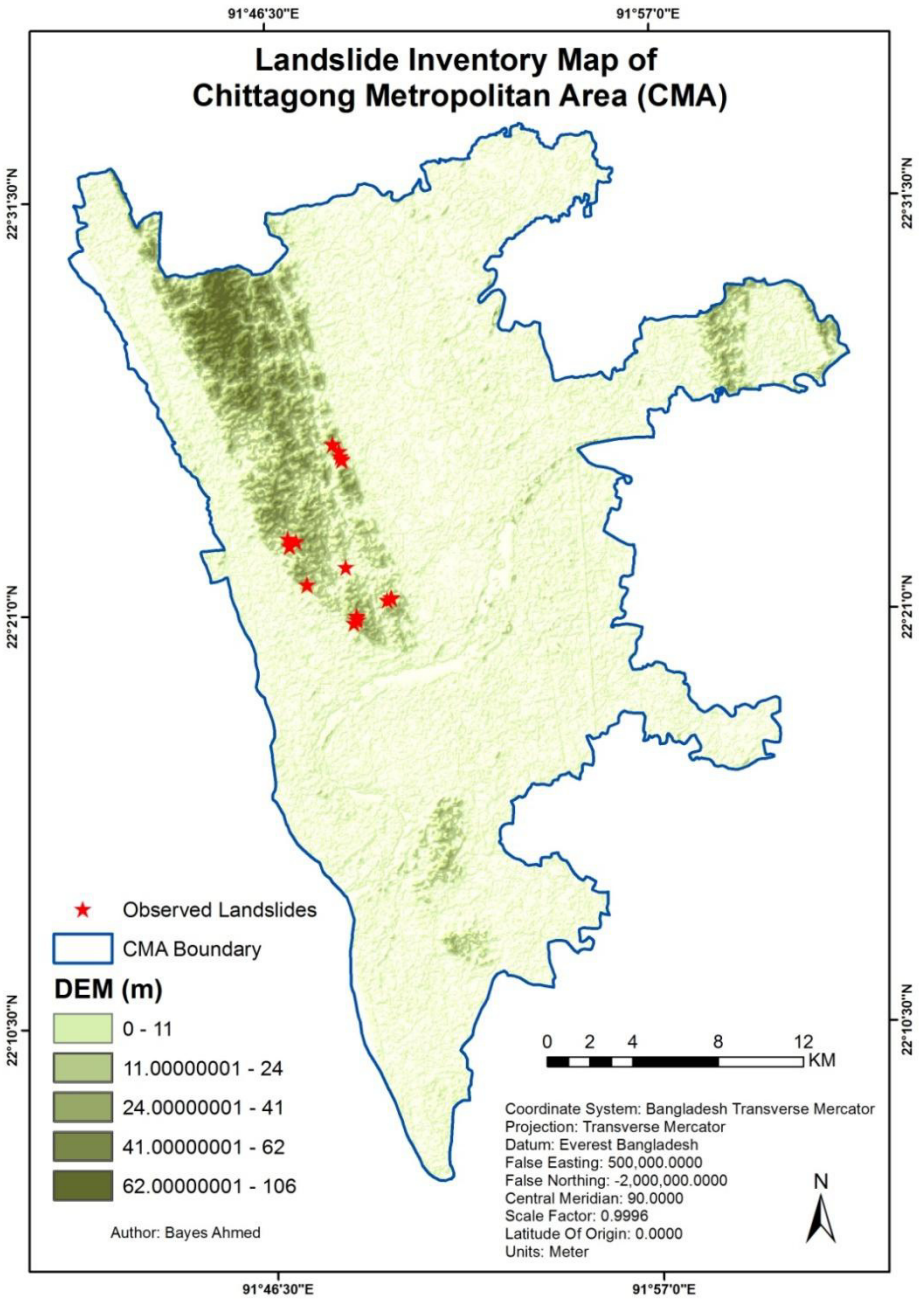

Figure 3.4. Observed landslide locations in CMA

3.2.4. Elevation and Slope Map

Elevation and slope maps can be produced from DEM layer. The maps were then classified using Natural Breaks (Jenks) method with 5 classes (Figure 3.5 and Figure 3.6). Natural Breaks classes are based on natural groupings inherent in the data. Class breaks are identified that best group similar values and that maximize the differences between classes. The features are divided into classes whose boundaries are set where there are relatively big differences in the data values. Natural breaks are data-specific classifications and not useful for comparing multiple maps built from different underlying information [48].

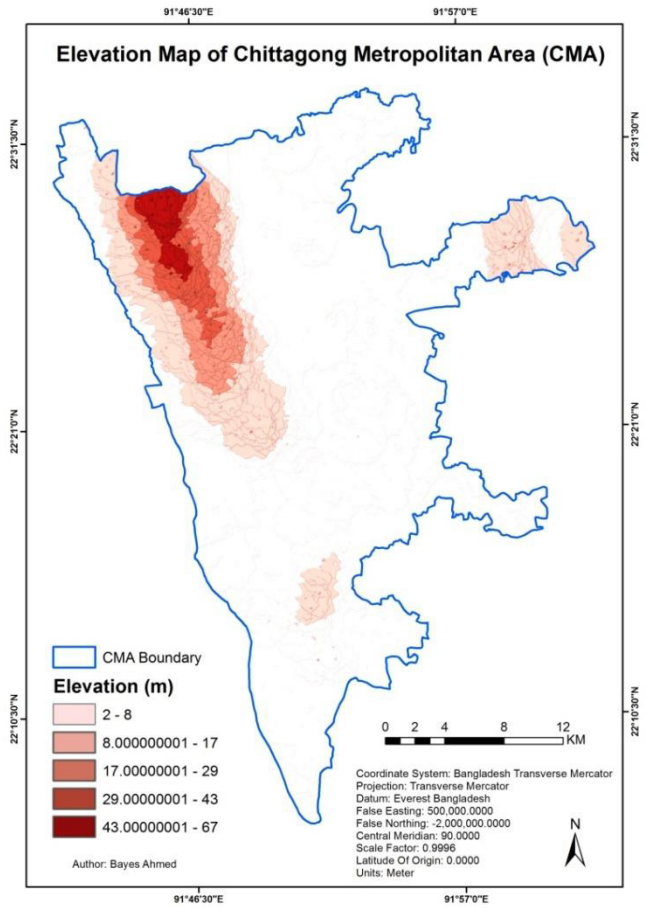

Figure 3.5. Elevation map

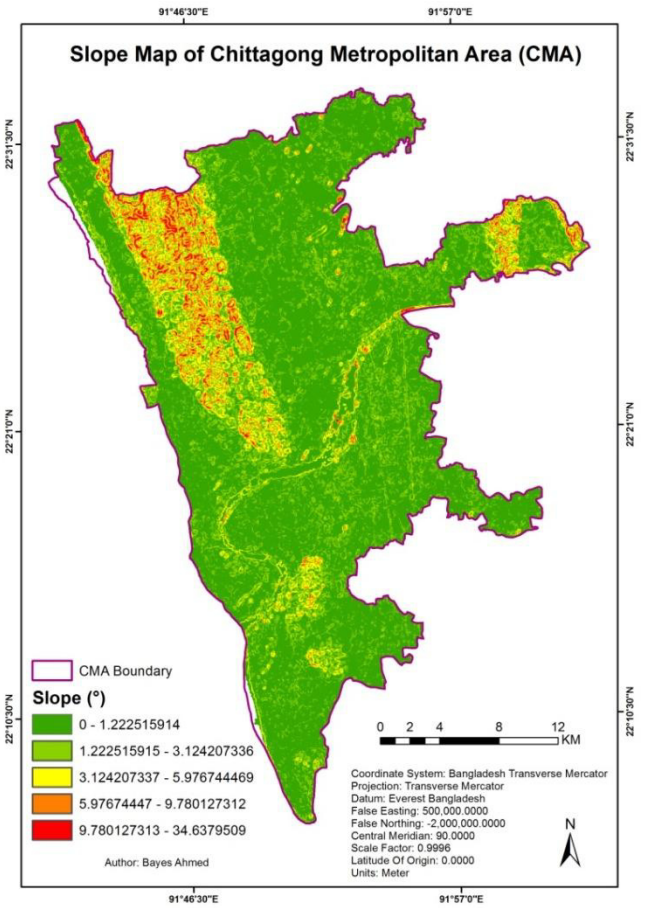

Figure 3.6. Slope map

3.2.5. NDVI Map

The Normalized Difference Vegetation Index (NDVI) is a standardized index allowing you to generate an image displaying greenness (relative biomass). This index takes advantage of the contrast of the characteristics of two bands from a multispectral raster dataset- the chlorophyll pigment absorptions in the red band and the high reflectivity of plant materials in the near-infrared (NIR) band [48]. The documented and default NDVI equation is as follows:

NDVI = ((IR - R)/ (IR + R))

where, IR = pixel values from the infrared band (band 4)

R = pixel values from the red band (band 3)

This index outputs values between -1.0 and 1.0, mostly representing greenness, where any negative values are mainly generated from clouds, water, and snow, and values near zero are mainly generated from rock and bare soil. Very low values of NDVI (0.1 and below) correspond to barren areas of rock, sand, or snow. Moderate values represent shrub and grassland (0.2 to 0.3), while high values indicate temperate and tropical rainforests (0.6 to

0.8) [48]. In this research, the Landsat 4-5 TM images from the same season (dry and summer) were acquired from GLOVIS USGS website. The specifications of the collected satellite images are described in Table 3.3. Finally the NDVI map (Figure 3.7) of CMA was prepared by analysing band 3 and band 4.

Table 3.3. Details of the satellite images for NDVI analysis

Satellite	Sensor	Path	Row	Date (DD/MM/YY)	Source Agency	Cloud Coverage	Quality
Landsat 4-5	TM	136	44	05/02/2009	USGS	0%	9
		136	45	09/03/2009			

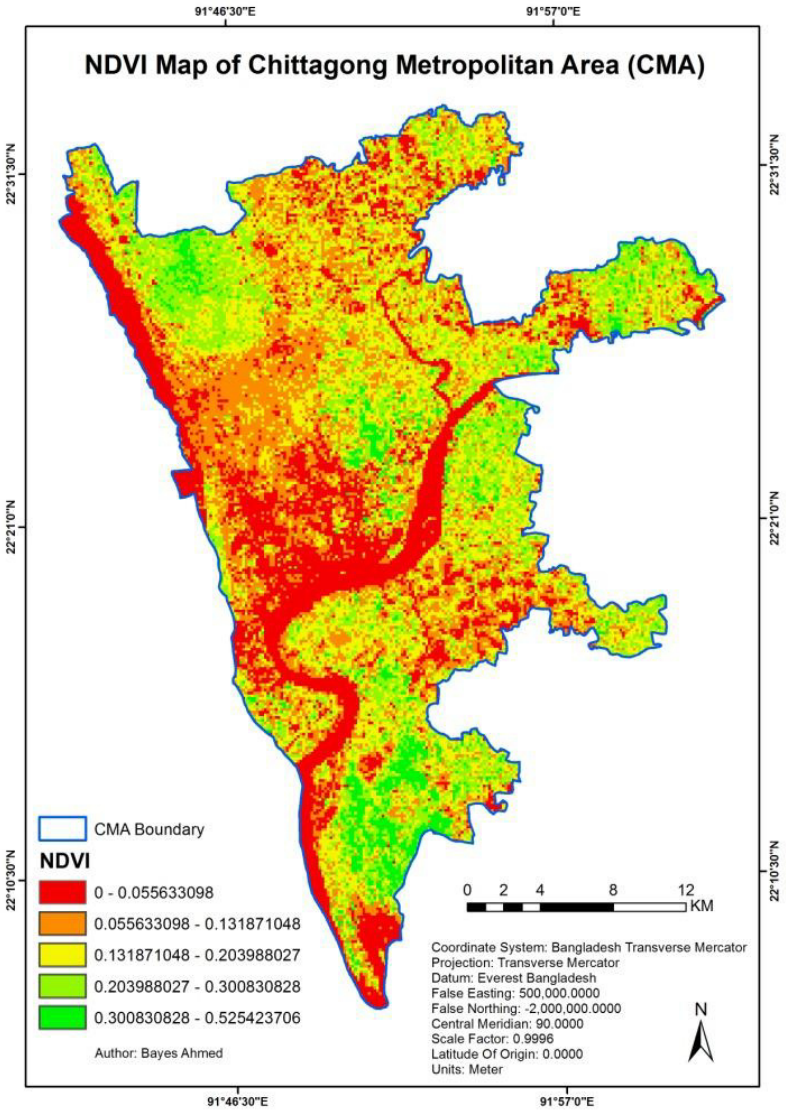

Figure 3.7. NDVI map

3.2.6. Other Layers

The road network, drainage network and water body layers were collected from the Chittagong Development Authority (CDA). The distance images from all these layers were prepared using 'Euclidean Distance' technique which gives the distance from each cell in the raster to the closest source (Figure 3.7-3.10). The Euclidean distance tools give you information according to Euclidean, or straight-line, distance. Euclidean distance is calculated from the center of the source cell to the center of each of the surrounding cells. True Euclidean distance is calculated in each of the distance tools [48].

The soil permeability map (Figure 3.11) was collected from Bangladesh Agricultural Research Council (BARC).

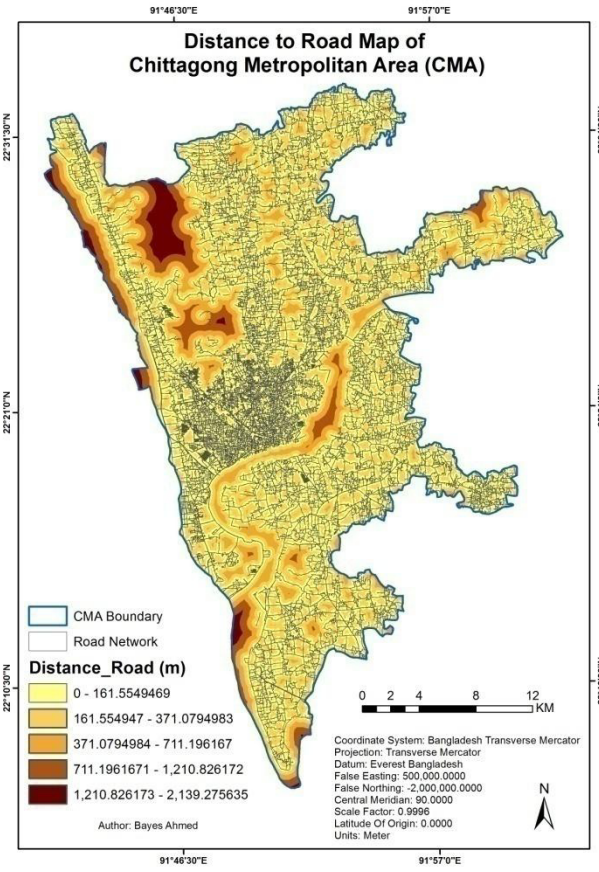

Figure 3.8. Distance to road map

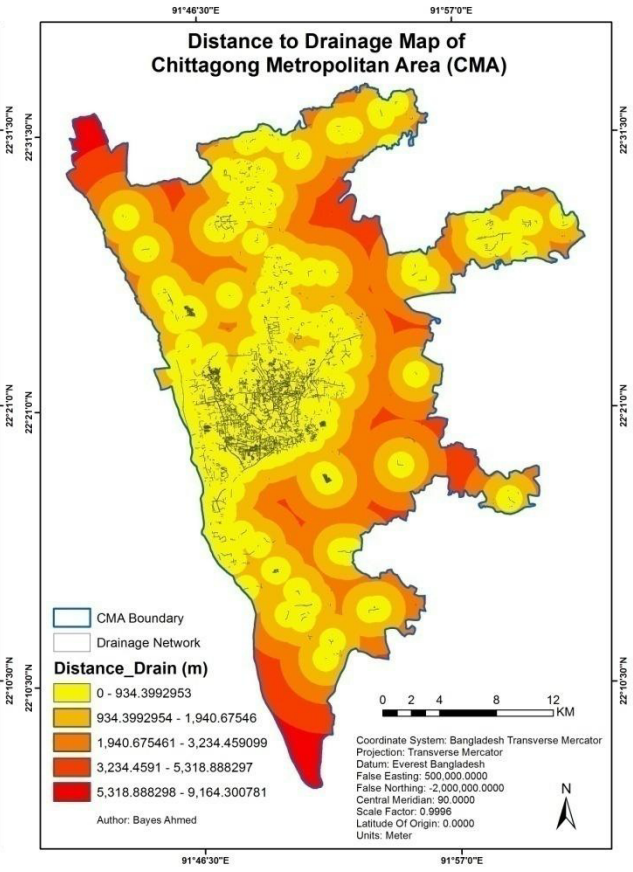

Figure 3.9. Distance to drain map

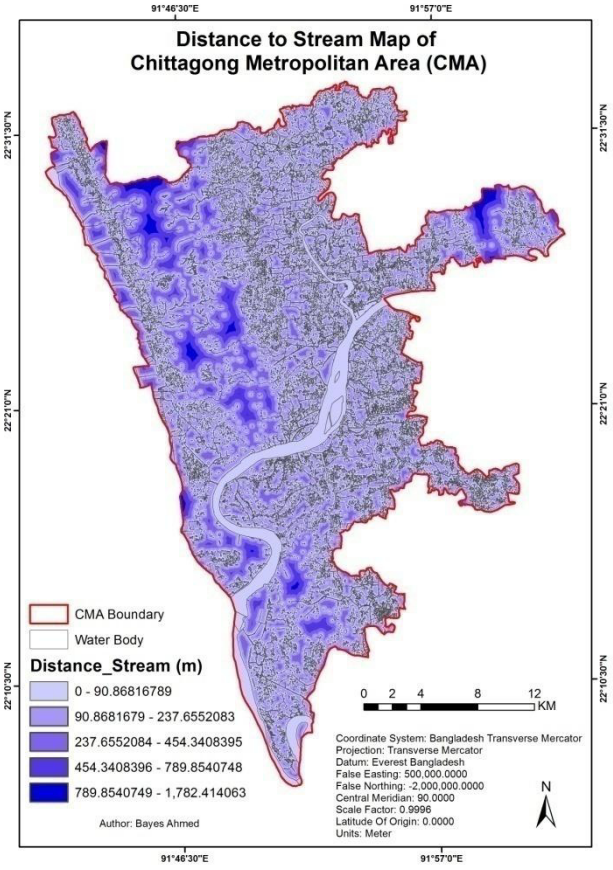

Figure 3.10. Distance to stream map

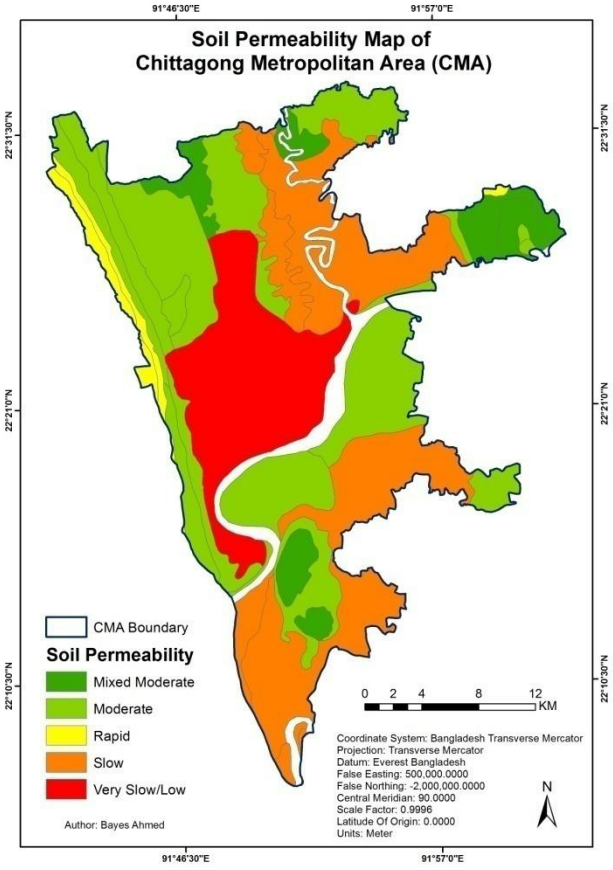

Figure 3.11. Soil permeability map

3.3. Soil Sample Collection

Soil samples were collected from 17 locations of CMA, which are vulnerable to landslides, to analyze different properties of soil related to shear strength.

Chapter 4

LANDSLIDE SUSCEPTIBILITY MAPPING

For the predictive landslide susceptibility mapping of CMA, three different techniques have been implemented. These are:

a. Weighted Linear Combination
b. Logistic Regression
c. Multiple Regressions

4.1. Weighted Linear Combination (WLC)

The GIS-multicriteria decision analysis (GIS-MCDA) technique is increasingly used for landslide hazard mapping and zonation. It enables the integration of different data layers with different levels of uncertainty. The WLC method is one of the most commonly used GIS-MCDA [49]. The WLC technique is a popular method that is customized in many GIS and is applicable for the flexible combination of maps. The tables of scores and the map weights can be adjusted to reflect the judgment of an expert in the domain of the application being considered [42]. This method initially requires the standardization of the classes in each factor to a common numeric range. WLC can be considered as a hybrid between qualitative and quantitative methods. In the WLC method, each criterion is multiplied by its weight from the pairwise comparison and the results are summed:

$$S = \sum_i w_i \mu_i$$

In this formula, S represents the final score, w_i represents the weight of the criterion i, and μ_i represents the criterion standardized score [50]. Weights can have a tremendous influence on the solution. Due to the criterion weights being summed to one, the final scores of the combined solution are expressed on the same scale. Also, weights given to each criterion determine the trade-off level relative to the other criteria, which implies that high scores and weights from standardized criteria can compensate for low scores from other criteria. However, when scores from standardized criteria are low while the weights are high, they can only weakly compensate for the poor scores from other criteria [42,50].

WLC (or simple additive weighting) is based on the concept of a weighted average. The decision-maker directly assigns the weights of 'relative importance' to each attribute map layer. A total score is then obtained for each alternative by multiplying the weight assigned to each attribute by the scaled value given to the alternative on that attribute, and summing the products of all attributes. When the overall scores are calculated for all of the alternatives, the alternative with the highest overall score is chosen. The method can be operationalized using any GIS system with overlay capabilities. The overlay techniques allow the evaluation criterion map layers (input maps) to be combined, in order to determine the composite map layer (output map) [42,49].

In this method, criteria may include both weighted factors and constraints. WLC starts by multiplying each factor by its factor/trade-off weight and then adding the results; constraints are then applied by successive multiplication to "zero out" excluded areas. This procedure is characterized by full trade-off between factors and average risk. Factor weights, not used at all in the case of Boolean intersection (no trade-off), are very important in WLC because they determine how individual factors will trade-off relative to each other. In this case, the higher the factor weight the more influence that factor has on the final suitability map. (Contrast this with method 3 below where the importance of factor weights is variable). Along with full trade-off, this combination procedure is characterized by an average level of risk, as it is exactly midway between the minimization (AND operation) and maximization (OR operation) of areas to be considered suitable in the final result [51].

The class rating within each factor was based on the relative importance of each class according to experts opinion, practical experience, field observations in the study area and existing literature, indicating certain conditions as the most favourable to slope failure. For this research purpose, some assumptions were undertaken for the factors. The susceptibility to landslides for a certain area increases:

1. The more the distance from drainage network
2. The higher the elevation
3. The closer to urban area land cover type
4. The lower the NDVI
5. The higher the precipitation
6. The farther the distance from road network
7. The steeper the slope

8. The slower the soil permeability
9. The closer to water body

Based on the above assumptions, three different combinations of factor weights (Table 4.1) were chosen for producing three different WLC maps. Finally the WLC maps were reclassified into low, medium and high landslide susceptibility zones (Figure 4.1-4.3).

Table 4.1. Factor weights for WLC analysis

Factor	Factor Weight_1	Factor Weight_2	Factor Weight_3
Distance to Drain	0.05	0.10	0.10
Elevation	0.10	0.10	0.15
Land Cover	0.10	0.15	0.15
NDVI	0.10	0.10	0.10
Precipitation	0.05	0.05	0.05
Distance to Road	0.05	0.05	0.05
Slope	0.10	0.15	0.15
Soil Permeability	0.40	0.25	0.20
Distance to Stream	0.05	0.05	0.05
Total	**1.00**	**1.00**	**1.00**

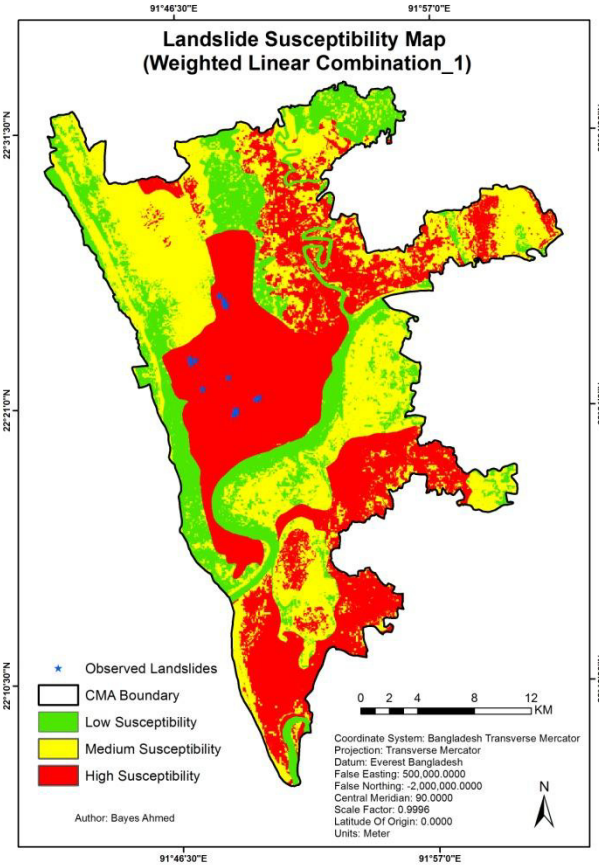

Figure 4.1. WLC_1 map

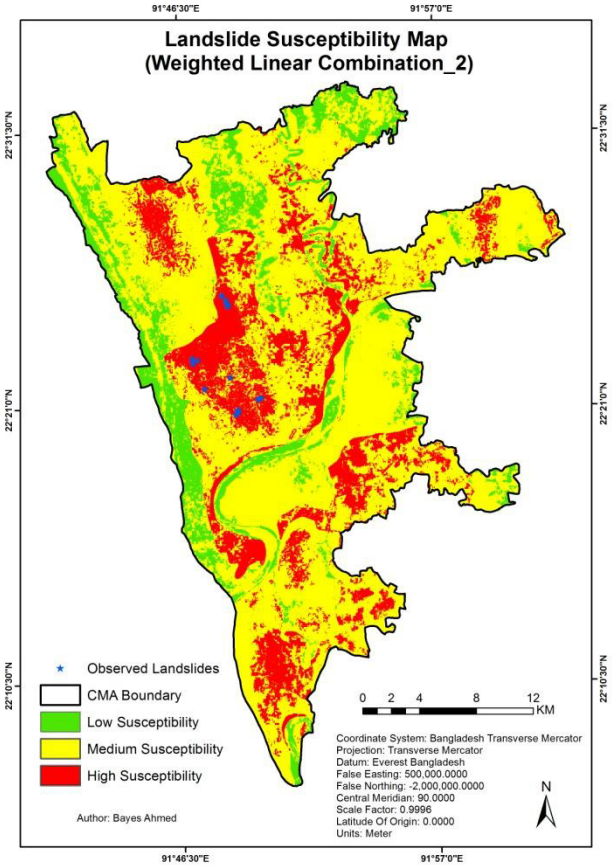

Figure 4.2. WLC_2 map

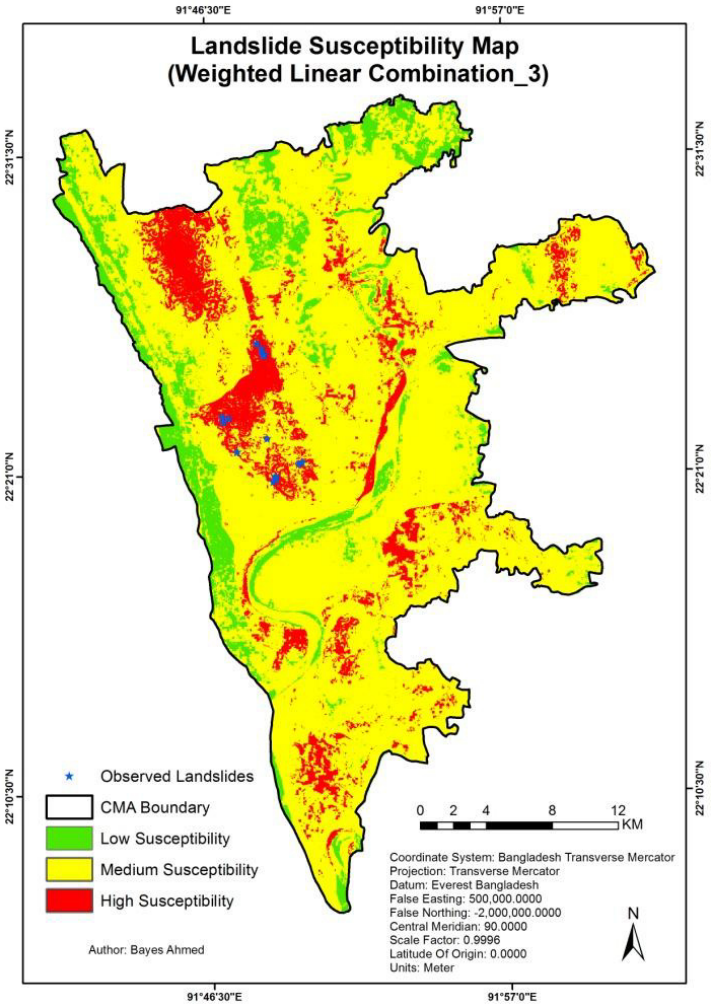

Figure 4.3. WLC_3 map

4.2. Logistic Regression (LR)

Logistic regression (LR), a type of multivariate analysis, is useful for predicting the presence or absence of a characteristic or outcome based on the values of a set of predictor variables [52]. The LR model, which was developed by McFadden (1973), uses independent variables to create a mathematical formula for the probability that an event will occur on any given parcel of land [53]. The key to LR is that the dependent variable is dichotomous [33]. The independent variables in this model are predictors of the dependent variable and can be measured on a nominal, ordinal, interval, or ratio scale. The relationship between the dependent and independent variables is nonlinear [33, 54].

For this research, the 'LOGISTICREG' tool of IDRISI Taiga software was used. LOGISTICREG performs binomial logistic regression, in which the input dependent variable must be binary in nature, that is, it can have only two possible values (0 and 1). Such regression analysis is usually employed in estimating a model that describes the relationship

between one or more continuous independent variable(s) to the binary dependent variable. The basic assumption is that the probability of dependent variable takes the value of 1 (positive response) follows the logistic curve and its value can be estimated with the following formula [51,55]:

$$P(y=1|X) = \frac{exp(\sum BX)}{1+exp(\sum BX)}$$

where, P = the probability of the dependent variable being 1; X is the independent variables,

$X = (x_0, x_1, x_2, \ldots x_k), x_0 = 1$

B is the estimated parameters

$B = (b_0, b_1, b_2, \ldots b_k)$

To linearize the above model and to remove the 0/1 boundaries for the original dependent variable (probability), the following transformation are usually applied [51,55]:

$P' = Ln(P/(1-P))$

This transformation is referred to as the logit or logistic transformation. Note that after the transformation P' can theoretically assume any value between minus and plus infinity. By performing the logit transformation on both sides of the above logit regression model, we obtain the standard linear regression model [51,55]:

$Ln(p/(1-p)) = b_0 + b_1*x_1 + b_2*x_2 + \ldots\ldots + b_k*x_k + error\_term$

Notice that the logit transformation of dichotomous data ensures that the dependent variable of the regression is continuous, and the new dependent variable (logit transformation of the probability) is unbounded. Furthermore, it ensures that the predicted probability will be continuous within the range from 0-1.

Assumptions of the logistic regression model [51]:

- the dependent random variable, Y, is assumed to be binary, taking on only two values (0 and 1).

- the outcomes on Y are assumed to be mutually exclusive and exhaustive.

- Y is assumed to depend on K observable variables X_k and the relationship is non-linear and follows the logistic curve.

- the data are generated from a random sample of size N, with a sample point denoted by i, i = 1, ..., N.

- no restriction on the independent variables except that they cannot be linearly related; (implies that N>K).

- the error term of each observation is assumed to be independent of the error terms of all other observations.

LOGISTICREG employs Maximum Likelihood Estimation (MLE) procedure to find the best fitting set of parameters (coefficients). The maximum likelihood function used by LOGISTICREG is the following [51,55]:

$L = \prod_i^N \mu * (1-\mu_1)^{(1-y_i)}$

where, L is the likelihood

μ_i is the predicted value of the dependent variable for sample i

$\mu_i = \exp(\sum_{k=0}^{k} b_k x_{ik}) / (1 + \exp \sum_{k=0}^{k} b_k x_{ik})$

y_i is the observed value of the dependent variable for sample i

To maximize the above likelihood function, it thus requires the solution for the following simultaneous nonlinear equations [51,55]:

$\sum_{i=1}^{N} .(y_i - \mu_i) * x_{ij} = 0$

Where x_{ij} is the observed value of the independent variable j for sample i.

The rest is the same as for the likelihood function. In solving the above equations, LOGISTICREG uses the Newton-Raephson algorithm [51]. Moreover, the LOGISTICREG text output includes the following:

The regression equation and the individual regression coefficient;

In the Regression Statistics section [51]:

Number of Total Observations:	the number of observations used in study area
Number of 0s in Study Area:	the number of observations with dependent value as 0 in study area
Number of 1s in Study Area:	the number of observations with dependent value as 1 in study area
Percentage of 0s in Study Area:	equal to 100*(Number of 0s in study area / Number of observations in study area)
Percentage of 1s in Study Area:	equal to 100*(Number of 1s in study area / Number of observations in study area)
Number of Auto-sampled Observations:	the number of observations sampled for analysis
Number of Os in Sampled Area:	the number of observations with dependent value as 0 in analysis
Number of 1s in Sampled Area:	the number of observations with dependent value as 1 in analysis
Percentage of 0s in Sampled Area:	actual percentage of 0s used in analysis
Percentage of 1s in Sampled Area;	actual percentage of 1s used in analysis

The basis for testing the goodness of fit in logistic regression is the likelihood ratio principle. The ratio is based on the following two statistics [51,55]:

-2log(L0)

where L0 is the value of the likelihood function if all coefficients except the intercept are 0;

-2log(Likelihood)

where Likelihood is the value of the likelihood function for the full model as fitted;

Based on the above two statistics, the following two are calculated [51]:

Pseudo R_square = 1- (log(Likelihood)/log(L0);

Thus, pseudo R_square = 1 indicates a perfect fit, where as pseudo R_square = 0 indicates no relationship.

Pseudo R_square greater than 0.2 is considered a relatively good fit [56].

ChiSquare(k) = -2(log(likelihood) –log(L0));

This is also known as the likelihood ratio statistic which follows, approximately, a chi-square distribution when the null hypothesis is true. This statistic tests the hypothesis that all coefficients except the intercept are 0. Thus, it is a similar test as the F statistic in liner

regression analysis. The degrees of freedom for this chi-square statistic is K (the number of the independent variables included) [51].

The last statistic in this group that bears some measure of goodness of fit is calculated based on the difference between the observed and the predicted values of the dependent variable [51]:

$$Goodess\_of\_fit = \sum_{i=1}^{N}.(y_i-\mu_i)^2/\mu_i*(1-\mu_i)$$

Thus, the smaller of this statistic, the better fit it indicates. The classification is based on the predicted probability with 0.5 as the dividing point, i.e., classify a case as 0 if its predicted probability is less than 0.5 and as 1 otherwise. The odds ratio is calculated from the classification table with the following formula [51]:

$$Odds\_ratio = (f_{11} * f_{22})/(f_{12} * f_{21})$$

where,

Observed	Pred_0	Pred_1
0	f_{11}	f_{12}
1	f_{21}	f_{22}

In the last section, this version of LOGISTICREG offers two additional statistics [51]:

(1) Instead of reclassifying the case using the probability of 0.5 as the cutting point, it offers an alternative classification of cases based on a new cutting point, which is determined by matching the quantity of the number of 1s in the observed values of the dependent variable. Accordingly, an Adjusted Odds Ratio is calculated. In addition, as a transition to the ROC statistic that follows, True and False Positive are also calculated based on this new classification, where [51]:

$$True\_Positive = f_{22} /(f_{21}+ f_{22}) \text{ and}$$

$$False\_Positive = f_{12} /(f_{11}+ f_{12})$$

(2) ROC (Relative Operating Characteristic) ROC is an excellent method to compare a Boolean map of "reality" versus a suitability map (for detailed explanation, see help for the ROC module). Thus, ROC is included here as an excellent statistic for measuring the

goodness of fit of logistic regression. The ROC value ranges from 0 to 1, where 1 indicates a perfect fit and 0.5 indicates a random fit. A ROC value between 0.5 and 1 indicates some association between the X variables and Y. The larger the ROC, the better the fit [51,57].

Now applying the above mentioned method, the landslide susceptibility map of CMA was produced (Figure 4.4). The detailed statistical output of this LR analysis is attached in Appendix-IV.

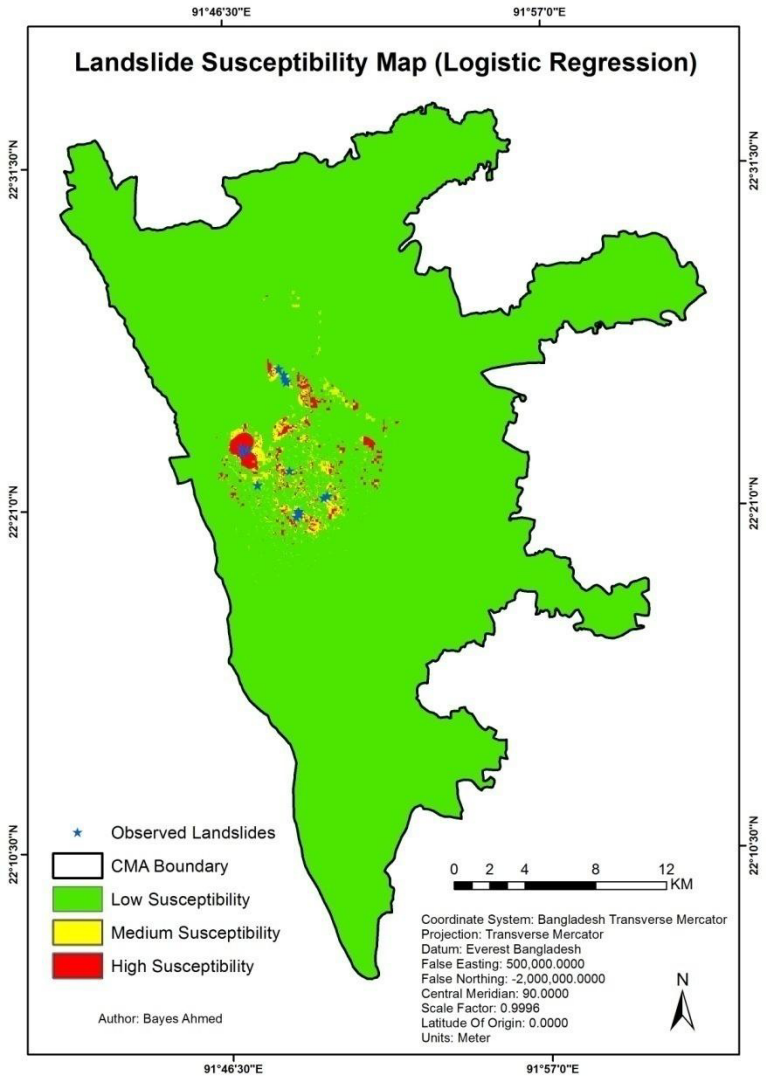

Figure 4.4. Landslide susceptibility map derived from LR model

4.3. Multiple Regressions (MR)

For this research, the 'MULTIREG' tool of IDRISI Taiga software was used. MULTIREG undertakes a multiple linear regression to analyze the relationship of one or more independent variables to a single dependent variable. The regression can be conducted for image files or

attribute values files. MULTIREG adopts a least-squares approach to multiple regressions [59,60].

In multiple regressions, a linear relationship is assumed between the dependent variable and the independent variables. For example, in the case of three independent variables, the multiple linear regression equation can be written as [51]:

$$Y = a + b1*x1 + b2*x2 + b3*x3$$

where Y is the dependent variable, x1, x2, and x3 are the independent variables, a is the intercept, and b1, b2 and b3 are the coefficients of the independent variables x1, x2, and x3 respectively. The intercept represents the value of Y when values of the independent variables are zero, and the coefficient indicates unit change of Y with a one-unit increase in the corresponding independent variable.

The independent variables can be continuous (e.g., interval, ratio, or ordinal) or discrete (dummy variable), but the dependent variable should be continuous and unbounded. Some assumptions underlie the use of multiple linear regressions, such as [51]:

(1) The observations are drawn independently from the population, and the dependent variable is normally distributed;

(2) The number of observations are larger than number of independent variables; and

(3) No exact or near-linear relationship exists among independent variables.

The susceptibility map derived from MR approach is depicted in Figure 4.5. Moreover, the detailed statistical output of this MR model is attached in Appendix-V.

4.4. Model Validation and Comparison

To evaluate the performances of the models in analyzing landslide susceptibility, it is important to validate the models or techniques. To do this validation Relative Operating Characteristic (ROC) method is used in this research. The ROC module employs an excellent method to assess the validity of a model that predicts the location of the occurrence of a class by comparing a suitability image depicting the likelihood of that class occurring (i.e., the input image) and a Boolean image showing where that class actually exists (i.e., the reference image). For example, the ROC could be used to compare an image of modelled probability for landslides against an image of actual observed landslides [51].

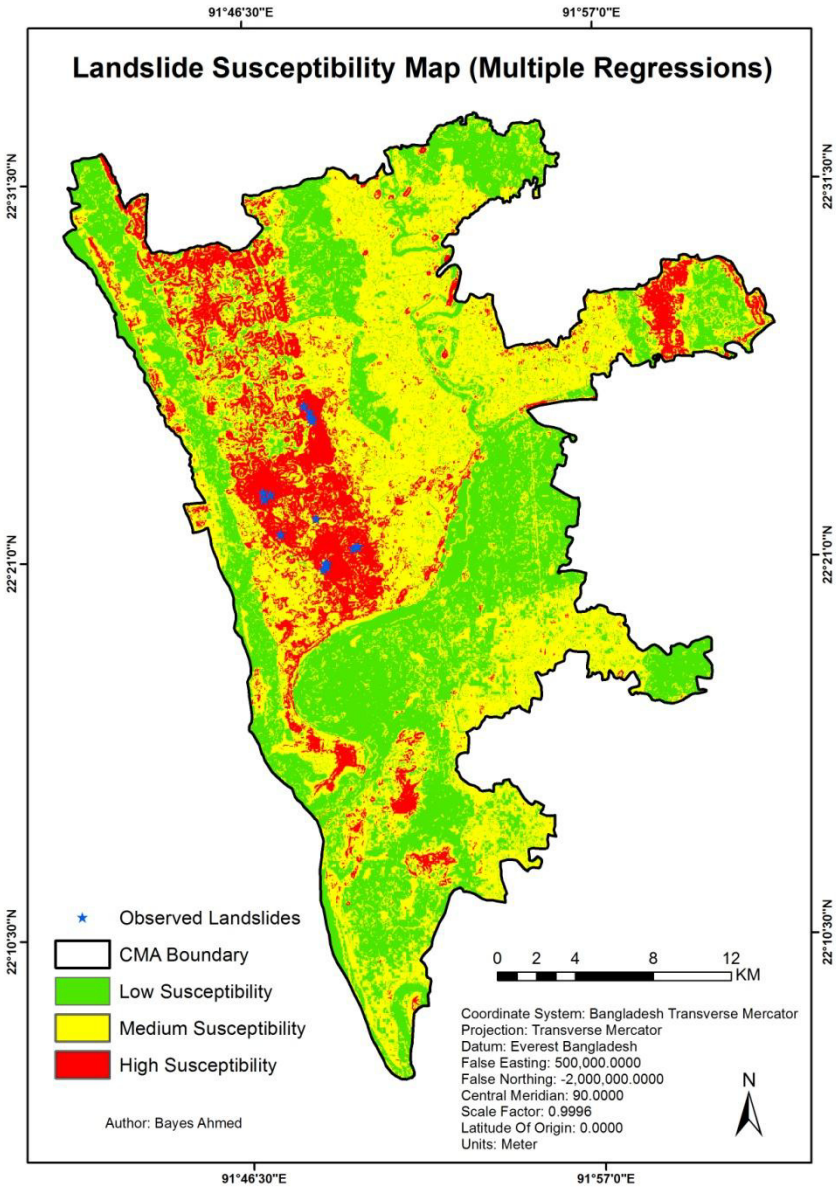

Figure 4.5. Landslide susceptibility map derived from MR model

The ROC module offers a statistical analysis that answers one important question: "How well is the category of interest concentrated at the locations of relatively high suitability for that category?" The answer to this question allows the scientist to answer the general question, "How well do the pair of maps agree in terms of the location of cells in a category?" while not being forced to answer the question "How well do the pair of maps agree in terms of the quantity of cells in each category?" Thus the ROC analysis is useful for cases in which the scientist wants to see how well the suitability map portrays the location of a particular category but does not have an estimate of the quantity of the category [51].

ROC is a summary statistic derived from several two-by-two contingency tables (Table 4.2), based on a comparison of the simulated image with the reference image. Each table corresponds to a different threshold in the suitability map [57,61].

Table 4.2. Contingency table for ROC

		Reference Image	
		In class of interest (1)	Not in class of interest (0)
Simulated Image	In class of interest (within threshold)	A (true positive)	B (false positive)
	Not in class of interest (not within threshold)	C (false negative)	D (true negative)

The true positive % value is derived from A/(A+C) while the false positive % value is derived from B/(B+D), where A, B, C, D are pixel counts in the contingency table for each threshold [57,61].

Figure 4.6 shows the ROC graph for three input images. A point for each threshold is plotted with the percentage of true positives on the vertical axis and the percentage of false positives on the horizontal axis [51,57,61].

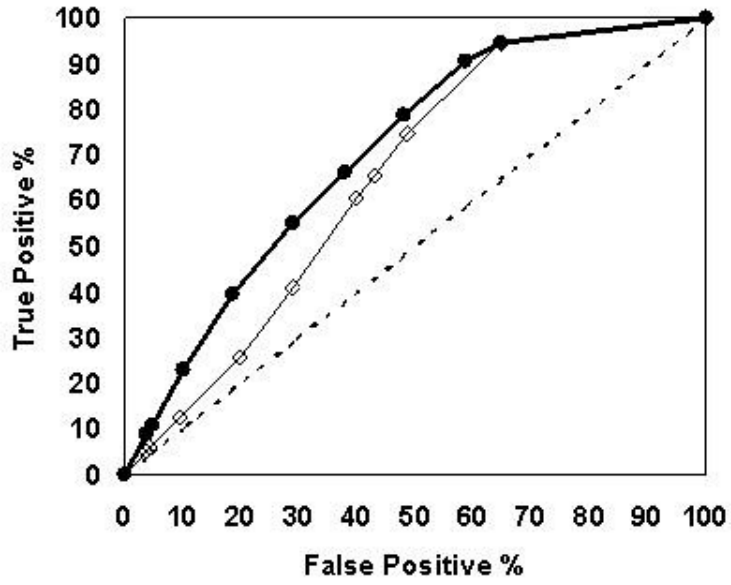

Figure 4.6. ROC graph for three input images [51]

The ROC statistic is the area under the curve that connects the plotted points. IDRISI uses the trapezoidal rule from integral calculus to compute the area, where x_i is the rate of false positives for threshold i, y_i is the rate of true positives for threshold i, and n+1 is the number of thresholds [57,61].

$$AreaUnderCurve = \sum_{i=1}^{n} [x_{i+1} - X_i] \times [y_i + (y_{i+1} - y_i)/2]$$

The dashed diagonal line derives (Figure 4.6) from an input image in which the locations of the image values were assigned at random (AUC=0.50). The other two lines derive from different models. The model that produced the thin line with open squares (AUC=0.65) is shown to be performing more poorly than the model that produced the thin line with closed circles (AUC=0.70).

4.4.1. Comparison of Models

To assess the spatial effectiveness of the susceptibility maps using ROC curves were also constructed in this research. The landslide-susceptibility analysis results were verified using the landslide location sites for CMA. The verification method was then performed by comparing the landslide test data and landslide-susceptibility analysis results for each of the models. Two basic assumptions are then needed to verify the landslide susceptibility calculation methods. One is that landslides are related to spatial information, such as topography, land cover, soil, and geology; the other is that future landslides will be precipitated by a specific impact factor, such as rainfall [62]. In this research, both the two assumptions were satisfied because the landslides were shown to be related to the spatial information (Figure 4.7), and the landslides were precipitated by heavy rainfall (Figure 4.8).

The area under ROC curves (AUC) constitutes one of the most common used accuracy statistics for the prediction models in natural hazard assessments [63]. The minimum value of AUC is 0.5 means no improvement over random assignment while the maximum value of that is 1 denotes perfect discrimination [64]. The comparison results are shown in Figure 4.7 as a line graph (threshold type is equal interval and number of thresholds is 25%). The AUC values are indicating the accuracy of the models for landslide prediction. The WLC_1, WLC_2, WLC_3, LR and MR models had AUC values of 0.839, 0.911, 0.885, 0.767 and 0.967, respectively. Generally, the verification results showed satisfactory agreement between the susceptibility map and the existing data on the landslide location (AUC values from 0.767-0.967). The MR model fits best for this research area (Figure 4.7).

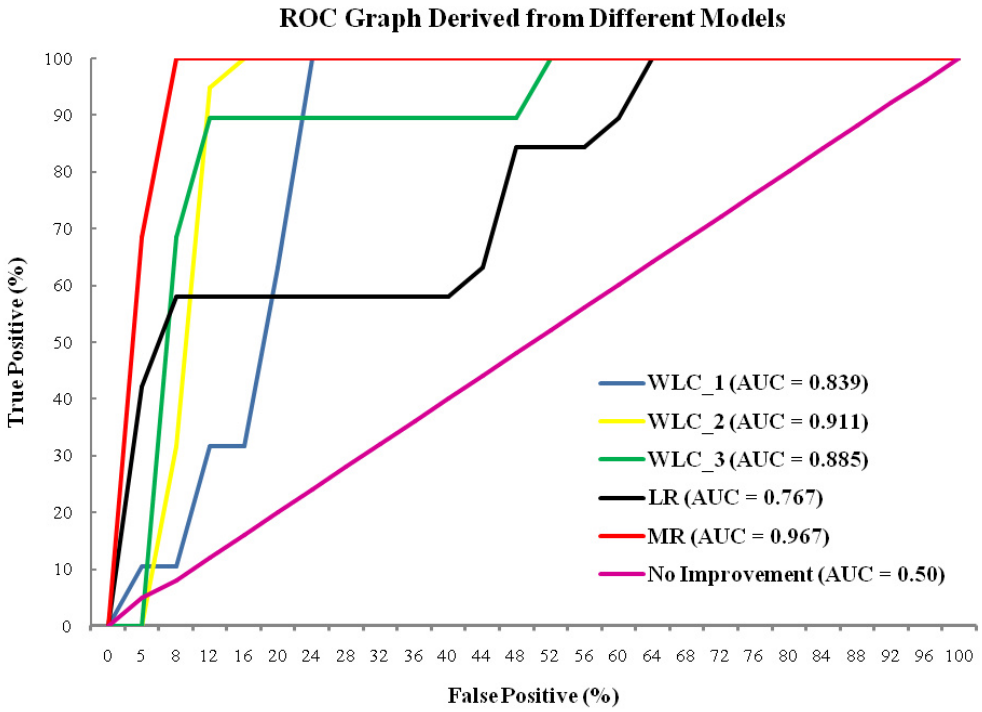

Figure 4.7. Assessment of the model performance based on the ROC curves

The detailed statistics of the ROC results for all the models are attached in Appendix VI. Moreover it has already been stated that, due to climate change, Chittagong City is experiencing high intensity of rainfall in recent years which is making the landslide situation worse. Existing evidences to date also justify the above argument because of a gradual upward shift in precipitation has been noted for the last five decades (1960-2010), with an abrupt fluctuation in the mean annual precipitation levels (Figure 4.8).

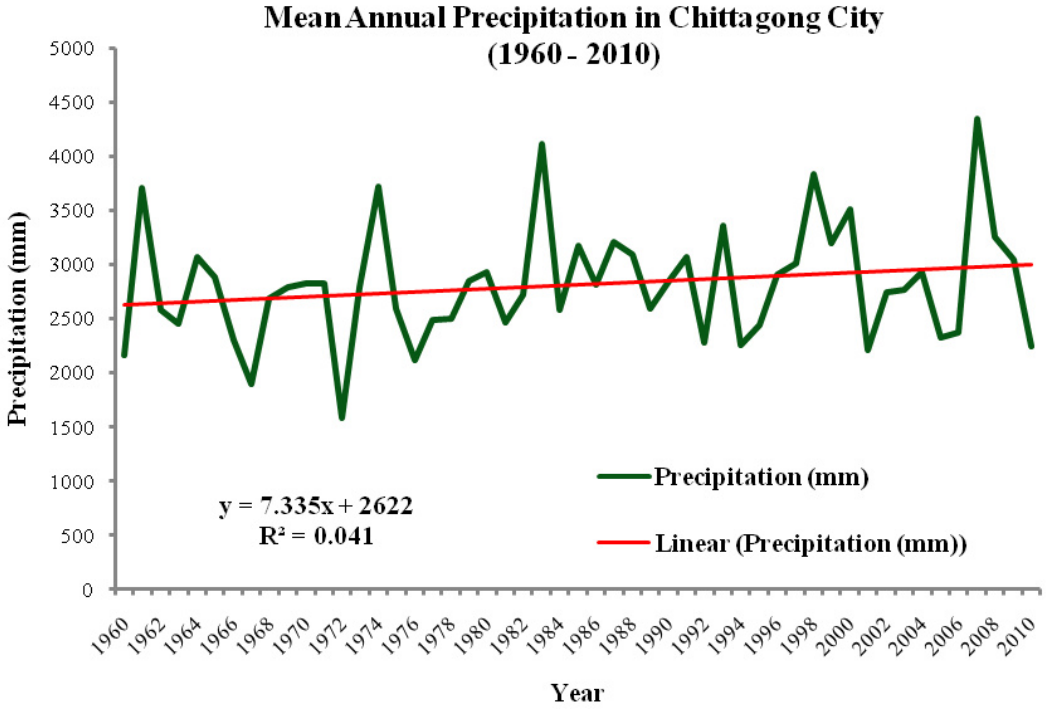

Figure 4.8. Annual rainfall patter in Chittagong City from 1960-2010

Chapter 5

GEOTECHNICAL ISSUES

5.1. Geotechnical Causes of Landslides

Many approaches for classifying landslide have been introduced by many resource persons and institutions. Almost all the soils are clayey in test samples. Amount of clay in any type of soil has a strong contribution in landslide occurrence. The greater the amount of clay in soil the lesser the drainage means soil cannot drain out water properly. Therefore the remaining water in clayey soils increase pore water pressure by losing effective strength and finally trigger landslides**.** Shear strength of soil is a function of different parameters like natural water content, ground water level, cohesion, particle size, Atterberg indexes, permeability etc. In this paper only those parameters have been considered whose are responsible for water triggering landslides. As different parameters of soil are responsible for landslide so a brief of its type, strength and component has been described here.

5.2. Soil

5.2.1. Definition

Soil is an important element of earth without which we can't think our existence in the world. From the inception of the earth different types of soil has furnished the world with many shapes. This clearly indicates the different types and formation process of soil.

5.2.2. Component of Soil

Atoms Oxygen, Silicon, Hydrogen organized in various crystalline forms along with calcium, sodium, potassium, magnesium, and carbon constitute over 99 percent of the solid mass of soils. It also contains air void and water in small portion.

5.2.3. Types of Soil

If we see around we could find two things which are rock and soil. Rock is considered to be the natural aggregate of mineral grains with strong binding materials (cohesive force) that tied the rock forming elements together. In the other hand soil is the aggregate of minerals with relatively low cohesive force and binding materials among the elements. Upon the presence of organic matter the soils are termed as inorganic or organic soil.

In engineering perspective soils mainly classified in two groups that are coarse grain and fine grain soil. Coarse soils are subdivided into sand and gravel where fine soils are subdivided into clay and silt.

These two basic types of inorganic soils are formed due to the weathering of rock. Coarse grained soil is formed by the physical weathering of rock whereas the fine grained is formed by chemical weathering process. The basic difference of these two types' soils arises because of the variation of size and shape of the soil particles. Smaller fine grained soils are often called cohesive soil as they influenced by physiochemical interactions resulting plastic deformation in different moisture content. Coarse grained soils are cohesion less soils dominated by the physical characteristics of the particles.

The common clay minerals are montmorillonite or smectite, illite, and kaolinite or kaolin. These minerals tend to form in sheet or plate like structures, with length typically ranging between 10−7 m and 4x10−6 m and thickness typically ranging between 10−9 m and 2x10−6 m, and they have a relatively large specific surface area. The specific surface area (SSA) is defined as the ratio of the surface area of particles to the mass of the particles. Clay minerals typically have specific surface areas in the range of 10 to 1,000 square meters per gram of solid. Due to the large surface area available for chemical, electrostatic, and van der Waals interaction, the mechanical behaviour of clay minerals is very sensitive to the amount of pore fluid available and the type and amount of dissolved ions in the pore fluid.

5.2.4. Strength of Soils

Soils are subjected to normal and shear stress in every geotechnical aspects (e.g. - slope stability, foundation engineering, retaining wall, dam, and embankment). Shear strength and stiffness of soils denotes the stability of soils or its deformation due to stress. Soil strengths are the contribution of interlocking angles, frictional resistance, cohesion, minerals as well as type of the soil. Shear strength enables soil to remain its equilibrium when the surface is not horizontal. Therefore knowledge of the strength is necessary to determine if a slope will be stable.

5.2.5. Indicating Parameters of Soil Strength

It is important to know the strength of soil prior to any modification or development of the soil. Various tests are being performed to know the strength of soils. In this research different

index values found by the Atterberg limit test (i.e. - Plasticity Index, Flow Index, Liquidity Index, Linear Shrinkage etc.) and sieve analysis have been used to determine the strength as well as types of soils. As the strength of soils greatly depends on its types, soil classification has been done in three different ways as stated hereafter.

5.2.6. Soil Classification

As the natural soils are infinitely varied several systems of classification have been developed both have certain advantages and disadvantages depending on purpose. For determining slope stability and the types of soil sample collected from the vulnerable hillside AASHTO (developed by American Association of State Highway and Transportation Officials) and Unified Soil Classification System (USCS) have been used. Grain size analysis and Atterberg limit test have also been performed to find the different terms of AASHTO and USCS system. Both coarse and fine particles in the soil sample collected, from different sites where landslide occurred or like to occur, for sieve and hydrometer analysis have been performed. ASTM C136-06 code has been followed in this gradation test.

Following the presence of different sizes of particles soil maybe classified in two types that are well graded and poorly graded soils (Table 5.1).

Table 5.1. Soil classification scheme

Liquid Limit	Plastic Limit	Soil Type
25-40	20-30	Silt Clay Mixture
40-70	20-40	Kaolinite Clay
300-600	100-200	Montmorillonite Clay

Well Graded: This types soils contain all sizes particles ranging from 4.75mm to 0.075mm diameter. As the soil has a good representation of all sizes particles the soil shows more strength than poorly and gap graded as it has enough interlocking capacities and low drainage probability.

Poorly Graded: This soils doesn't have good representation of all sizes of particles ranging from 4.75mm to 0.075mm diameter. Poorly graded soils maybe uniformly graded or gap graded.

The soils that have most of its particles are in same sizes which decrease the interlocking efficiency resulting bad quality of soil. The gap graded soil is the representation of that group of soil where a certain sizes particles are absent.

Soil Consistency: Soil consistency indicates the degree and variety of cohesion and adhesion between the moisture and soils also the rough estimation of rupture or deformation of soil due to change in moisture content. Slope failures are greatly dependent on soil consistency and Atterberg parameters help to understand the degree of consistency of soils.

5.2.7. Landslides Triggering Factors

Ground water is a very important factor that causes landslide. Rising ground water table and increasing water pressure greatly contribute to the landslide as most of the landslides cause in rainy season. Pour water pressures become very high when soils absorb much water in rainy season decreasing effective strength by losing internal friction. Water itself is not a lubricant of landslide but it made clayey soils lubricant by taking the soils in saturated state. Volume expansion or swelling occurs when water content of soils change. One or two percent increase in water content may cause severe swelling by decreasing shear strength of clayey soil. The greater the swelling tendency the smaller the shearing strength hence the more the landslides risk. In this paper contribution of water in triggering landslide has been broadly discussed with some solutions. For better understanding some sources of soil water with some examples of that water triggered landslides outside Bangladesh is described.

5.2.8. Sources of Input Water

Sources of soil water are very important in analyzing the water induced landslides. Here many water resources, their affect in landslides and some worldwide examples of water aided landslides are discussed.

Rainstorms: High rainfalls from individual storms cause numerous shallow slides where high water pressures can rapidly reach slip surfaces. Hundreds of slides in Jordan, in early 1992, due to rare heavy snowfall and rapid melt in a normally semi-desert terrain; soils, rocks and fills all equally affected. Destructive 1988 slide at Catak, Turkey, failed during the first period of high rainfall since road widening had steepened the slope four years previously. Shallow earth slides and debris flows are annual events during rainstorms on steep slopes of the shanty town favellas in Rio de Janeiro.

Rainfall seasons: Deep-seated slides are more affected by annual fluctuations of water table. Winter groundwater maxima create a landslide season lasting from November to March in Britain. Monsoons trigger most of the landslides in South East Asia. Spring snowmelt is the main factor in alpine regions, after slopes have been stable during winter freeze. Numerous sets of data show correlation between rainfall and slide movement; mostly on small scale with rapid response or on large scale with response delayed 1–10 weeks.

Artificial inputs: Impounding water in a reservoir raises regional water tables. De-vegetation of a slope allows increased infiltration. Irrigation of farmland or gardens has caused many terrace edge failures in dry regions such as California.

5.2.9. Landslides Distributions

Bangladesh is the most landslides vulnerable of all the South Asian countries because of its formation and geographic location. In 2010 landslides almost 29% of total landslides induced death toll in South Asia was in Bangladesh (Figure 5.1 and Table 5.2).

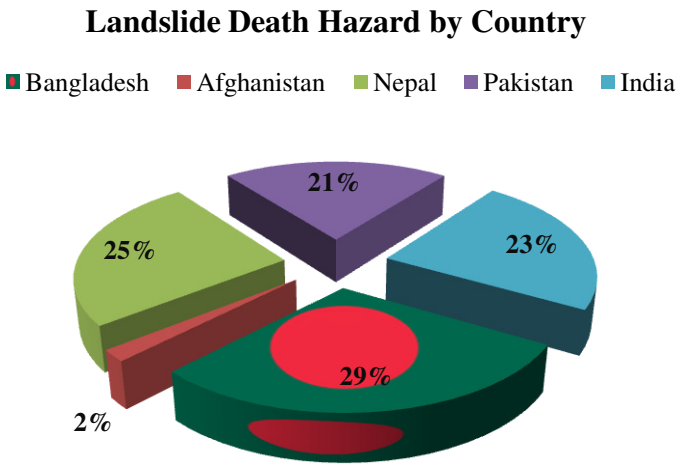

Figure 5.1. People killed by landslides in South Asia, 2010

Table 5.2. Damages caused by landslides in South Asia in 2010

Country	Death	Injuries	Missing
Afghanistan	4	6	-
Bangladesh	62	27	12
India	59	14	6
Nepal	54	16	19
Pakistan	44	16	-

Source: Media report, BBC, CNN

5.2.10. General Causative Factors of Landslides

Rainfall: From statistics it has been found that most of the landslide occurred during the rainy season which indicates the strong relation between landslide and rainfall. In one single event in 2011, about 90 people were killed by landslide triggered by heavy rainfall in port city Chittagong. In rainy season people living beside hill pass their every moment in anxiety.

Many researchers have published many research papers where they showed strong relationship between landslide and rainfall. Neil Caine of Institute of Arctic and Alpine Research, University of Colorado, USA, mentioned the relation between rainfall and landslide in 1980 by the following equation:

$I = 14.83 * D^{-0.39}$

Where I = Rainfall intensity in mm/hr

D = Duration of rainfall in hours

We can estimate the threshold rainfall intensity for 24 hours that can create landslide. Landslide occurs for duration of less than 12 hours at 6mm/hr intensity but the rainfall continues for more than 100 hours then 2mm/hr intensity is enough to cause landslide. If precipitation continued for 1 month then 1mm/hr precipitation intensity is more than enough for triggering landslide in that condition landslide may occur anytime at any intensity [58].

Earthquake: Frequent earthquake impart shearing stress also reduce the resistance of slope materials hence slopes become unstable. The greater the steepness of slopes is the greater the degree of amplifications of intensity of earthquake. As Chittagong lies in the low seismic danger zone it doesn't have great influence in Chittagong landslide.

Water Level Change: When water level falls drastically then the pore water pressure dissipates imparting instability of slope. Detailed analysis of this term is presented in the case study pages.

Artificial Reasons: These include-

- Changing landcover
- Agricultural practice on steep slope
- Housing
- Water reservoir which increase pore water pressure decreasing effective pressure of soil

- Road construction aside the hill
- Soil collection from hill
- Converting hillside into recreational site

5.3. Soil-Water Interactions in Causing Landslides

5.3.1. Atterberg Limit

It is obvious that rain is the main trigger of landslide hence it can be stated that behaviour of soils are greatly depend on water content in it. Atterberg (Swedish soil scientist in the early 1990's) first identified that a gradual decrease in water content of clay soil slurry causes the soil to pass through four states of consistency. These are liquid, plastic, semi-solid and solid.

Liquid State: When fine grained soils exist in liquid condition then the soils would flow on its weight.

Plastic State: Plastic state is a condition at which soils can be remoulded without making any crack.

Semi-Solid State: At this stage the soils can be remoulded with the development of crack.

Solid State: At this stage the soils can't be remoulded at any cost, if done then crack would form suddenly.

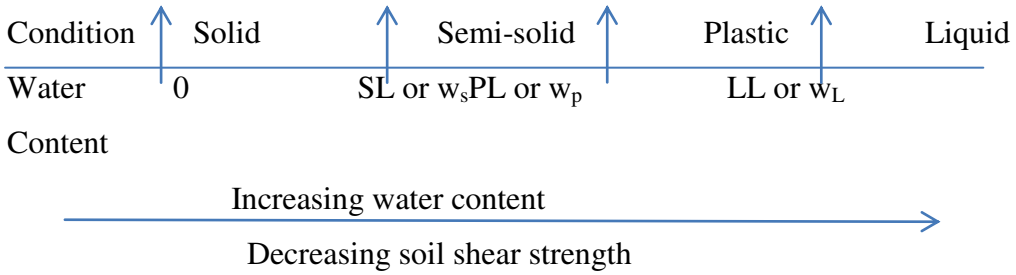

5.3.2. Shear Strength of Soil

The resistance to the deformation or failure of soil at the state of non-equilibrium plane is called shear strength of soil. Shear strength of soil greatly depend upon the state consolidation. Over consolidated soil shows high shear strength than unconsolidated soil. Liquidity Index demonstrates the consolidation state of clay soil though there is no empirical formula for the relationship. Consolidation state of clayey soil can be estimated from Liquidity Index by equation $Su = e^{(0.026-1.21IL)}$. Soils in liquid state have no shear strength

whereas in solid state it has some shear strength to maintain its equilibrium in inclined surface. Shear force in soils greatly come from the cohesion which is indicated by the term consistency. Table 5.3 shows soil consistency according to soil types with vulnerability to the landslides. Stiffness of soils increased with cohesion hence imparting high shear strength and has very less vulnerability to landslides.

Table 5.3. Soil Consistency BSI 1975

Un-drained Shear Strength (kPa)	Soil Condition	Vulnerability to Landslide
>150	Very stiff soil	Very less vulnerable
75-150	Stiff	Less vulnerable
40-75	Firm	Vulnerable
20-40	Soft	Highly vulnerable
<20	Very Soft	Still in danger

5.4. Laboratory Test Analysis

Soil samples were collected from different hills where landslides occurred, yet to occur and seem to occur very soon to analyse different properties of soil related to shear strength. Atterberg limit test has been done by remoulded clayey soil that collected from 2-4 meter depth of different locations. Slopes consist with high strength soil are very stable even in steep state but become start losing shear strength with the change of moisture in soil.

In total 17 soil samples have been tested in laboratory for observing the correlation between water, strength and soil composition. There might be some small error due to difficulty in sample collection, rain before digging for sample, long transportation and also not very good facilities in laboratory. Despite these drawbacks it seems the result is good enough to meet the experimental objectives. The sample soil test method and data calculation procedures for two sites (Motijharna and Foys Lake Hill) are attached in Appendix-VII.

In total 7 soil parameters of the soil samples was tested. The detail results are in Table 5.4.

Table 5.4. Results of soil tests

Sl. No.	Site	LL	PL	NWC	LS	FI	PI	LI	Comment
1	Tigerpass wall	42.39	21.45	28.75	9.73	11.67	20.94	0.35	Two very devastating landslides
2	Motijharna	50.25	23.56	32.53	12.14	10.94	26.69	0.34	Landslides occur almost every year
3	Batali Hill	39.91	19.64	30	9.28	13.75	20.26	0.314	Very alarming condition because of frequent landslides
4	Foys Lake Railway Society	38.23	21.05	26.25	8.06	9.12	17.18	0.30	Landslides happened two times in last 20years Now the hill is cut to make a housing area by Railway Authority
5	Akber Shah Majar Hill	44.24	23.07	28.15	9.78	11.32	21.17	0.24	Very Devastating landslides
6	Red Hill AS Majar	45.76	22.43	28.74	10.75	14.58	23.33	0.27	Frequent landslides, still vulnerable
7	South Khulshi	38.23	19.45	23.45	8.85	8.49	18.78	0.22	No devastating landslide yet
8	Foys Lake Zoo Hill	41.89	19.85	24.92	10.29	14.79	22.04	0.23	No landslides yet but vulnerable
10	CU Campus	38.56	18.79	23.68	9.20	12.66	19.77	0.25	Only one landslide till now
15	BFRI Rest House Hill	36.96	19.07	23.12	8.47	7.87	17.89	0.21	No landslide yet but vulnerable
16	Jharna Hill	46.45	23.02	31	10.65	15.63	23.43	0.34	Very tragic landslides
17	AK Khan Hill Panchlaish	39.67	20.48	27.5	8.93	14.92	19.19	0.36	Vulnerable but now AK Khan company going to construct a hotel by cutting the hill

Description of Table 5.4: Liquid limit of the samples were found in between 38.23 and 50.25. Plastic limit are in between 18.79 and 23.56. Therefore it can be said that almost all the soils are with very small quantity consolidated sand, kaolinite clay, shales of the DupiTila Formation. The soils were yellow to brown and slightly acidic. From the dispersion test about 5-11% sand, 28-32% silt, 49-54% clay and 2-3% organic matter were found in the soil samples. The soil has 49% porosity and 1.31 gm./cc bulk density. Based upon the evaluations for extrusion pressures corresponding to plastic and liquid limits, which are 2000 kPa and 20

kPa, respectively, it can be asserted that the shear strength at plastic limit is about 100 times the shear strength at liquid limit. For better understanding of Table 5.4, let's consider two locations Motijharna where many people died by landslides and BFRI Hill where yet to occur any landslide.

5.4.1. Liquid Limit (LL or W_L)

The liquid limit is the amount of water (amount, in percent of soil) at which soil changes to liquid from plastic behaviour. A large liquid limit indicates high compressibility and high shrinks swell tendencies (Table 5.5). Clays over the range of 30-200% indicates that the range of un-drained shear strength at liquid limit is from 1.3 to 2.4 kPa with an average value of 1.7 kPa. Also, it is the minimum water content at which soil mass is still in liquid state but has enough shearing strength to prevent flowing.

Table 5.5. Range of liquid limit

Liquid Limit	<39	39-50	50-63	>63
Swelling Potential	Low	Medium	High	Very High
Soil Quality	Very Good	Good	Bad	Very Bad Soil

Soils in liquid state have no shear strength whereas in solid state it has some shear strength to maintain its equilibrium in inclined surface. Shear force in soils greatly come from the cohesion which is indicated by the term consistency. So when soil reaches to its liquid limit then all the particles become segregated by breaking their cohesion bond also lose all the shear strength. When by absorbing water soil become liquid by going its liquid limit then it can't sustain even self-weight because of this slope collapse down.

A large liquid limit indicates high compressibility of soil also high swelling and shrinking capacities. As because of high compressibility the soil changes its volume rapidly by absorbing or expelling water which lessen shear strength of soil. Therefore high liquid limit soil is very vulnerable to rain triggered landslides. Soil sample of Motijhorna has a liquid limit 50.25 where BFRI Hill has 36.96; it means the soil of Motijharna is very compressible also highly swelling potential than the soil of BFRI Hill.

5.4.2. Flow Index (FI)

Flow Index indicates the loss of shear strength of soil with the increasing water content. Soil with high FI is very vulnerable to landslide as its shear strength changes very rapidly with water content. The lower the Flow Index the less chance to occur landslide as its shear strength decrease slowly with increasing of water. FI=6 has better shear strength as a function of water than FI=10 (Figure 5.2).

Figure 5.2. Flow curve the soil Sample from Batali Hill

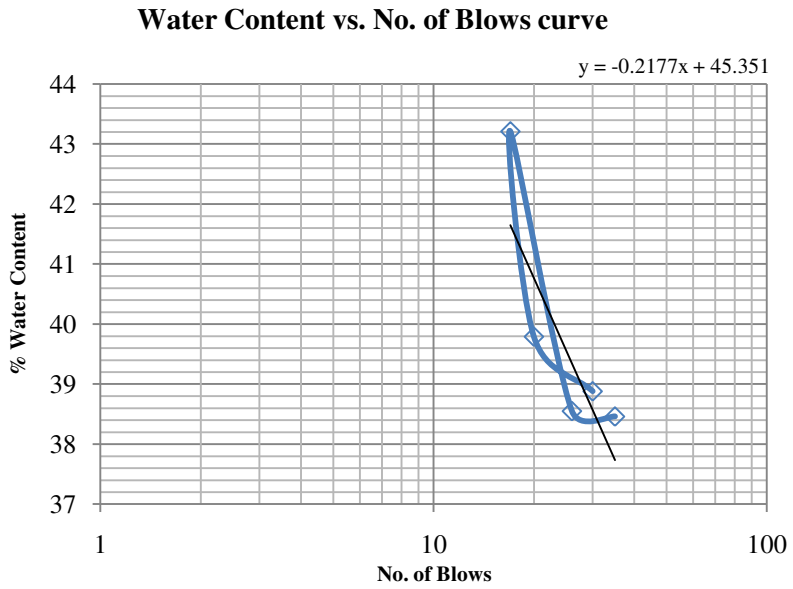

N.B.: Slope of the line denotes Flow Index

The Flow index of Motijharna soil is 10.94 which mean that for one percent increase of water content shear strength of the soil decrease by 10.94. The same index were found for the BFRI Hill 7.87 which is lower than 10.94 that means soil of BFRI hill loose shear strength in a lower rate than the soil of Motijharna as a function of water content. So for the same soil type, precipitation others factor remaining same there is not yet any landslide in BFRI hill though there is frequent landslide in Motijharna. Therefore the higher flow index indicates the low strength of soil hence very vulnerable to landslides.

5.4.3. Plastic Limit (PL or W_p) and Plasticity Index (PI)

The plastic limit is the threshold point at which soil begins to behave as a plastic material. At plastic limit the soil must gain some minimum strength. According to Skempton and Northey (1953) the shear strength at plastic limit is about 100 times that at liquid limit. We may expect 170 kPa shear strength as the requisite strength of the soil at plastic limit.

Plasticity Index is an indication of plasticity of soils. Plasticity Index greater than 20 indicates high plastic soil, 10-20 indicates medium plastic and less than 10 indicates non-plastic soils. It is known that high percentage of clay exhibit high plastic properties. Plasticity Index also a measure of the range of water content for which it remains plastic. Table 5.6 shows the quality of soil based on the vulnerability to landslides.

Table 5.6. Plasticity index indicators

Plasticity Index	<18	15-28	28-47	>47
Swelling Potential	Low	Medium	High	Very High
Soil Quality	Very Good	Good	Bad Soil	Very bad soil

Almost all the samples show the plasticity index greater than 20, so all the hills are composed with high plastic soil that is high percentage of clay. Let's consider these two locations for the Plasticity Index. Plasticity Index of Motijharna is 26.69 and BFRI hill is 17.89 which means that soil of Motijharna is highly plastic. By comparing these values with table- it is clear that soil of Motijharna has high swelling potential than BFRI hill. So the soil of Motijharna would change its volume rapidly by absorbing water reducing shearing strength of soil hence occurring landslide. This is another reason of why landslide occurred in Motijharna but not in BFRI Hill.

5.4.4. Shrinkage Limit (SL or W_s) and Linear Shrinkage

The shrinkage limit is the smallest water content below which a soil sample will not reduce its volume anyway. It indicates the maximum amount of water that could be injected without changing the volume (Table 5.7). It is known that amount of water decrease with the volume from liquid limit to the shrinkage limit resulting increase in the shear strength of soils.

Table 5.7. Shrinkage limit range

Shrinkage Limit	>15	10-16	7-12	<11
Linear Shrinkage	0-4	4-7	7-9	>9
Welling Potential	Low	Medium	High	Very High
Soil Quality	Very Good	Good	Bad	Very Bad

The higher the value of Linear Shrinkage (LS) is the more swelling potential of that soil. Soil with high swelling potential has very low shear strength compared to others. Table 5.7 shows that soil with LS greater than 8 has very high swelling potential that means the soil absorb or

spell out water very rapidly by changing volume. In all the soil samples we found every LS greater than 8 but Motijharna has very high Linear Shrinkage (12.14) than the Linear Shrinkage of BFRI Hill soil (8.47). One or two percent increase in moisture content may cause severe swelling by decreasing shear strength of clayey soil. The greater the swelling tendency the smaller the shearing strength hence the more the landslides risk.

5.4.5. Liquidity Index

Liquidity Index is more reliable than the liquid or plastic limit to characterize the soil strength (Table 5.8). Liquidity Index, LI = $(W_n-W_p)/PI$. From the liquidity index equation it is clear that when the soil absorbed water fully and reaches its liquid limit then the liquidity index becomes 1. Liquidity index 1 the corresponds undrained shear strength is 1.5 kPa (Figure 5.3) which is not enough to remain its equilibrium in any case hence just after or before reaching liquid limit the soils collapsed for maintaining equilibrium. This is happened during long time rainfall.

Table 5.8. Liquidity index indicators

Liquidity Index (LI)	Consolidation State	Landslide Vulnerability
Below -0.2	Highly Over consolidated	Low
-0.2 to 0.5	Over Consolidated	Medium
0.5 to 1.2	Normally Consolidated	High
Above 1.2	Sensitive Soil	Very High

Figure 5.3. Liquidity index against un-drained shear strength of soil graph

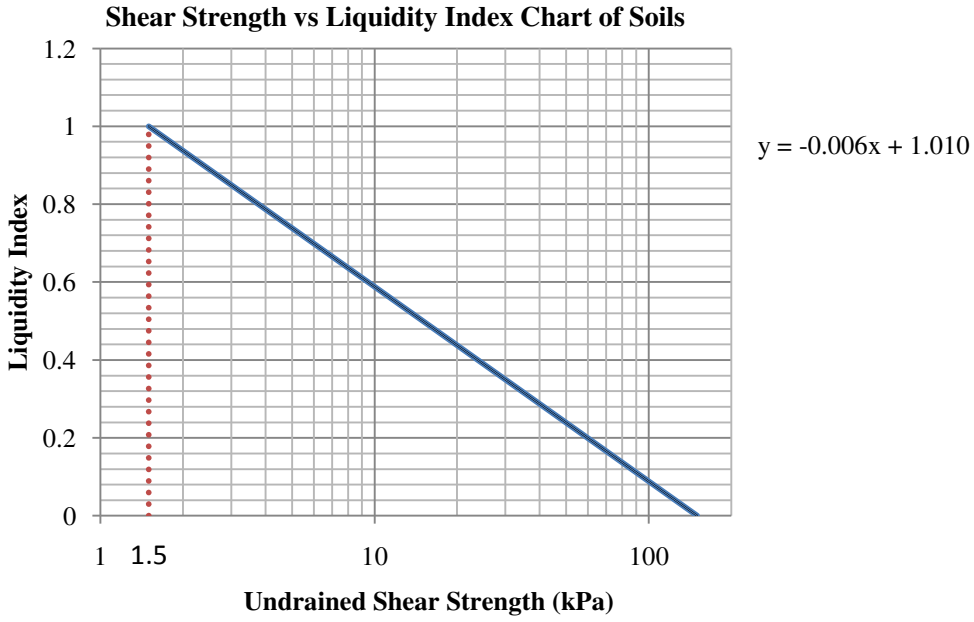

If LI is 1 then the soil in its liquid limit with un-drained shear strength of 1.5kPa and if the value of LI becomes zero then the soil is said to be in its plastic limit with un-drained shear strength of 150kPa. Most soil deposits show the liquidity index in between 0 to 1. Liquidity Index provides a reliable indication of the degrees of consolidation of clayey soils. IL is zero for over consolidated soil and IL is negative for highly over consolidated soil.

From Table 5.4 it is found that Liquidity Index of Motijhorna soil is 0.34 and for BFRI hill the index value is 0.21. This means soil of Motijharna has lower shear strength than soil of BFRI hill. For the same intensity precipitation the soil of Motijhorna would reach to its liquid limit very faster than the soil of BFRI Hill. This is another reason for the landslide in Motijhorna than the BFRI Hill.

5.5. Causes of Water Induced Landslides from Experiment

From the experiment with the soils that collected from landslides prone areas, several causes for water induced landslides have been identified as the description stated above. Hills composed of the soils that have following properties are very vulnerable to landslide in moderate long precipitation in rainy season.

1. High Liquidity
2. High Flow Index
3. High Plasticity Index
4. High percentage of clay
5. High Liquidity Index
6. High Liner Shrinkage
7. Soil surface directly expose to air
8. High Ground Water Level
9. Low drainage capacity of soil
10. Disturbed soil
11. Soil Particle Size Distribution

5.6. Some Engineering and Technological Solutions for Landslides

Now in Bangladesh the only technology which is used to stable slope is Retaining wall. Constructing and maintaining retaining wall is very costly also recent failures of retaining wall prove its insufficiency in withstanding soil pressure. Therefore we need to explore new affordable and sustainable technology to stable hill slopes.

5.6.1. Landslides Susceptibility Maps

From above discussion it is clear that soil properties have much more effect in causing landslides than other parameters like land cover and surroundings. Therefore landslide susceptibility maps should be prepared in such a way that the maps include all the geotechnical parameters with the physical parameters of the landslide vulnerable areas. While identifying and categorizing landslide prone areas these parameters might help to identify more correctly and precisely.

5.6.2. Wire Mesh

Figure 5.4. Roadside Slope Stabilization by wire mesh (Source: ROTEC Intl, USA)

In unstable slope wire mesh covering is a sustainable solution for landslide risk. Wire mesh stabilize risky slope by imparting shear strength in the soils. This would be very useful for protecting road networks passing through the hill in hilly region from landslide destructions. Many countries have already been started this technology to stabilize roadside slope which could protect huge landslides brought damages. Depending on landslide susceptibility maps produces base on soil properties different sizes wire net would be designed by civil engineer.

5.6.3. Earth Retaining Wall

Earth retaining wall can make stable the unstable slope only if it is designed and constructed in proper way. Defects in design and construction may induce huge damages than to stable slope. In 2007 about 90 were killed by falling earth retaining wall on some houses in Chittagong where the wall made to retain the hilly road at Batali Hill (Figure 5.5 and Figure 5.6).

Figure 5.5. Retaining wall

Figure 5.6. Retaining wall failure

Source: Field Visit, March, 2013

Retaining walls (Figure 5.5 and Figure 5.6) were constructed in Chittagong to protect the road that was constructed through the Batali Hill. Some people intended to construct some shops on the wall that's why engineers designed the wall in like small wall foundation keeping great hole inside the square wall. They didn't keep enough drainage facility to allow the foundation to drain the rain water out. When high precipitation had happened then huge amount of water accumulated in the hole of structures after making the soil completely saturated. Then the walls collapsed on nearby houses as the walls couldn't sustain saturated soils weight, extra water weight and its self-weight. About 90 people were killed in the wall failure due to poor design and construction of retaining wall.

5.6.4. Soil Reinforcing

Soil can take only compression not the tension so when tension comes from self-weight then it falls down which is termed as landslide. By adding some grasses, fibres and lignin strength of soil can easily be increased to withstand soil self weight which causes landslides. A team headed by Professor Dr. Abdul Jabbar Khan of Bangladesh University of Engineering and

Technology has been trying to use local Jute fibre in reinforcing unstable soils to make them strength reducing landslides vulnerability. The team has gone so far and likely to publish their report very soon. The process would be very easy and economically feasible as the fibres are locally produced and cheap.

5.6.5. Tree Plantation and Vegetation

Land cover type has a great effect on landslides as infiltration is a function of soil type and land use type. Hill soil directly exposed to rain has high infiltration rate because of low surface run off. Exposed soil get saturated by water earlier than the soil covered with plants. Also roots of trees reinforced soil increasing shear strength. So vegetation and planting more trees in landslides prone hills are the sustainable solutions.

5.6.6. Geotechnical Properties based Landslides Warning System

In developed countries peizometric warning is being used to get a probability of landslide for a certain precipitation. In USA Emergency Alert System (EAS) is established to alert the vulnerable people in any emergency case. Existing landslide early alert system is based on precipitation rate considering the existing water level of soil. If precipitation for a certain period exceeds the limit then a signal is sent to the central server then the signal dissipated to the government emergency departments concerning disasters to taka necessary initiatives. Installation and maintenance of the system is costly also very lengthy. People living in vulnerable areas don't get the instant alarm to go to safe places. As the system is costly developing countries government have some limitations to install the alarming system. Considering these drawbacks we propose an economically feasible, user friendly and effective alarming system.

Considering every possible causes and parameters that trigger landslides a model would be formed for different landslides prone areas. From the model equation required precipitation to reach the soils liquid limit would be measured. Simple and low cost rainfall measure instrument would be installed in every vulnerable area which would also be connected with a local siren to alert local people. When rainfall pot will be poured to the calibrated water mark then the siren would sound to alert people for moving into safe place. Geotechnical properties based Landslide susceptibility maps can help the stakeholders to establish a landslide early warning system.

The outreach activities are described in Appendix-VIII.

Chapter 6

RECOMMENDATIONS AND CONCLUSION

In general, the term 'Natural Disaster' refers to extreme natural events like tsunami, earthquakes, landslides, floods etc. But it has been argued that these events are not disasters until a vulnerable group of people is exposed [65]. At this drawback, it is important to understand the main reasons for this progression of urban landslide vulnerability in Chittagong Metropolitan Area (CMA). Moreover, even being aware of the landslide risks people are living in those areas. This situation needs to be analysed.

As discussed earlier, the highly urbanized hilly city like CMA is experiencing more and more rainfall-induced fatal landslides (RFLs) in recent years. Moreover, the rate of urbanization and population growth is also increasing quite evidently in these areas. In this situation it is important to reveal the consequences of landslides in those affected areas. Some major consequences can be as follows:

a) Loss of life and property
b) Economic instability
c) Lower living standard
d) Degraded social norms and values
e) Political unrest
f) Declining community feelings
g) Fear of becoming landless or losing a job
h) Change in economic activities
i) Environmental threats

Therefore, based on the predicted landslide vulnerable zones and its relations with the geotechnical issues, some recommendations and ideas for future research are demonstrated.

6.1. Recommendations

6.1.1. To understand human adaptation to landslide risks under the condition of rapid urbanization in a fast growing city like CMA.

To achieve this goal, it is important to know-

a) Why and how long people are living in this area?

b) Why they do not want to leave this risky place?
c) What will be the consequences of leaving this place?
d) What steps the local people are taking to stay here for longer?
e) What are the possible threats or risks living here?
f) How these areas can be planned in a proper way incorporating sustainable development strategies?

Filed level questionnaire survey can be carried out in this case. Different questionnaires should be produced to conduct the survey- the inhabitants living in risky zones, the local community or committee, local political groups, expert opinion survey and concerned institution or organizations.

6.1.2. To understand the processes and mechanism of landslides in CMA.

The followings steps can be performed to achieve this objective:

i. Landslide classification (using different available schemes)
ii. Landslide dimensions (different widths and lengths)
iii. Landslides activity and its distribution (advancing, enlarging, moving, widening etc)
iv. Rate of movement of landslides (extremely slow to extremely rapid)
v. Potential causes of landslides (geological, morphological, physical, human induced etc)
vi. Landslide triggering mechanism (excessive rain, water level change, earthquake, human activities)
vii. Factors influencing slope stability (gradient, slope geometry, stress, vegetation, disturbance etc)

Extensive filed surveying and soil testing is recommended be perform for this section.

6.1.3. To develop a Web-GIS based dynamic model to warn the people in landslide vulnerable zones.

After knowing how people are living with landslide risks, the mechanisms of landslides and producing the predictive vulnerability maps (as done in this research); it is possible to

create a model. This model will be a kind of early warning system. Web-GIS techniques can be used to create suck kind of model.

This model will be dynamic. It means the vulnerable zones of a certain area will be changed based on the intensity of rainfall. It is known that the bearing capacity of different types of soil changes due to different amount of rainfall. The climatic condition of the coming days (at least 7 days) is possible to know through different weather stations data. Moreover, the vulnerable zones are changed due to the change in precipitation level, soil characteristics, geomorphological issues and other relevant control variables. Therefore, by considering the future climatic conditions and its association with the control variables, the model will automatically generate future landslide vulnerable zones. This will be represented through graphical representation (e.g. dynamic susceptibility maps) in a website.

Finally this website will be linked with concerned organizations or institutions (e.g. the Red Crescent, local volunteering groups, local political representatives, Governmental officials and other related NGOs). Whenever a particular section or area turns into vulnerable zone, it will send digital warning (e.g. email, text messages, automatic siren) to the community in risks or all the relevant authorities.

6.1.4. The 'Chittagong Metropolitan Master Plan' was published by the Chittagong Development Authority (CDA) in March 1995. This master plan was gazetted by the Government of Bangladesh on 9 December, 1999. It consists of the Structure Plan (1995-2015), the Urban Development Plan (1995-2005), the Detailed Area Plan, a Drainage Master Plan and a Transportation Plan [14]. But it is unfortunate that the CDA authority is not being able to implement the master plan properly. The master plan will be outdated within 2 years but still there is no sign of revising it. It proves there is lacking in integrating urban planning policies within the city boundary. This issue needs to be solved and implementation of the master plan is mandatory.

6.1.5. Creating awareness among the local people based on the predictive landslide susceptibility maps as prepared in this research, increasing cooperation among different public/private/autonomous/NGOs organizations and generating facilities for proper evacuation system in crisis moment are highly recommended.

6.2. Research Gap and Future Work

Till now, in all cases, the researchers have used the previous or existing land cover images to project/predict the landslide susceptibility maps. But land use/ land cover map can be treated as a dynamic variable. Because within few decades, the land use of a particular area can be abruptly changed (e.g. CMA). This change in land use pattern (e.g. deforestation, hill-cutting) can put positive impacts occurring landslides [44]. Therefore, while modelling landslide hazard maps, it is very important to take into account a new thematic layer-'the future projected land cover map'.

Same thing can happen for the trend in precipitation. It is already indicated that due to climate change, a significant increase of annual and pre-monsoon rainfall in Bangladesh is observed [45]. Moreover, the recent landslide events were related to the extreme rainfall intensities (40 mm/day) having short period of time (2-7 days). All the major landslide events occurred at much higher rainfall amount compared to the normal monthly average as well [46]. Therefore, it is also important to consider future rainfall pattern while producing landslide susceptibility maps for the future. These are the current research gaps in landslide modelling.

In this drawback, future research should try to take into consideration the dynamic variables like- the simulated land cover map and future rainfall pattern, to predict the future landslide scenario of CMA. This will be a new kind of analysis. It will help answering whether using the simulated dynamic variables will give much better results or not. It is expected that preparing landslide hazard maps, using this kind of new modelling concept will add new knowledge to the landslide susceptibility mapping in modern science. The flowchart of this new idea is depicted in Figure 6.1.

6.3. Conclusion

The outcome of this research shall help the endangered local inhabitants/communities, urban planners and engineers to reduce losses caused by existing and future landslides by means of prevention, mitigation and avoidance. The results will also be useful for explaining the driving factors of the known existing landslides, for supporting emergency decisions and upholding the efforts on the mitigation of future landslide hazards in CMA, Bangladesh.

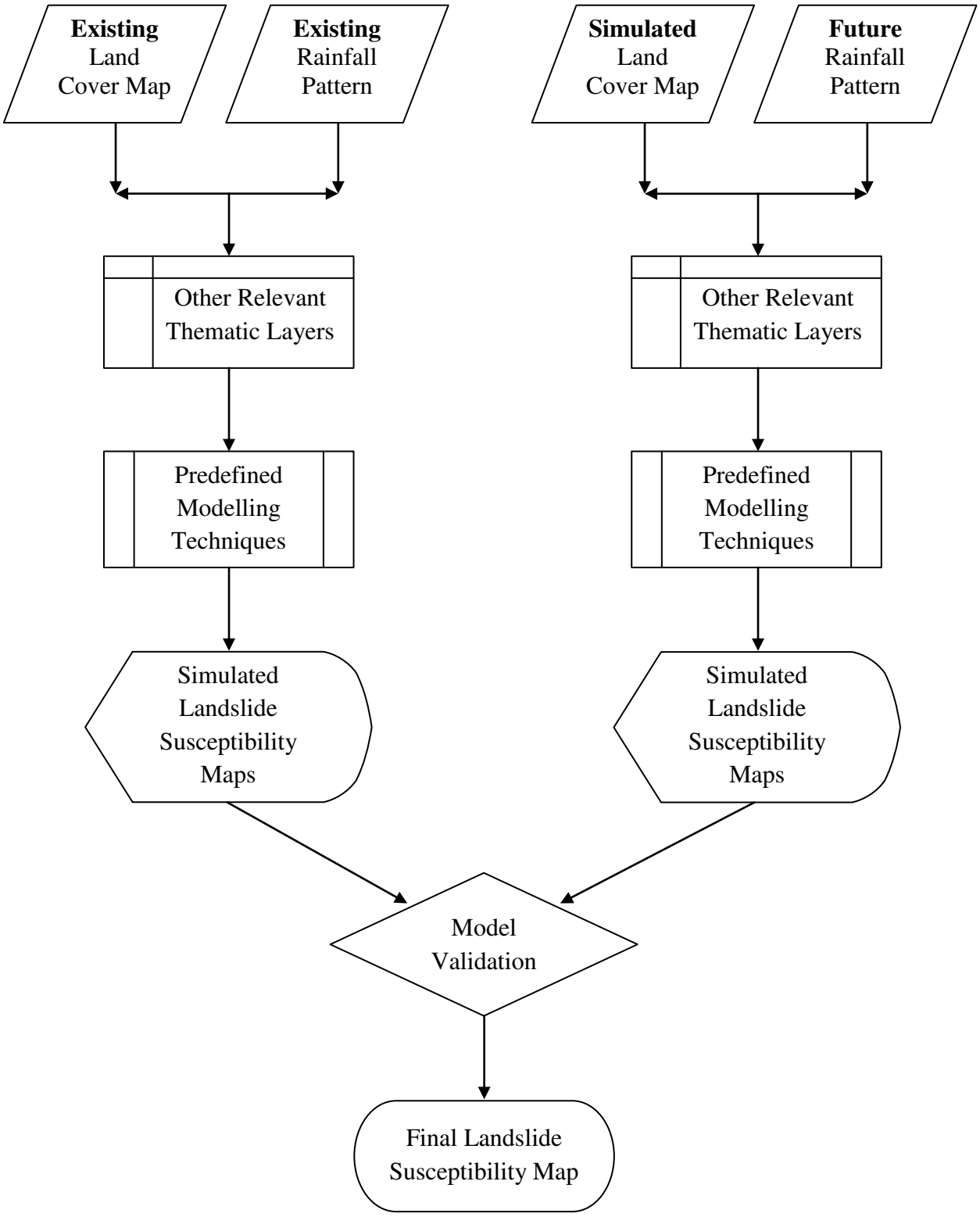

Figure 6.1. Flowchart of new concept for landslide susceptibility mapping

REFERENCES

[1] Thomas Glade, Landslide occurrence as a response to land use change: a review of evidence from New Zealand, Catena, 51 (2003) 297–314.

[2] Deepak Chapagai, Landslide problem of South Asia and vis-a-vis Global Scenario, SAARC training program on landslide risk management in South Asia, SAARC Disaster Management Centre (SDMC), New Delhi, May 02-08, 2011.

[3] SAARC EXPERT GROUP MEETING ON LANDSLIDE TERMINOLOGY, CLASSIFICATIONS, DOCUMENTATION AND HAZARD MAPPING; Published by the SAARC Disaster Management Centre (SDMC), New Delhi, 2011.

[4] F. Mugagga, V. Kakembo and M. Buyinza, Land use changes on the slopes of Mount Elgon and the implications for the occurrence of landslides, Catena, 90 (2012) 39–46.

[5] Xiaojun Yang and Liding Chen, Using multi-temporal remote sensor imagery to detect earthquake-triggered landslides, International Journal of Applied Earth Observation and Geoinformation, 12 (2010) 487–495.

[6] I. Alcantara-Ayala, O. Esteban-Chavez and J.F. Parrot; Landsliding related to land-cover change: A diachronic analysis of hillslope instability distribution in the Sierra Norte, Puebla, Mexico; Catena, 65 (2006) 152–165.

[7] H.L. Perotto-Baldiviezo, T.L. Thurow, C.T. Smith, R.F. Fisher & X.B. Wu; GIS-based spatial analysis and modeling for landslide hazard assessment in steeplands, southern Honduras; Agriculture, Ecosystems and Environment, 103 (2004) 165–176.

[8] José M. García-Ruiz, Santiago Beguería, Luis Carlos Alatorre & Juan Puigdefábregas; Land cover changes and shallow landsliding in the flysch sector of the Spanish Pyrenees; Geomorphology, 124 (2010) 250–259.

[9] Kirschbaum MUF, et al, Quantifying the climate-change consequences of shifting land use between forest and agriculture, Sci Total Environ (2013), http://dx.doi.org/10.1016/j.scitotenv.2013.01.026

[10] Quaas, J., 2011. Global warming: the soot factor. Nature 471, 456-457.

[11] Cities and climate change: global report on human settlements, 2011, United Nations Human Settlements Programme.

[12] IPCC (2007) 'Climate change 2007: Synthesis report', in R. K. Pachauri and A. Reisinger (eds) Contribution of Working Groups I, II, and III to the Fourth Assessment Report of the Intergovernmental Panel on Climate Change, Cambridge University Press, Cambridge, UK; URL:

www.ipcc.ch/publications_and_data/publications_ipcc_fourth_assessment_report_synthesis_report.htm, last accessed 23 April 2013.

[13] Bayes Ahmed, 2011, Urban land cover change detection analysis and modeling spatio-temporal Growth dynamics using Remote Sensing and GIS Techniques: A case study of Dhaka, Bangladesh; unpublished MSc thesis, Erasmus Mundus Program, Universidade Nova de Lisboa (UNL), Instituto Superior de Estatística e Gestão de Informação (ISEGI), Lisboa, Portugal.

[14] Chittagong Metropolitan Master Plan, 1995, Urban Development Plan, Chittagong Development Authority, the Government of the People's Republic of Bangladesh.

[15] BANGLADESH POPULATION AND HOUSING CENSUS 2011, COMMUNITY REPORT, ZILA: CHITTAGONG, June 2012, POPULATION AND HOUSING CENSUS 2011, BANGLADESH BUREAU OF STATISTICS, STATISTICS AND INFORMATICS DIVISION, MINISTRY OF PLANNING, GOVERNMENT OF THE PEOPLE'S REPUBLIC OF BANGLADESH.

[16] Smyth, C. and S. Royle (2000) 'Urban landslide hazards: Incidence and causative factors in Niterói, Rio de Janeiro State, Brazil', Applied Geography 20(2): 95–117.

[17] "Heavy rains and landslides in Bangladesh kill 90", 27 June 2012, BBC News.

[18] Younus Ahmed Khan, Habibah Lateh, M. Azizul Baten & Anton Abdulbasah Kamil, Critical antecedent rainfall conditions for shallow landslides in Chittagong City of Bangladesh, Environmental Earth Sciences, September 2012, Volume 67, Issue 1, pp 97-106.

[19] Rain causes water logging in Chittagong city, Sunday, May 05, 2013, The Daily Star, Assessed on 6 May 2013.

http://www.thedailystar.net/beta2/news/rain-causes-waterlogging-in-ctg-city/

http://www.eprothomalo.com/contents/2013/2013_05_05/content_zoom/2013_05_05_3_0_b.jpg

[20] Amanullah Bin Mahmood & Mamunul H. Khan, Landslide Vulnerability of Bangladesh Hills and Sustainable Management Options: A Case Study of 2007 Landslide in Chittagong City, paper presented in the *International Seminar on "Management and Mitigation of Water Induced Disaster"*, 21-22 April 2008, Kathmandu, Nepal.

[21] Ronju Ahammad, 2009, Understanding Institutional Changes for Reducing Social Vulnerability to Landslides in Chittagong City, Bangladesh, Unpublished Master's thesis; Ecosystems, Governance and Globalization programme 2007/2009, Stockholm Resilience Center, Stockholm University, Sweden.

[22] Introduction & History, Chittagong and CDA, the official website of Chittagong Development Authority (CDA). Assessed on 10 September, 2013.

http://portal.cda.gov.bd/index.php?option=com_content&view=article&id=85&Itemid=107

[23] Shireen Hasan Osmany, Chittagong City, BANGLAPEDIA, National Encyclopaedia of Bangladesh, Asiatic Society of Bangladesh, Dhaka, Bangladesh. Assessed on 12 September, 2013. http://www.bpedia.org/C_0208.php

[24] Sifatul Quader Chowdhury, Chittagong City, BANGLAPEDIA, National Encyclopaedia of Bangladesh, Asiatic Society of Bangladesh, Dhaka, Bangladesh. Assessed on 14 September, 2013. http://www.bpedia.org/C_0215.php

[25] I. Alcantara-Ayala, O. Esteban-Chavez, J.F. Parrot. Landsliding related to land-cover change: A diachronic analysis of hillslope instability distribution in the Sierra Norte, Puebla, Mexico. Catena 65 (2006) 152–165.

[26] R. RAJAKUMAR, S. SANJEEVI, S. JAYASEELAN, G. ISAKKIPANDIAN, M. EDWIN, P. BALAJI AND G. EHANTHALINGAM. LANDSLIDE SUSCEPTIBILITY MAPPING IN A HILLY TERRAIN USING REMOTE SENSING AND GIS. Journal of the Indian Society of Remote Sensing, Vol. 35, No. 1, 2007.

[27] Saro Lee & Touch Sambath. Landslide susceptibility mapping in the Damrei Romel area, Cambodia using frequency ratio and logistic regression models. Environ Geol (2006) 50: 847–855.

[28] Ram Avtar, C. K. Singh, Gulab Singh, R. L. Verma, S. Mukherjee & H. Sawada. Landslide susceptibility zonation study using remote sensing and GIS technology in the Ken-Betwa River Link area, India. Bull Eng Geol Environ (2011) 70:595–606.

[29] F. Karsli, M. Atasoy, A. Yalcin, S. Reis, O. Demir & C. Gokceoglu. Effects of land-use changes on landslides in a landslide-prone area (Ardesen, Rize, NE Turkey). Environ Monit Assess (2009) 156:241–255.

[30] Prabin Kayastha, Megh Raj Dhital & Florimond De Smedt. Landslide susceptibility mapping using the weight of evidence method in the Tinau watershed, Nepal. Nat Hazards (2012) 63:479–498.

[31] Christine Gassner, Catrin Promper, Helene Petschko, and Thomas Glade. Scenarios of future landslide susceptibility - incorporating changes in land cover and climate. Geophysical Research Abstracts, Vol. 15, EGU2013-6786, 2013.

[32] Tahir Ali Akbar & Sung Ryong Ha. Landslide hazard zoning along Himalayan Kaghan Valley of Pakistan—by integration of GPS, GIS, and remote sensing technology. Landslides, December 2011, Volume 8, Issue 4, pp 527-540.

[33] Soyoung Park, Chuluong Choi, Byungwoo Kim & Jinsoo Kim. Landslide susceptibility mapping using frequency ratio, analytic hierarchy process, logistic regression, and artificial neural network methods at the Inje area, Korea. Environ Earth Sci (2013) 68:1443–1464.

[34] Fausto Guzzetti, Alberto Carrara, Mauro Cardinali & Paola Reichenbach. Landslide hazard evaluation: a review of current techniques and their application in a multi-scale study, Central Italy. Geomorphology 31 1999 181–216.

[35] Shi-Biao Bai, Jian Wang, Guo-Nian Lü, Ping-Gen Zhou, Sheng-Shan Hou & Su-Ning Xu. GIS-based logistic regression for landslide susceptibility mapping of the Zhongxian segment in the Three Gorges area, China. Geomorphology 115 (2010) 23-31.

[36] Duman TY, Can T, Emre O, Kecer M, Dogan A, Ates S, Durmaz S (2005) Landslide inventory of north-western Anatolia, Turkey. Eng Geol 77:99–114.

[37] Godt JW, Baum RL, Savage WZ, Salciarini D, Schulz WH, Harp EL (2008) Transient deterministic shallow landslide modeling: Requirements for susceptibility and hazard assessment in a GIS framework. Eng Geol 102:214–226.

[38] Isik Yilmaz, Landslide susceptibility mapping using frequency ratio, logistic regression, artificial neural networks and their comparison: A case study from Kat landslides (Tokat—Turkey). Computers & Geosciences 35 (2009) 1125–1138.

[39] Yilmaz I, Yildirim M (2006) Structural and geomorphological aspects of the Kat landslides (Tokat-Turkey), and susceptibility mapping by means of GIS. Environ Geol 50(4):461–472.

[40] Dieu Tien Bui, Biswajeet Pradhan, Owe Lofman, Inge Revhaug & Øystein B. Dick. Regional prediction of landslide hazard using probability analysis of intense rainfall in the Hoa Binh province, Vietnam. Nat Hazards (2013) 66:707–730.

[41] J.L. Zêzere, R.A.C. Garcia, S.C. Oliveira & E. Reis. Probabilistic landslide risk analysis considering direct costs in the area north of Lisbon (Portugal). Geomorphology 94 (2008) 467–495.

[42] Bakhtiar Feizizadeh & Thomas Blaschke. GIS-multicriteria decision analysis for landslide susceptibility mapping: comparing three methods for the Urmia lake basin, Iran. Nat Hazards (2013) 65:2105–2128.

[43] Chandra Prakash Poudyal, Chandong Chang, Hyun-Joo Oh & Saro Lee. Landslide susceptibility maps comparing frequency ratio and artificial neural networks: a case study from the Nepal Himalaya. Environ Earth Sci (2010) 61:1049–1064.

[44] F. Mugagga, V. Kakembo & M. Buyinza. Land use changes on the slopes of Mount Elgon and the implications for the occurrence of landslides. Catena 90 (2012) 39–46.

[45] Shamsuddin Shahid. Trends in extreme rainfall events of Bangladesh. Theor Appl Climatol (2011) 104:489–499.

[46] Younus Ahmed Khan, Habibah Lateh, M. Azizul Baten & Anton Abdulbasah Kamil. Critical antecedent rainfall conditions for shallow landslides in Chittagong City of Bangladesh. Environ Earth Sci (2012) 67:97–106.

[47] T. Tachikawa, M. Hato, M. Kaku and A. Iwasaki, 2011, The characteristics of ASTER GDEM version 2, IGARSS, July 2011. Assessed on 23 October, 2013. http://www.jspacesystems.or.jp/ersdac/GDEM/E/1.html

[48] ArcGIS® 10 Help; Environmental Systems Research Institute: Redlands, CA, USA, 2012. Available online: http://help.arcgis.com/en/arcgisdesktop/10.0/help/ (accessed on 7 November 2013).

[49] Malczewski J (2000). On the use of weighted linear combination method in GIS: common and best practice approaches. Trans GIS 4(1):5–22.

[50] Gorsevski PV, Jankowski P, Gessler PE (2006) An heuristic approach for mapping landslide hazard by integrating fuzzy logic with analytic hierarchy process. Control Cybern 35:21–141.

[51] Ron Eastman, The IDRISI Selva Help, 2012 Clark Labs, Clark University 950 Main Street, Worcester MA 01610-1477 USA.

[52] Lee S, Sambath T (2006) Landslide susceptibility mapping in the damrei romel area, cambodia using frequency ratio and logistic regression models. Environ Geol 50:847–855.

[53] McFadden D (1973) Conditional logit analysis of quantitative choice behavior. In: Zarembka P (ed) Frontiers in Econometrics. Academic Press, New York, pp 105–142.

[54] Yesilnacar E, Topal T (2005) Landslide susceptibility mapping: A comparison of logistic regression and neural networks methods in a medium scale study, Hendek region (Turkey). Eng Geol 79:251–266.

[55] Aldrich, John H. and Forrest D. Nelson, 1984. Linear, Probability, Logit, and Probit Models (in Series L Quantitative Applications in the Social Sciences). Newbury Park: Sage University Publication.

[56] Clark, W.A., and P.L. Hosking,1986. Statistical Methods for Geographers (Chapter 13). New York: John Wiley &Sons.

[57] Pontius, R. G. Jr. and L. Schneider. 2001. Land-use change model validation by a ROC method for the Ipswich watershed, Massachusetts, USA. Agriculture, Ecosystems & Environment 85(1-3) p. 239-248.

[58] Larsen MC. Simon A(1993) A rainfall intensity-duration threshold for landslides in a humid tropical environment, Puerto Rico. Geogr Ann 75:13-18.

[59] Kleinbaum, D. G., L. L. Kupper and K.E. Muller 1988 (second edition). Applied Regression Analysis and Other Multivariable Methods. Boston: PWS-KENT Publishing Company.

[60] Clark, W. A. V. and P. L. Hosking 1986. Statistical Methods for Geographers. New York: John Wiley & Sons.

[61] Schneider, L and R.G. Pontius. 2001. Modeling landuse change in the Ipswich watershed, Massachusetts, USA. Agriculture, Ecosystems & Environment 85(1-3) p. 83-94.

[62] Chung, C. F., & Fabbri, A. G. (1999). Probabilistic prediction models for landslide hazard mapping. Photogrammetric Engineering and Remote Sensing, 65(12), 1389–1399.

[63] Begueria, S., 2006. Validation and evaluation of predictive models in hazard assessment and risk management. Natural Hazards 37, 315–329.

[64] H.A. Nefeslioglu, C. Gokceoglu and H. Sonmez. An assessment on the use of logistic regression and artificial neural networks with different sampling strategies for the preparation of landslide susceptibility maps. Engineering Geology 97 (2008) 171–191.

[65] Ben Wisner, Piers Blaikie, Terry Cannon and Ian Davis. 2003 (Second edition). At Risk: Natural Hazards, People's Vulnerability and Disasters. Routledge, New York, USA.

Appendix-I

PHOTOGRAPHS FROM FIELD SURVEYING IN CHITTAGONG METROPOLITAN AREA (CMA)

1. Tree Plantation to Protect Landslides

2. Tree Plantation to Protect Landslides

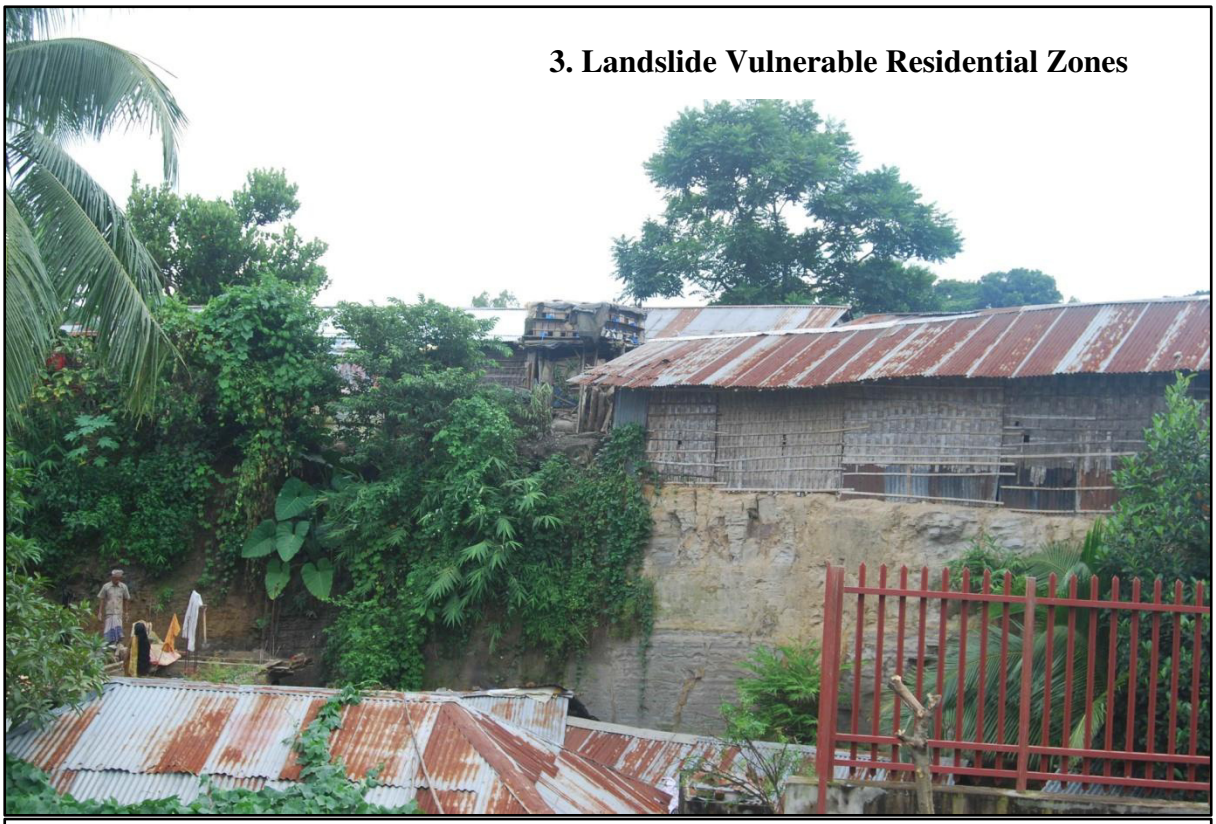

3. Landslide Vulnerable Residential Zones

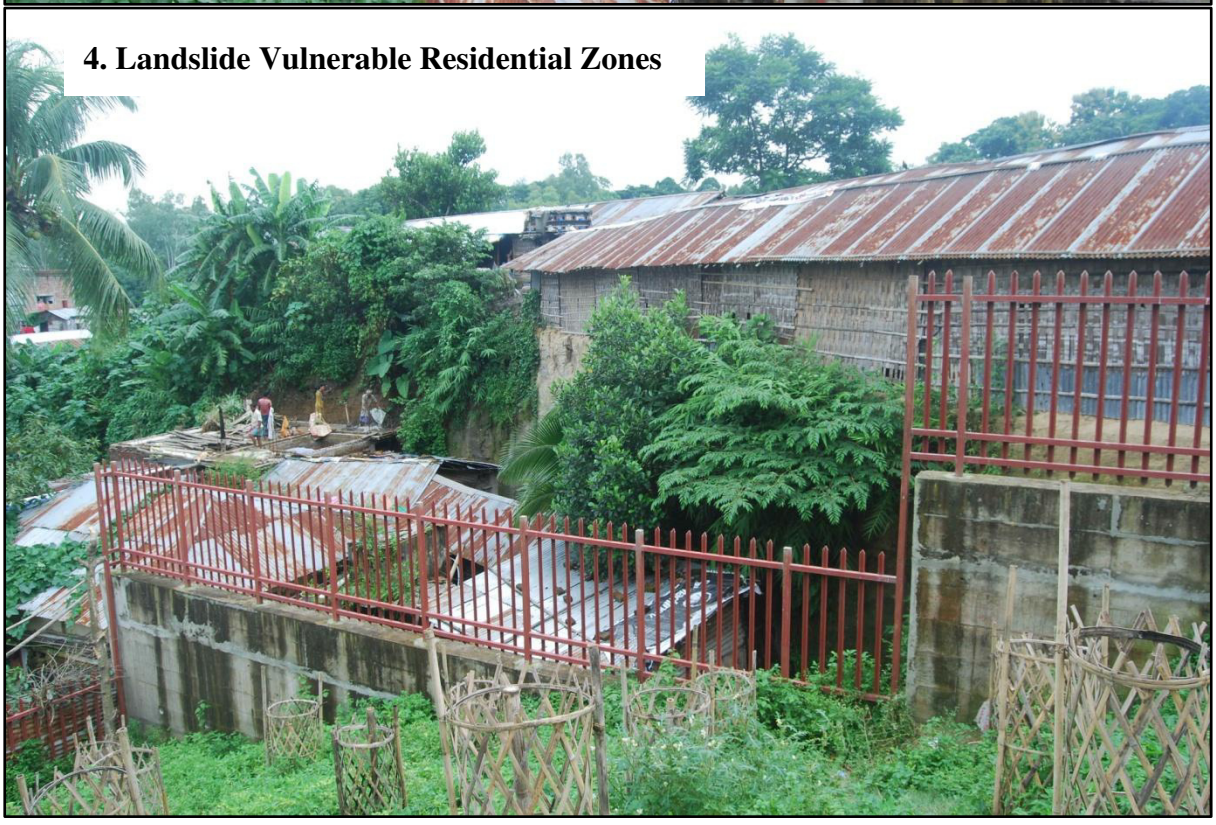

4. Landslide Vulnerable Residential Zones

5. Landslide Vulnerable Residential Zones

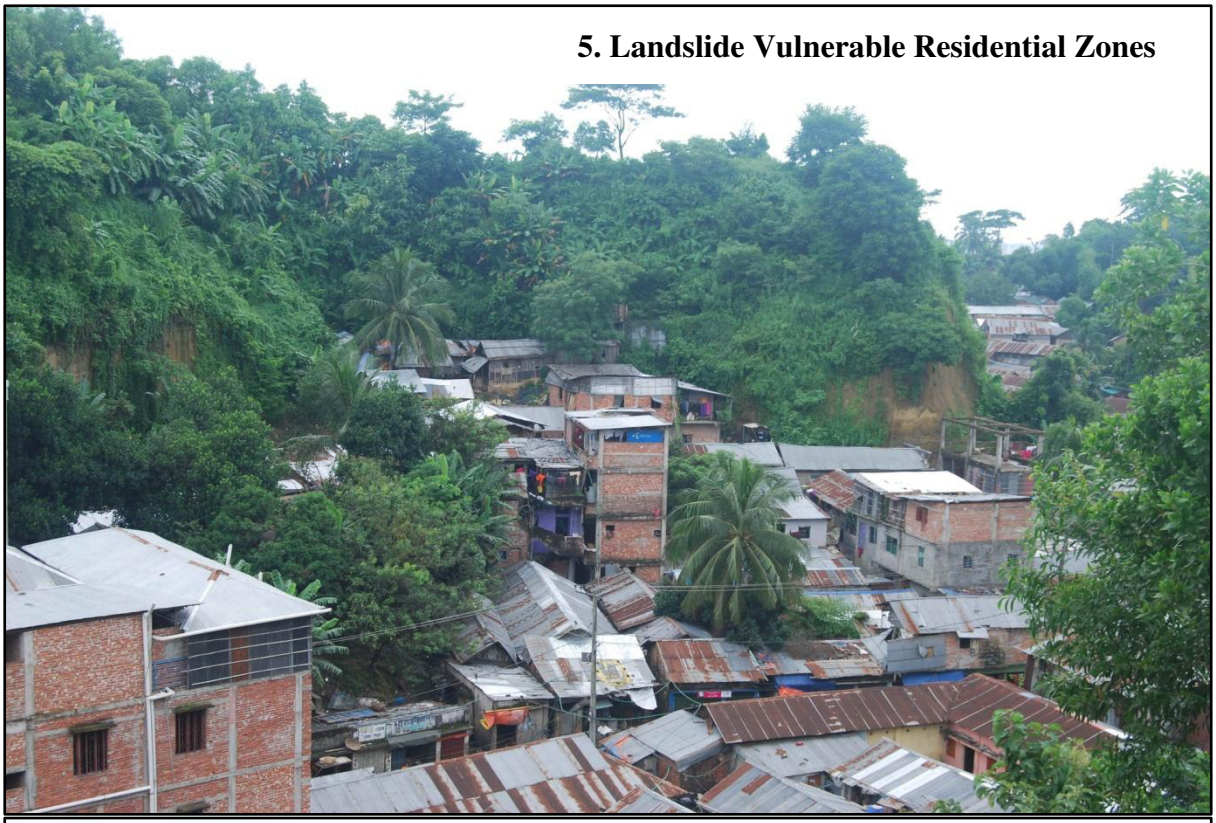

6. Landslide Vulnerable Residential Zones

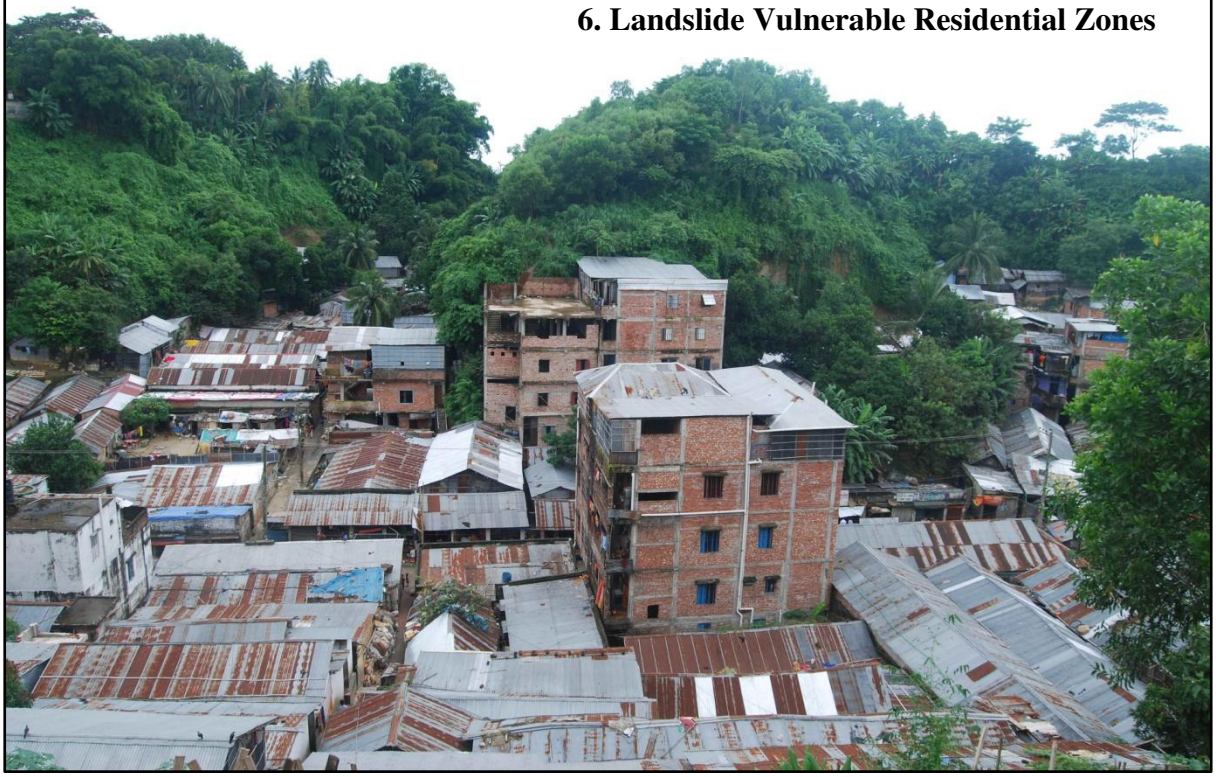

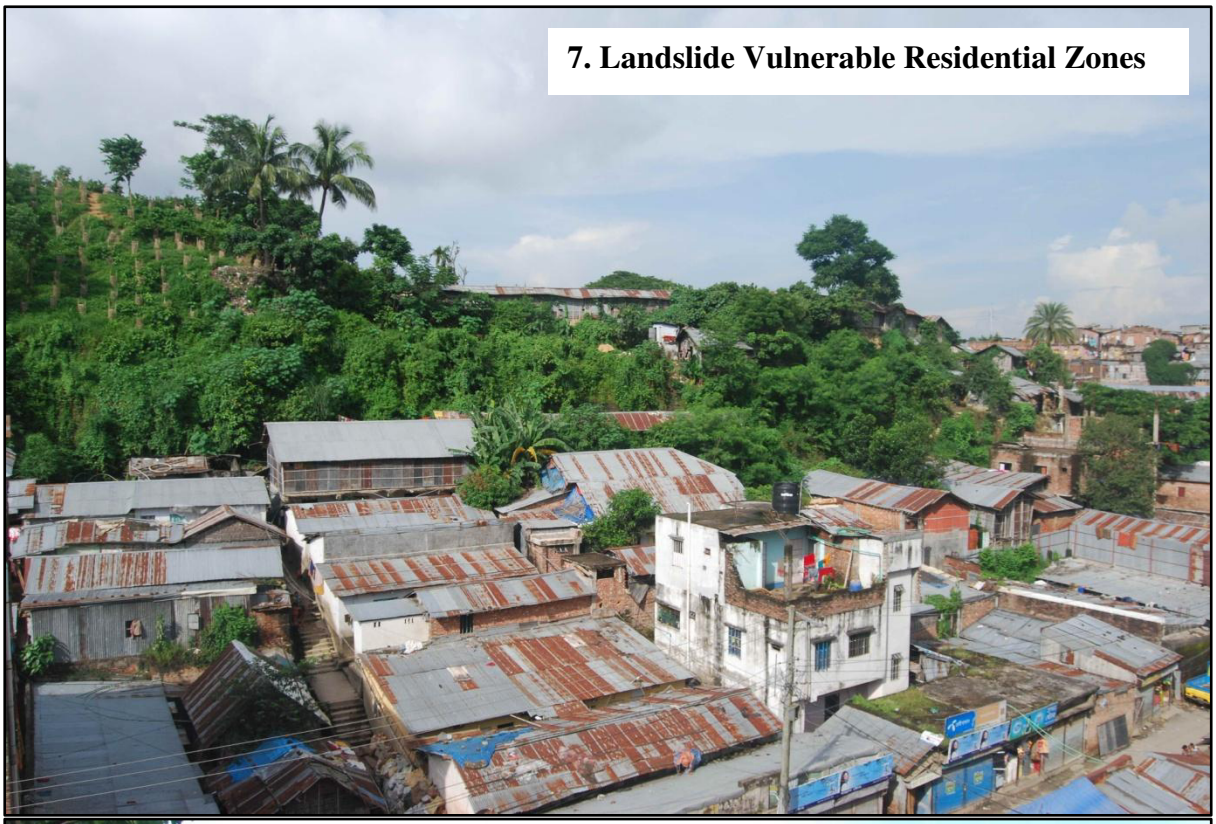

7. Landslide Vulnerable Residential Zones

8. Hill Cutting near Residential Zones

9. Temporary Accommodation for the Landslide Vulnerable People

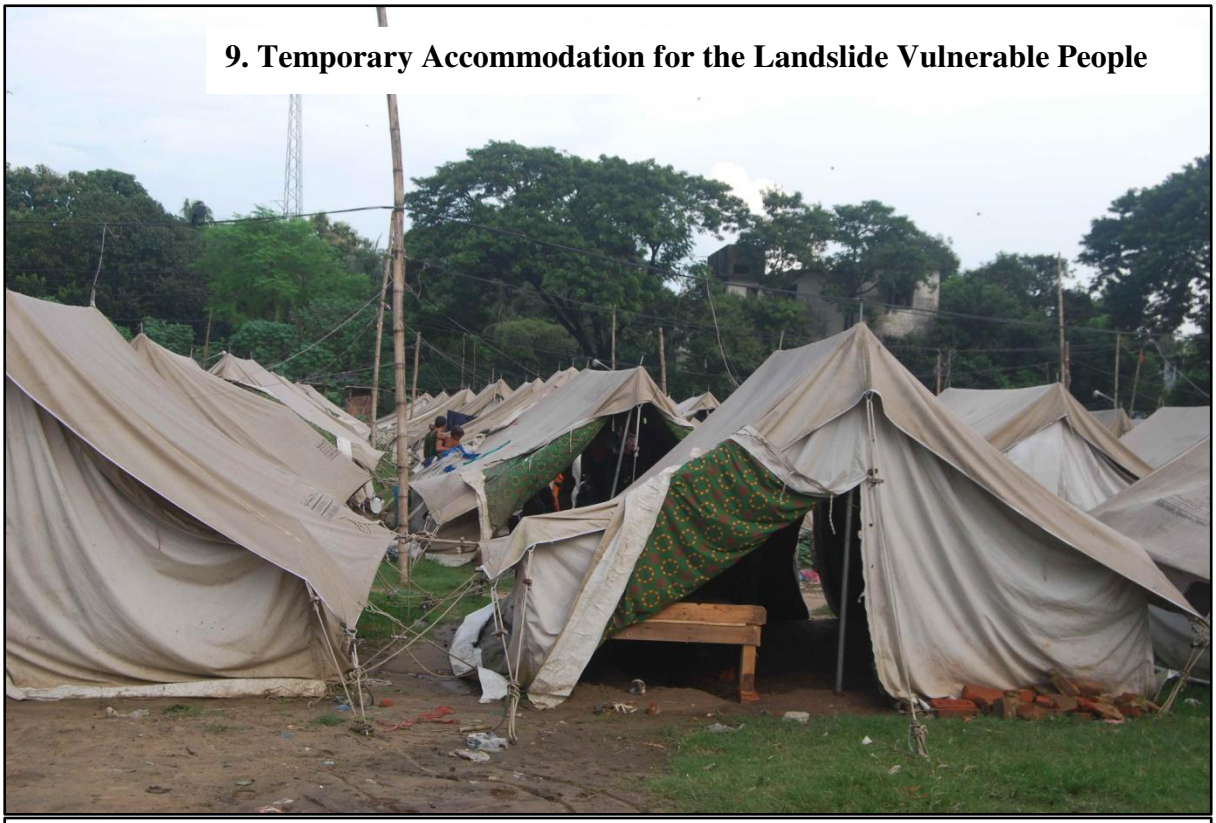

10. Mr. Bayes Ahmed (Mentor) with the Landslide Refugees

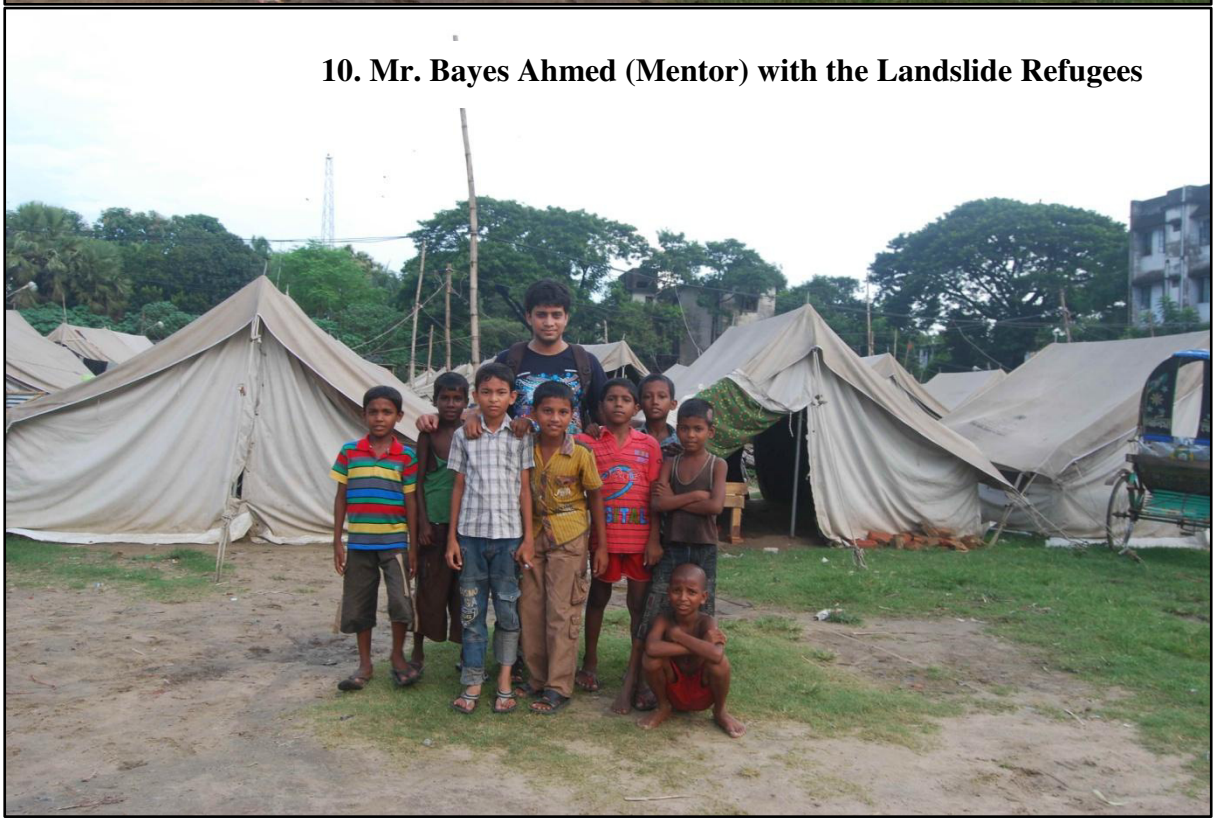

Photograph-11

Photograph-12

These two pictures taken from the Red Hill (Photograph-11) and Akbar Shah Majar Hill (Photograph-12) represent how low income people are forced to live in highly danger areas though they know that every year a considerable number of people died in Landslides.

Photograph-13

Photograph-14

Poor drainage facility (Photograph-13) and unhealthy latrine (Photograph-14) in landslide prone slum dwelling at Batali Hill, Chittagong. The houses are rebuilt after big landslides in that hill.

Photograph-15

Photograph-16

The dwellers don't want to provide enough info about past landslides fearing eviction by government from the place they are living. They told when reporters write about the dangerous houses in instable hillside then the government authorities force them to leave the place. Questioning a landslide refuge in Motijharnahill (Photograph-15). A landslide victim in Akbar Shah Hill (Photograph-16) showed me where he lost his family in sudden landslides.

Photograph-17

Photograph-18

A road in Chittagong University is in great danger of landslides (Photograph-17). Several road ways in Bangladesh blocked due to slope failure in rainy season. Some playing spots for children at Chittagong Foy's Lake are also in great danger of landslides (Photograph-18).

Photograph-19

Photograph-20

The red sign board in the Photograph-19 tells the area is very vulnerable to landslide and warns people not to live near the hill. Despite of the warning finding not a place almost 100 people are living there area with a risk of huge damage during rainy season. Newly immigrated people are often building buildings by cutting down hills in Chittagong imparting high landslides risk in rainy season (Photograph-20).

Photograph-21

Photograph-22

Soil tests performed by Yiaser Arafat Rubel for determining landslides occurring factors performed by me in Geotechnical Engineering Laboratory, Bangladesh University of Engineering and Technology (Photographs 21 and 22).

Appendix-II

EXISTING LITERARY WORKS ON LANDSLIDE SUSCEPTIBILITY MAPPING/MODELLING

Authors/ Citations	Location/ Context	Main Theme	Data	Methods/ Techniques	Results	Recommendations
Gassner et al. **2013**	Waidhofen/Ybbs, Lower Austria.	Land cover change and precipitation	Precipitation data, land cover maps, derivations of a DEM (e.g. slope, curvature) and a matching landslide inventory (1962-2007).	Logistic Regression; extrapolation of the landslide susceptibility to the future (1962-2100).	A tendency towards an increasing susceptibility, however this trend is not continuous over all time periods.	Landslides are usually triggered by short but intense rainfall events occurring during summer.
Ayala, Chavez & Parrot, **2006**	Sierra Norte, Puebla, Mexico	Land use change (deforestation)	Landsat TM (1989) & ETM+ (1999).	A diachronic analysis for NDVI & vegetation fragmentation calculation.	Significant vegetation reduction (1989-99). Landslide concentration was much higher on surfaces that were bare and had low vegetation index (0-50%).	Land use change and land degradation are precursors to mass movement events.
Lee & Lee, **2006**	Gangneung area, Korea	Heavy rainfall	KOMPSAT-1 (Korea Multipurpose Satellite) EOC (Electro Optical Camera) images. 16 factors (Topography, geology, soil, forest, lineaments and land cover etc.).	Frequency ratio, one of the probabilistic model.	The prediction accuracy showed 86.76%	Lack of data- rainfall, earthquakes, slopes cutting etc, combining with hydrological model. Risk analysis could not be performed- lack of data to vulnerability of buildings & other properties.
Mugagga, Kakembo & Buyinza, **2012**	Mount Elgon, Eastern Uganda	Land use changes on the slopes (woodlands and forest cover)	Aerial photographs, Landsat TM, SPOT MS image, DEM.	Maximum Likelihood Supervised Classification.	Drastic decimation of forest and woodland cover, due to agricultural encroachment. The vulnerability to landsliding of steep concave slopes with a northerly orientation.	It is recommended that forest cover be restored, and the local communities restrained from opening up new areas for cultivation on critical slopes.
Do Minh Duc, **2012**	Van Canh District, Binh Dinh Province, Vietnam	Heavy Rainfall	Topographical map, geological map, daily rainfall (1976-2010), site investigations (geological settings,	Map of landslide susceptibility is produced by overlaying factors affecting landslide susceptibility	The landslides occurred after 3 months of heavy rain. Landslides were triggered when the slopes were almost	The effective counter measure is to resettle local people to safe sites and disseminate the early

			characteristics of weathering crust, geotechnical properties of soils and rocks, and landslide properties).	(slope angle, distance to faults, and slope aspect).	saturated.	warning signs of potential landslides (such as tension cracks and scarps) in the area to the local people
Ayalew, Yamagishi & Ugawa; **2004**	Tsugawa area of Agano River, Niigata Prefecture, Japan	High precipitation	Aspect, Elevation, Lithology, Plan Curvature, Profile Curvature, Slope Gradient	Weighted Linear Combination (WLC)	High scale of susceptibility lies on mid-slope mountains where relatively weak rocks such as sandstone, mudstone and tuff are outcropping as one unit.	The spatial distribution of landslides is a result of the interaction of many parameters. A reliable and accurate susceptibility map depends on the inclusion and proper determination of the role of these parameters.
Pellicani, Van Westen & Spilotro; **2013**	Western part of the Apulia region, in Southern Italy	Meteoric events and earthquakes	Slope angle, Lithology, land use, aspect, rainfall and seismicity. (1) Physical (buildings, cultural buildings and transportation networks), (2) social (population), (3) economic (land value) and (4) environmental (land cover and protected areas).	Spatial multi-criteria evaluation (ILWIS-GIS)	The higher level of exposure is localised in urban areas where the importance of social, physical and economical assets is greater.	As no information is available on the temporal and spatial probability of landslide events, it is not possible to generate landslide risk map based on historical information.
Kavzoglu, Sahin & Colkesen; **2013**	Trabzon province, NE Turkey	The highly saturated loamy formation, continuous exposure to heavy rain & human factors (infrastructure, superstructure, and deforestation).	Lithology, slope, land cover, aspect, topographic wetness index, drainage density, slope length, elevation, and distance to road.	Multi-criteria decision analysis (MCDA), support vector regression (SVR), and logistic regression (LR)	The GIS-based MCDA method was superior to the other methods with slight difference with the SVR method. The LR method produced the lowest performance.	The main difficulty in the use of the MCDA is the determination of optimal values of the weights assigned for each parameter pair, whereas the selection of kernel parameters and determination of their optimal values are crucial for the success of the SVR method. Although the logistic regression is a

						simple and widely used method, it was found inferior in shallow landslide susceptibility mapping considered in this study.
Rajakumar et al. **2007**	Ooty Region, Tamil Nadu, India	Land use change (e.g. deforestation, urbanization), inadequate drainage, more soil thickness.	Indian Remote Sensing Satellite Imagery, DEM, Slope, Land cover, Drainage frequency map, Lineament incidence & lineament intersection map and Aspect.	Overlay Analysis (Delphi Approach).	Very high susceptible areas are characterized by non-forested areas indicating the influence of vegetation on the initiation of slope instability.	Layers missing- roads, railway, soil & geology.
Saro Lee & Touch Sambath, **2006**	Damrei Romel area, Cambodia	Heavy rainfall in steep slopes.	Slope, aspect, curvature, distance to drainage, lithology, distance to lineament, geology, the detected landslide locations and land cover.	Frequency ratio and logistic regression.	The frequency ratio model (86.97%) and logistic regression model (86.37%) showed high accuracy.	The frequency ratio model and the logistic regression model showed a similar accuracy.
Pandey et al. **2008**	Dikrong river basin, Arunachal Pradesh, India	Soil erosion due to Jhum cultivation practices & wet tropical and sub-tropical climate accompanied with humid condition.	Slope, aspect, photo-lineament buffer, thrust buffer, relative relief map, geology and land use / land cover map.	The weighting rating system based on the relative importance of various causative factors.	The high susceptibility to landslides is mainly due to a complex geological setting, varying slopes and relief, heavy rainfall, along with ever increasing human interference in the ecosystem.	Developed maps can be used as an elementary form of landslide hazard map because they show the spatial location of susceptible zones of landslides.
Avtar et al. **2011**	Ken-Betwa River Link area, India	Land use change (the construction of roads, etc., will affect the stability of slope and cause deforestation) & heavy rainfall.	Geology, land use/land cover, lineament, drainage, slope, aspect, normalized difference vegetation index and soil type. Rainfall data, groundwater level data and a petrological study of rock thin sections.	Numerical rating schemes were used for ranking the thematic layers & a multi-criteria decision-making technique.	The LSZ map produced in this study divides the area into high, moderate, low and very low susceptibility zones, which have been shown to correlate well with rainfall and groundwater level.	The basic data will assist in slope management and land-use planning as exposure of rocks, deforestation, construction of the canal, etc. will affect the hydrological conditions of the slopes.
Karsli et al. **2009**	Ardesen, Rize, NE Turkey	Mountainous topographic character,	Lithology, slope gradient, slope aspect, vegetation cover,	The geometrical changes in the landslide area are	Landslides occurred regularly after precipitation. 95% of the	Increase in both the number of new houses constructed

		land cover change and high frequency of heavy rain.	land class, climate, rainfall and proximity to roads.	determined by using the photogrammetric techniques.	landslides identified in the region occurred in highly or completely decomposed rock (tea agriculture).	and in the length of road network affect the stability of slopes negatively and thus causes new landslide developments.
Kayastha, Dhital & Smedt, **2012**	Tinau watershed, Nepal.	Adverse geological conditions, prolonged and high-intensity rainfall and anthropogenic factors.	Slope angle, slope aspect, slope shape, relative relief, geology, distance from faults, land use, distance from drainage and mean long-term annual precipitation.	The weight of evidence method.	72 % of the observed landslides fall on the high and very high susceptible zones, which that constitute 30 % of the study area.	Due to the dynamic nature of precipitation, rapid urbanization, deforestation and anthropogenic activities, the presented landslide susceptibility map is subjected to change.
Feizizadeh & Blaschke, **2013**	Urmia lake basin, Iran.	Unstable slopes combined with the geological tectonic settings.	Lithology, distance to fault, distance to roads, distance to stream, elevation, slope, aspect, land use/cover, precipitation & the landslides inventory database.	Analytic hierarchy process (AHP), weighted linear combination (WLC) and ordered weighted average (OWA). Dempster-Shafer theory for uncertainty analysis.	The AHP performed best in the landslide susceptibility mapping closely followed by the OWA method while the WLC method delivered significantly poorer results.	It is evident that each method has its advantages and inherent limitations that must be fully understood and accepted by the decision maker before applying it.
Bui et al. **2013**	Hoa Binh province, Vietnam.	Heavy rainfall, clear-cut logging, deforestation, and infrastructural expansion.	Landslide inventory map, rainfall data & five landslide susceptibility maps.	The rainfall threshold Model, Poisson probability model, support vector machines, logistic regression, evidential belief functions, Bayesian regularized neural networks, and neuro-fuzzy models.	A total of 15 specific landslide hazard maps were generated considering three time periods of 1, 3, and 5 years.	The details of soil thickness and soil strength properties are not available. An assessment of the change of land use and road system should be carried out for the considered period.
Mohamed O. Arnous, **2011**	Wadi Watier area, South Sinai, Egypt.	Earthquakes, poor quality soils, diverse geomorphology, and steep slope gradient.	Lithology, structural lineaments, land-cover/land-use, terrain analysis, seismic map, slope, aspect, height elevation, and 3D.	The weighting-rating system based on the relative importance of various causative factors.	The distribution of landslides is largely governed by the combined effect of various geo-environmental conditions.	Detail investigation on existing infrastructure or communities can provide information to ensure a stable design.
Poudyal et al. **2010**	Panchthar district,	Groundwater,	Slope angle, slope aspect,	Frequency ratio and	Most of the highly hazardous	The respective accuracy of

	Nepal.	stratigraphic condition, and precipitation.	stream power index (SPI), topographic wetness index (TWI), combined slope length (LS), geology, distance from drainage system, distance from lineament, and land use.	artificial neural networks.	areas lie near the drainage line whereas some are located near lineaments. Elevation has a minor influence on the occurrence of landslides.	82.2% and 78.2% obtained for the frequency ratio and artificial neural network approaches shows that the map derived using the frequency ratio has a greater accuracy than that produced from the artificial neural network result.
Reis et al. **2012**	Rize province, NE Turkey.	Climatic conditions (rainfall), urbanization and tea gardens, and geomorphologic characteristics.	Lithology, slope angle, slope aspect, land cover, distance to stream, drainage density, distance to road & landslide inventory map.	Frequency ratio (FR) and analytical hierarchy process (AHP).	The active landslide zones coincided with a high percentage for the high and very high susceptibility class in the FR and AHP maps, as around 73% and 70%, respectively.	When field conditions and characteristics are accurately determined by professional expertise, the FR method gives better results in the study area.
Park et al. **2013**	Inje area, Korea.	Intensive rainfall.	Topographic factors (elevation, slope, aspect), hydrological factors (distance to drainage, stream power index, topographic wetness index), soil factors (soil texture, soil effective thickness), forest factors (tree type, tree diameter, tree age, crown density), and land-cover factors (land-use/land-cover type).	Frequency ratio, analytic hierarchy process, logistic regression, and artificial neural network. Area under the curve (AUC) values of relative operating characteristic (ROC) curves & cross-tabulation.	The ANN, LR, FR, and AHP models had over all accuracies of 68.47, 65.51, 65.27, and 64.35 %, respectively.	The slightly lower accuracy may have been because we did not take geologic factors (such as lithology and lineament) into account, and these factors are closely related to landslides.
Ali Yalcin, **2008**	Ardesen, Turkey	Climate conditions (heavy rainfall), geologic, and geomorphologic characteristics.	Lithology-weathering, slope, aspect, land cover, distance to stream, drainage density, distance to road & landslide inventory map.	The analytical hierarchy process (AHP), the statistical index (Wi), and weighting factor (Wf) methods.	81.3% of the landslide zones fall into the high and very high susceptibility zones of the AHP method while this is 62.5% in the case of Wi method, and 68.8% with the Wf method.	The AHP method gave a more realistic picture of the actual distribution of landslide susceptibility, than the Wi and Wf methods.

Ermini, Catani & Casagli, **2005**	The Reno River, Northern Apennines, Italy.	Geomorphological and geological settings.	Lithology, slope angle, profile curvature, land cover, up-slope contributing area & landslide inventory.	Artificial Neural Networks (ANNs): Multi-Layered Perceptron (MLP) the Probabilistic Neural Network (PNN).	Geographic representations of the model predictions show satisfactory results for both networks.	Estimation errors can be due to the following causes: Problems in the network construction, Wrong or insufficient variables & Noisy data.
Pradhan, Lee & Buchroithner, **2010**	Penang Island, Cameron Highland and Selangor; Malaysia.	Tropical rainfall, flash floods, continuous development and urbanization lead to deforestation and erosion of the covering soil layers.	Landslide inventory, the slope, aspect, curvature, altitude, distance from drainage, stream power index, distance from road, distance from faults, geology, land use, normalized difference vegetation index (NDVI), topography, topographic wetness index, soil texture and soil material.	An artificial neural network (ANN) method. Verification through ‘‘area under the curve” (AUC) method.	The verification results showed satisfactory agreement between the susceptibility map and the existing data on the landslide location.	If data on rainfall, earthquake shaking, or slope cutting existed, then the possibility analysis could be performed. Similarly, if the factors relevant to the vulnerability of buildings and other property were available, the risk analysis could also be performed.
Chau et al. **2004**	Hong Kong Island	Rainfall	Terrain data (slope angle and elevation), environmental effect (rainfall), geology information (soil deposit and lithology), landslide information (potential run-out coverage and landslide inventory. Population map for risk analysis.	A frequency–volume relation & multi-dimensional regression analysis.	Strong correlation between rainfall and landslide occurrence is obtained.	In terms of being hit by a landslide, squatter areas and roads are at the highest risk.
Blahut, Westen & Sterlacchini, **2010**	The Valtellina Valley, the Central Italian Alps.	Rainfall-induced small slides and soil slips which are the sources for debris flows.	Land use, geology, faults, altitude, aspect, internal relief, planar curvature, profile curvature, slope and flow accumulation.	The Weights-of-Evidence modelling technique (WofE), Success rate curves & Prediction rate curves. [An ArcGIS 9.2 extension SDM—Spatial Data Modeller]	The spatial distribution of susceptible areas in the best performing maps disagrees by 20% to 30%. It is highly variable and dependent on the combination of the factor maps used.	It is better not to perform statistical analysis over a large area because particular differences in susceptibility conditions are not shown.
Nefeslioglu,	The town Ispir and its	Geomorphometric	Lithology, land use,	Logistic regression and	The susceptibility maps	To find out the best

Gokceoglu & Sonmez, **2008**	close vicinity, Northeastern part of Turkey.	conditions.	Geomorphometric parameters (altitude, slope angle, slope aspect, curvature, plan & profile curvature, Sediment tran. cap. Index, Stream power index, Topogr. wetness index, Distance to- drainage, ridge, road, drainage & road density).	artificial neural networks. The area under curve (AUC).	produced mapping the outputs of the back-propagation artificial neural networks could be interpreted as highly optimistic, while of those generated using the resultant probabilities of the logistic regression equations might be considered as pessimistic.	algorithm and the most appropriate accuracy and precision levels, there is still an indispensable need for further investigations with more realistic validation applications and data.
Pradhan & Lee, **2010**	Klang Valley area, Malaysia	Heavy tropical rainfalls.	Slope angle, slope aspect, curvature, altitude, distance to roads, distance to rivers, lithology, distance to faults, soil type, landcover and the normalized difference vegetation index value.	Back-propagation artificial neural network model, frequency ratio and bivariate logistic regression modelling.	ANN results are better than the other two methods. The best accuracy (94%) was obtained in the case of the 7 factors weight, whereas 11 factors based weight showed the worst accuracy (91%).	The scientific weights and ratings are essential to landslide susceptibility mapping. To obtain higher prediction accuracy it is recommended to use a suitable dataset of landslide data.
Bai et al. **2010**	Three Gorges area, China	The construction of the dam and other human engineering activities severely affect the geological environment.	Geological map, landslide inventory map, elevation, slope angle, aspect, terrain roughness, shape of the slope parameters, plan curvature and profile curvature, land cover,	Logistic regression method, the correct classification percentage and the root mean square error (RMSE).	2.8% of the study area was identified as an area with very high-susceptibility. The correct classification percentage and RMSE values for the validation data were 81.4% and 0.392, respectively.	Both precipitation and seismicity were not considered for the analyses. The main types of maps related to landslide mitigation are landslide-inventory, susceptibility, hazard and risk maps.
Yilmaz, **2009**	The Kat County, Tokat, Turkey.	Heavy rainfall, the saturated conditions of the sliding material & the presence of clays.	Geology, faults, drainage system, topographical elevation, slope angle, slope aspect, topographic wetness index (TWI) and stream power index (SPI).	Frequency ratio, logistic regression & artificial neural networks. Area under curve (AUC).	The map obtained from ANN model is more accurate than the other models.	Logistic regression and neural networks require the conversion of data to ASCII or other formats.
Zêzere, Garcia & Reis, **2008**	Lisbon, Portugal	Rainfall	Slope angle, Slope aspect, Transversal profile of slope,	A probabilistic approach using Spatial Data	Elements at risk within the test site include 2561 buildings and	Prediction risk models are always a simplified version

			Lithology, Superficial deposits, Geomorphological units & land use.	Analysis techniques.	roads amounting to 169 km.	of a complex reality, and model reliability and performance are strongly influenced by uncertainties in input data.
Remondo, Bonachea & Cendrero, **2008**	Bajo Deba area, Northern Spain	Intense rainfall and indirectly by human activities.	Terrain geometry, land cover and use, geology, regolith type, geomorphology, thickness and hydrologic conditions.	A susceptibility model based on statistical relationships between past landslides and terrain parameters related to instability.	Total monetary value at risk for the Bajo Deba area in the next 50 years is about 2.4×10^6 Euros.	Successful spatial modelling of landslide risk depends critically on detailed analysis and quantification of geomorphic processes.
Neuhäuser & Terhorst, **2007**	The Jurassic escarpment, Swabian Alb, SW-Germany.	Climatic factors (precipitation) & geological conditions.	Soil type, Geological units, Distance escarpment, Hydro-geological units, Lineament-density, Lineament distance, Geomorphological units, Slope angle & Curvature.	Weights-of-evidence method.	Slopes with angles from 11° to 26°, consisting of colluvial layers, particular soils, or a set of diverse geological layers were identified as indicators for slope instability.	Further studies using a more detailed terrain model are required.
Akbar & Ha, **2011**	Western Himalayan Kaghan Valley, Pakistan.	Monsoon intense rainfall.	Landuse, elevation, geology, rainfall intensity, slope inclination, soil, slope aspect, distances from- main roads, secondary roads, main river & trunk streams.	The information value model.	100% accuracy of the hazard zonation map is found. The major risk of landslide was on the main road of the study area.	The artificial excavation of lands at steep slopes along the main and secondary roads might increase the occurrences of landslides.

Appendix-III

LANDSLIDE INVENTORY FOR CHITTAGONG METROPOLITAN AREA

Id	Location	Date	X	Y
1	Mukbul Ahmed primary school	Prior to '69	91°48'33.73"E	22°22'11.02"N
2	Akbarshah colony	6/26/2012	91°47'30.68"E	22°21'44.79"N
3	Akbarshah colony	6/26/2012	91°47'30.04"E	22°21'44.76"N
4	Gazjr math (Biswa colony) B Block	6/26/2012	91°47'2.86"E	22°22'43.63"N
5	Gazjr math (Biswa colony) B Block	6/26/2012	91°47'2.11"E	22°22'44.21"N
6	North part of Pahratoli	6/26/2012	91°46'59.73"E	22°22'55.26"N
7	Motijharna Batali hill	8/23/2008	91°48'46.49"E	22°20'45.54"N
8	Motijharna Tankir Pahar I	4 years back	91°48'50.73"E	22°20'56.28"N
9	Motijharna Tankir Pahar II	4-5 years back	91°48'51.70"E	22°20'54.52"N
10	Motijharna hill beside Batali hill	4-5 years back	91°48'51.40"E	22°20'50.11"N
11	Badshah Mjah road	Yearly May-June	91°49'48.10"E	22°21'24.20"N
12	Kanan Dhara Abashik Prokolpo	6/26/2012	91°49'48.74"E	22°21'23.00"N
13	Badsha Mjah road, private park-Finlay State	6/11/2007	91°49'41.11"E	22°21'20.35"N
15	North part of Pahratoli	4-5 years back	91°47'12.91"E	22°22'51.17"N
14	Lebubagan Kaccha Ghona	6/11/2007	91°48'29.11"E	22°24'55.75"N
16	Lebubagan Kaccha Ghona	6/11/2007	91°48'27.05"E	22°25'0.08"N
17	Lebubagan Kaccha Ghona	6/11/2007	91°48'24.89"E	22°25'7.82"N
18	Lebubagan Kaccha Ghona	6/11/2007	91°48'29.12"E	22°24'54.02"N
19	Lebubagan Kaccha Ghona	6/11/2007	91°48'15.00"E	22°25'18.94"N
20	Lebubagan Kaccha Ghona	6/11/2007	91°48'14.11"E	22°25'18.13"N

Source: Asian Disaster Preparedness Centre (ADPC), 2013

MyCOE/SERVIR Himalayas Fellowship Program

This inventory is prepared on the basis of the survey conducted in many locations of Chittagong district where landslide occurred/likely to occur.

Sl No.	Landslide Location	Lat-Lon-Alt	Total Landslide Occur	Last Landslide	Trigger	Stranded	Injured	Died	House before last landslide	House after last landslide	Total People now in danger
1	Tiger Pass Retaining Wall Hill	N22-20-42 E91-48-45.9 70	2	26 June 2012	Precipitation & Overloaded Side Wall	245	13	90	61	43	297
2	Batali Hill	N22-20-44.4 E91-48-45.9 109.7	Nil	No landslide affects the hill yet. But rapid cutting and current hill slope position vividly indicates its dangerous condition. Landslide causing great damage likely to happen very soon if no preventive measure would be taken.							
3	Moti Jharna	N22-20-52.7 E91-48-52.6 218.8	3	2009	Same as 2	43	21	5	31	57	235
4	Railway Society Foys Lake	N22-21-53.7 E91-47-31.7 96.4	3	2008	Hill Cut + Precipitation	68	13	17	72	23	94
5	Akbar Shah Majar Hill	N22-21-44.5 E91-47-32.0 45	5	2012	Housing+ Precipitation	135	36	7	86	11	60

Sl No.	Landslide Location	Lat-Lon-Alt	Total Landslide Occur	Last Landslide	Trigger	Stranded	Injured	Died	House before last landslide	House after last landslide	Total People now in danger
6	Red Hill, AS Majar	N22-21-48.3 E91-47-39.2 274.6	2	2011	Precipitation &Hillside Housing	145	25	4	43	28	105
7	South Khulsi		N/A	Landlords cut hill with the slope failure. Now many multiple story buildings have been built near the vulnerable hill bringing thousands of people at stake. The lion portion of the hill might fall over the building very soon if no proper measure would be taken.							200
8	Foys Lake-Chittagong Zoo Hill	N22-28-13.2 E91-47-13.5 222	3	2002	Same as 2 & Construction	Rain and development activities of Foys Lake occurs landslide causing great damage in existing infrastructures and amenities of lake. Also may cause death of visitors in rainy season.					
9	OR Nizam Road Housing Society Panchlaish		5	August 2005	Heavy Rains and Land Developing	56	10	2			
10	Market, Beside Shahid Minar Chittagong University	N22-27-21.3 E91-48-18.7 91	2	June 2000	Deforestation & Precipitation	54	23	15	30	Nil	N/A

Sl No.	Landslide Location	Lat-Lon-Alt	Total Landslide Occur	Last Landslide	Trigger	Stranded	Injured	Died	No. of Houses before last landslide	No. of Houses after last landslide	Total People now in danger
11	Foys Lake Observation Tower Hill	N22-22-06.8 E91-47-34.4 186.8	2	2011	Land Development and Rain	105	20	10	26	Nil	N/A
12	Dr.Yunus Bhaban Road Chittagong Univrsity	N22-28-23.0 E91-47-16.8 96	N/A	The connecting road between hostel area and academic building of Chittagong University is in dangerous position because of aside steeper slope hill. If high precipitation occurs for several hours continuously after long period of no-rain the road network would be crumbled due to landslide.							
13	Shantinagar Bayezid Bostami		3	October 2005	Rain and Housing	25	3	5	32	20	85
14	Nabinagar, Chittagong	N23-21-45.7 E90-44-78.8		September 2007	Monsoon Rain	13	0	2	26	56	140
15	Forest Research Institute Rest House Hill		N/A	No landslide yet but likely to occur because of rapid destruction of Bamboo and other tress roots.							

Sl No.	Landslide Location	Lat-Lon-Alt	Total Landslide Occur	Last Landslide	Trigger	Stranded	Injured	Died	No. of Houses before last landslide	No. of Houses after last landslide	Total People now in danger
16	Jharna Hill	N22-21-42.3 E91-49-46.1 112.5	3	2009	Heavy rain after long time	125	15	50	26	35	140
17	AK Khan Hill Panchlaish		1	2007	Hill Cutting then Rain	45	3	1	25	13	80

Source: Field Surveying, March and September, 2013

Appendix-IV

LOGISTIC REGRESSION RESULTS

Regression Equation:

logit(LS_locations) = -66.6424 - 3.118817*Drain_final + 2.958392*elevation_final- 0.151729*lc_final + 1.500556*NDVI_final - 13.020611*precipitation - 0.536982*Road_final - 0.291650*slope_final + 13.450597*soil_final + 0.138068*Water_final

Individual Regression Coefficient

Variables	Coefficient
Intercept	-66.64235202
Drain_Final	-3.1188169
Elevation_final	2.95839199
lc_final	-0.15172865
NDVI_final	1.50055576
Precipitation	-13.02061117
Road_final	-0.53698236
Slope_final	-0.29165029
soil_final	13.45059725
water_final	0.13806842

Regression Statistics:

Number of total observations = 800166

Number of 0s in study area = 800147

Number of 1s in study area = 19

Percentage of 0s in study area= 99.9976

Percentage of 1s in study area= 0.0024

Number of auto-sampled observations = 77021

Number of 0s in sampled area = 77019

Number of 1s in sampled area = 2

Percentage of 0s in sampled area = 99.9974

Percentage of 1s in sampled area = 0.0026

-2logL0 = 46.2347

-2log(likelihood) = 29.1549

Pseudo R_square= 0.3694

Goodness of Fit = 4258.7533

ChiSquare(9) = 17.0798

Means and Standard Deviations:

Variables	Mean	Standard Deviation
Drain_Final	2.305514	1.31106
Elevation_final	1.420807	0.858763
lc_final	2.717324	1.022174
NDVI_final	1.826593	1.094401
Precipitation	2.449202	1.411487
Road_final	1.073876	0.407564
Slope_final	1.507861	0.891945
soil_final	2.737565	1.690229
water_final	1.102089	0.714889
LS_locations	0.000026	0.005096

Classification of cases & odds ratio:

Observed	Fitted_0	Fitted_1	Percent Correct
0	77019	0	100
1	2	0	0

Odds Ratio = Not Applicable

Reclassification of cases & ROC (Sample-based computation when applicable):

(1) Select a new threshold value such that, after reclassification, the number of fitted 1s matches the number of observed 1s in the dependent variable

New cutting threshold = 0.0164

Classification of cases & odds ratio by using the new threshold

Observed	Fitted_0	Fitted_1	Percent Correct
0	77016	3	99.9961
1	2	0	0

Adjusted Odds Ratio = 0.0000

True Positive = 0.0000%

False Positive = 0.0039%

(2) ROC* Result with 100 thresholds (Sample-based computation when applicable):

ROC = 0.9900

* ROC=1 indicates a perfect fit; and ROC=0.5 indicates a random fit.

Appendix-V

MULTIPLE REGRESSIONS RESULTS

Regression Equation:

LS_locations = -0.0001 - 0.0000*Drain_final - 0.0000*elevation_final + 0.0000*lc_final - 0.0000*NDVI_final - 0.0000*precipitation- 0.0000*Road_final + 0.0001*slope_final + 0.0000*soil_final+ 0.0000*Water_final

Regression Statistics:

Apparent R = 0.014615

Apparent R square = 0.000214

Adjusted R = 0.014269

Adjusted R square = 0.000204

F (9, 800156) = 18.995455

ANOVA Regression Table:

	Apparent degrees of freedom	**Sum of squares**	**mean square**
Source			
Regression	9	0	0
Residual	800156	19	0
Total	800165	19	0

Individual Regression Coefficients:

	Coefficient	**t_test(800156)**
Intercept	-0.000086	-2.66416
Drain_final	-0.000007	-1.48423
Elevation_final	-0.000013	-1.32267
lc_final	0.000004	0.636121
NDVI_final	-0.000008	-1.56341
precipitation	-0.000007	-1.62925
Road_final	-0.000016	-1.0048
Slope_final	0.000059	7.487095
Soil_final	0.000015	4.367872
Water_final	0.000047	5.389963

Appendix-VI

RESULTS OF THE RELATIVE OPERATING CHARACTERISTIC (ROC)

1. Result of ROC for Weighted Linear Combination (1)

AUC = 0.839

The following section list detailed statistics for each threshold.

With each threshold, the following 2x2 contingency table is calculated

---

Reality (reference image)

Simulated by threshold 1 0

---

1 A (number of cells) B (number of cells)

0 C D

For the given reference image: A+C=19 B+D=800147

For the given reference image: A+C=19 B+D=800147

No.	Exp. Thrhlds (%)	Act. Thrhlds (%)	Act. raw cuts	A	True posi. (%)	B	False posi. (%)
1	0	0	0	0	0	0	0
2	4	4.0002	3	2	10.5263	32006	4
3	8	8.0001	3	2	10.5263	64012	8
4	12	12.0001	3	6	31.5789	96015	11.9997
5	16	16.002	3	6	31.5789	128022	15.9998
6	20	20.0001	3	12	63.1579	160022	19.9991
7	24	24.0001	3	19	100	192022	23.9983
8	28	28.0001	3	19	100	224028	27.9984
9	32	32.0001	3	19	100	256035	31.9985
10	36	36.0002	3	19	100	288042	35.9986
11	40	40.0001	3	19	100	320048	39.9986
12	44	44.0001	2	19	100	352055	43.9988
13	48	48.0002	2	19	100	384062	47.9989

14	52	52.0001	2	19	100	416068	51.9989
15	56	56.0001	2	19	100	448075	55.9991
16	60	60.0002	2	19	100	480082	59.9992
17	64	64.001	2	19	100	512088	63.9992
18	68	68.0001	2	19	100	544095	67.9994
19	72	72.0002	2	19	100	576102	71.9995
20	76	76.0001	2	19	100	608108	75.9995
21	80	80.0001	1	19	100	640115	79.9995
22	84	84.0001	1	19	100	672121	83.9997
23	88	88.0001	1	19	100	704128	87.9998
24	92	92.0002	1	19	100	736135	92
25	96	96.0001	1	19	100	768141	96
26	100	100	0	19	100	800147	100

** For the given reference image, the following seven statistics are the same for all thresholds. The unit of each statistic is the proportion correct attributable to a combination of information of location and quantity.

No info of location and no info of quantity: N(n) = 0.5000

Perfect info of location and perfect info of quantity: P(p) = 1.0000

Perfect info of location and no info of quantity: P(n) = 0.5000

No info of location and perfect info of quantity: N(p) = 1.0000

No info of location and no info of quantity: PerfectChance = 0.5000

No info of location and perfect info of quantity: PerfectQuantity = 0.5000

Perfect info of location given no info of quantity: PerfectLocation = 0.0000

No.	M(m)	N(m)	P(m)	M(p)	M(n)
1	1	1	1	1	0.5
2	0.96	0.96	0.96	1	0.5
3	0.92	0.92	0.92	1	0.5
4	0.88	0.88	0.88	1	0.5
5	0.84	0.84	0.84	1	0.5
6	0.8	0.8	0.8	1	0.5
7	0.76	0.76	0.76	1	0.5
8	0.72	0.72	0.72	1	0.5
9	0.68	0.68	0.68	1	0.5
10	0.64	0.64	0.64	1	0.5
11	0.6	0.6	0.6	1	0.5
12	0.56	0.56	0.56	1	0.5
13	0.54	0.54	0.54	1	0.5
14	0.48	0.48	0.48	1	0.5
15	0.44	0.44	0.44	1	0.5
16	0.4	0.4	0.4	1	0.5
17	0.36	0.36	0.36	1	0.5
18	0.32	0.32	0.32	1	0.5
19	0.28	0.28	0.28	1	0.5
20	0.24	0.24	0.24	1	0.5
21	0.2	0.2	0.2	1	0.5
22	0.16	0.16	0.16	1	0.5
23	0.12	0.12	0.12	1	0.5
24	0.08	0.08	0.5	1	0.5
25	0.04	0.04	0.04	1	0.5
26	0	0	0	1	0.5

No.	Kno.	Klocation	Kquantity	Kstandard
1	1	0	1	0
2	0.92	0	0.92	0
3	0.84	0	0.84	0
4	0.76	0	0.76	0
5	0.68	0	0.68	0
6	0.6	0	0.6	0
7	0.52	1	0.52	0
8	0.44	1	0.44	0
9	0.36	1	0.36	0
10	0.28	1	0.28	0
11	0.2	1	0.2	0
12	0.12	1	0.12	0
13	0.04	1	0.04	0
14	-0.04	1	-0.04	0
15	-0.12	1	-0.12	0
16	-0.2	1	-0.2	0
17	-0.28	0.998	-0.28	0
18	-0.36	1	-0.36	0
19	-0.44	1	-0.44	0
20	-0.52	0.999	-0.52	0
21	-0.6	0	-0.6	0
22	-0.68	0	-0.68	0
23	-0.76	0	-0.76	0
24	-0.84	0	-0.84	0
25	-0.92	0	-0.92	0
26	-1	0	-1	0

No.	Correct Chance	Correct Quantity	Correct Location	Error Location	Error Quantity
1	0.5	0.5	0	0	0
2	0.5	0.46	0	0	0.04
3	0.5	0.42	0	0	0.08
4	0.5	0.38	0	0	0.12
5	0.5	0.34	0	0	0.16
6	0.5	0.3	0	0	0.2
7	0.5	0.26	0	0	0.24
8	0.5	0.22	0	0	0.28
9	0.5	0.18	0	0	0.32
10	0.5	0.14	0	0	0.36
11	0.5	0.1	0	0	0.4
12	0.5	0.06	0	0	0.44
13	0.5	0.02	0	0	0.48
14	0.48	0	0	0	0.52
15	0.44	0	0	0	0.56
16	0.4	0	0	0	0.6
17	0.36	0	0	0	0.64
18	0.32	0	0	0	0.68
19	0.28	0	0	0	0.72
20	0.24	0	0	0	0.76
21	0.2	0	0	0	0.8
22	0.16	0	0	0	0.84
23	0.12	0	0	0	0.88
24	0.08	0	0	0	0.92
25	0.04	0	0	0	0.96
26	0	0	0	0	1

2. Result of ROC for Weighted Linear Combination (2)

AUC = 0.911

The following section list detailed statistics for each threshold.

With each threshold, the following 2x2 contingency table is calculated

---

	Reality (reference image)	
Simulated by threshold	1	0
1	A (number of cells)	B (number of cells)
0	C	D

For the given reference image: A+C=19 B+D=800147

No.	Exp. Thrhlds(%)	Act. Thrhlds(%)	Act. raw cuts	A	True posi.(%)	B	False posi.(%)
1	0	0	0	0	0	0	0
2	4	4.0002	3	0	0	32008	4.0003
3	8	8.0001	3	6	31.5789	64008	7.9995
4	12	12.0001	3	18	94.7368	96003	11.9982
5	16	16.002	3	19	100	128009	15.9982
6	20	20.0001	3	19	100	160015	19.9982
7	24	24.0001	3	19	100	192022	23.9983
8	28	28.0001	3	19	100	224028	27.9984
9	32	32.0001	3	19	100	256035	31.9985
10	36	36.0002	3	19	100	288042	35.9986
11	40	40.0001	3	19	100	320048	39.9986
12	44	44.0001	2	19	100	352055	43.9988
13	48	48.0002	2	19	100	384062	47.9989
14	52	52.0001	2	19	100	416068	51.9989
15	56	56.0001	2	19	100	448075	55.9991

16	60	60.0002	2	19	100	480082	59.9992
17	64	64.001	2	19	100	512088	63.9992
18	68	68.0001	2	19	100	544095	67.9994
19	72	72.0002	2	19	100	576102	71.9995
20	76	76.0001	2	19	100	608108	75.9995
21	80	80.0001	1	19	100	640115	79.9997
22	84	84.0001	1	19	100	672121	83.9997
23	88	88.0001	1	19	100	704128	87.9998
24	92	92.0002	1	19	100	736135	92
25	96	96.0001	1	19	100	768141	96
26	100	100	0	19	100	800147	100

For the given reference image, the following seven statistics are the same for all thresholds. The unit of each statistic is the proportion correct attributable to a combination of information of location and quantity.

No info of location and no info of quantity: N(n) = 0.5000

Perfect info of location and perfect info of quantity: P(p) = 1.0000

Perfect info of location and no info of quantity: P(n) = 0.5000

No info of location and perfect info of quantity: N(p) = 1.0000

No info of location and no info of quantity: PerfectChance = 0.5000

No info of location and perfect info of quantity: PerfectQuantity = 0.5000

Perfect info of location given no info of quantity: PerfectLocation = 0.0000

No.	M(m)	N(m)	P(m)	M(p)	M(n)
1	1	1	1	1	0.5
2	0.96	0.96	0.96	1	0.5
3	0.92	0.92	0.92	1	0.5
4	0.88	0.88	0.88	1	0.5
5	0.84	0.84	0.84	1	0.5
6	0.8	0.8	0.8	1	0.5
7	0.76	0.76	0.76	1	0.5
8	0.72	0.72	0.72	1	0.5
9	0.68	0.68	0.68	1	0.5
10	0.64	0.64	0.64	1	0.5
11	0.6	0.6	0.6	1	0.5
12	0.56	0.56	0.56	1	0.5
13	0.54	0.54	0.54	1	0.5
14	0.48	0.48	0.48	1	0.5
15	0.44	0.44	0.44	1	0.5
16	0.4	0.4	0.4	1	0.5
17	0.36	0.36	0.36	1	0.5
18	0.32	0.32	0.32	1	0.5
19	0.28	0.28	0.28	1	0.5
20	0.24	0.24	0.24	1	0.5
21	0.2	0.2	0.2	1	0.5
22	0.16	0.16	0.16	1	0.5
23	0.12	0.12	0.12	1	0.5
24	0.08	0.08	0.5	1	0.5
25	0.04	0.04	0.04	1	0.5
26	0	0	0	1	0.5

No.	Kno	Klocation	Kquantity	Kstandard
1	1	0	1	0
2	0.92	-0.043	0.92	0
3	0.84	0.255	0.84	0
4	0.76	0.941	0.76	0
5	0.68	1	0.68	0
6	0.6	1	0.6	0
7	0.52	1	0.52	0
8	0.44	1	0.44	0
9	0.36	1	0.36	0
10	0.28	1	0.28	0
11	0.2	1	0.2	0
12	0.12	1	0.12	0
13	0.04	1	0.04	0
14	-0.04	1	-0.04	0
15	-0.12	1	-0.12	0
16	-0.2	1	-0.2	0
17	-0.28	0.998	-0.28	0
18	-0.36	1	-0.36	0
19	-0.44	1	-0.44	0
20	-0.52	0.999	-0.52	0
21	-0.6	0	-0.6	0
22	-0.68	0	-0.68	0
23	-0.76	0	-0.76	0
24	-0.84	0	-0.84	0
25	-0.92	0	-0.92	0
26	-1	0	-1	0

No.	Correct Chance	Correct Quantity	Correct Location	Error Location	Error Quantity
1	0.5	0.5	0	0	0
2	0.5	0.46	0	0	0.04
3	0.5	0.42	0	0	0.08
4	0.5	0.38	0	0	0.12
5	0.5	0.34	0	0	0.16
6	0.5	0.3	0	0	0.2
7	0.5	0.26	0	0	0.24
8	0.5	0.22	0	0	0.28
9	0.5	0.18	0	0	0.32
10	0.5	0.14	0	0	0.36
11	0.5	0.1	0	0	0.4
12	0.5	0.06	0	0	0.44
13	0.5	0.02	0	0	0.48
14	0.48	0	0	0	0.52
15	0.44	0	0	0	0.56
16	0.4	0	0	0	0.6
17	0.36	0	0	0	0.64
18	0.32	0	0	0	0.68
19	0.28	0	0	0	0.72
20	0.24	0	0	0	0.76
21	0.2	0	0	0	0.8
22	0.16	0	0	0	0.84
23	0.12	0	0	0	0.88
24	0.08	0	0	0	0.92
25	0.04	0	0	0	0.96
26	0	0	0	0	1

3. Result of ROC for Weighted Linear Combination (3)

AUC = 0.885

The following section list detailed statistics for each threshold.

With each threshold, the following 2x2 contingency table is calculated

---

	Reality (reference image)	
Simulated by threshold	1	0
1	A (number of cells)	B (number of cells)
0	C	D

For the given reference image: A+C=19 B+D=800147

No.	Exp. Thrhlds(%)	Act. Thrhlds(%)	Act. raw cuts	A	True posi.(%)	B	False posi.(%)
1	0	0	0	0	0	0	0
2	4	4	3	0	0	32008	4.0003
3	8	8	3	13	68.4211	64001	7.9987
4	12	12	3	17	89.4737	96004	11.9983
5	16	16	2	17	89.4737	128011	15.9984
6	20	20	2	17	89.4737	160017	19.9985
7	24	24	2	17	89.4737	192024	23.9986
8	28	28	2	17	89.4737	224030	27.9986
9	32	32	2	17	89.4737	256037	31.9987
10	36	36	2	17	89.4737	288044	35.9989
11	40	40	2	17	89.4737	320050	39.9989
12	44	44	2	17	89.4737	352057	43.999
13	48	48	2	17	89.4737	384064	47.9992
14	52	52	2	19	100	416068	51.9989
15	56	56	2	19	100	448075	55.9991

16	60	60	2	19	100	480082	59.9992
17	64	64	2	19	100	512088	63.9992
18	68	68	2	19	100	544095	67.9994
19	72	72	2	19	100	576102	71.9995
20	76	76	2	19	100	608108	75.9995
21	80	80	2	19	100	640115	79.9997
22	84	84	2	19	100	672121	83.9997
23	88	88	2	19	100	704128	87.9998
24	92	92	1	19	100	736135	92
25	96	96	1	19	100	768141	96
26	100	100	0	19	100	800147	100

** For the given reference image, the following seven statistics are the same for all thresholds. The unit of each statistic is the proportion correct attributable to a combination of information of location and quantity.

No info of location and no info of quantity: N(n) = 0.5000

Perfect info of location and perfect info of quantity: P(p) = 1.0000

Perfect info of location and no info of quantity: P(n) = 0.5000

No info of location and perfect info of quantity: N(p) = 1.0000

No info of location and no info of quantity: PerfectChance = 0.5000

No info of location and perfect info of quantity: PerfectQuantity = 0.5000

Perfect info of location given no info of quantity: PerfectLocation = 0.0000

No.	M(m)	N(m)	P(m)	M(p)	M(n)
1	1	1	1	1	0.5
2	0.96	0.96	0.96	1	0.5
3	0.92	0.92	0.92	1	0.5
4	0.88	0.88	0.88	1	0.5
5	0.84	0.84	0.84	1	0.5
6	0.8	0.8	0.8	1	0.5
7	0.76	0.76	0.76	1	0.5
8	0.72	0.72	0.72	1	0.5
9	0.68	0.68	0.68	1	0.5
10	0.64	0.64	0.64	1	0.5
11	0.6	0.6	0.6	1	0.5
12	0.56	0.56	0.56	1	0.5
13	0.52	0.52	0.52	1	0.5
14	0.48	0.48	0.48	1	0.5
15	0.44	0.44	0.44	1	0.5
16	0.4	0.4	0.4	1	0.5
17	0.36	0.36	0.36	1	0.5
18	0.32	0.32	0.32	1	0.5
19	0.28	0.28	0.28	1	0.5
20	0.24	0.24	0.24	1	0.5
21	0.2	0.2	0.2	1	0.5
22	0.16	0.16	0.16	1	0.5
23	0.12	0.12	0.12	1	0.5
24	0.08	0.08	0.08	1	0.5
25	0.04	0.04	0.04	1	0.5
26	0	0	0	1	0.5

No.	Kno	Klocation	Kquantity	Kstandard
1	1	0	1	0
2	0.92	-0.043	0.92	0
3	0.84	0.656	0.84	0
4	0.76	0.881	0.76	0
5	0.68	0.876	0.68	0
6	0.6	0.87	0.6	0
7	0.52	0.861	0.52	0
8	0.44	0.853	0.44	0
9	0.36	0.847	0.36	0
10	0.28	0.837	0.28	0
11	0.2	0.826	0.2	0
12	0.12	0.812	0.12	0
13	0.04	0.797	0.04	0
14	-0.04	1	-0.04	0
15	-0.12	1	-0.12	0
16	-0.2	1	-0.2	0
17	-0.28	0.998	-0.28	0
18	-0.36	1	-0.36	0
19	-0.44	1	-0.44	0
20	-0.52	0.999	-0.52	0
21	-0.6	0	-0.6	0
22	-0.68	0	-0.68	0
23	-0.76	0	-0.76	0
24	-0.84	0	-0.84	0
25	-0.92	0	-0.92	0
26	-1	0	-1	0

No.	Correct Chance	Correct Quantity	Correct Location	Error Location	Error Quantity
1	0.5	0.5	0	0	0
2	0.5	0.46	0	0	0.04
3	0.5	0.42	0	0	0.08
4	0.5	0.38	0	0	0.12
5	0.5	0.34	0	0	0.16
6	0.5	0.3	0	0	0.2
7	0.5	0.26	0	0	0.24
8	0.5	0.22	0	0	0.28
9	0.5	0.18	0	0	0.32
10	0.5	0.14	0	0	0.36
11	0.5	0.1	0	0	0.4
12	0.5	0.06	0	0	0.44
13	0.5	0.02	0	0	0.48
14	0.48	0	0	0	0.52
15	0.44	0	0	0	0.56
16	0.4	0	0	0	0.6
17	0.36	0	0	0	0.64
18	0.32	0	0	0	0.68
19	0.28	0	0	0	0.72
20	0.24	0	0	0	0.76
21	0.2	0	0	0	0.8
22	0.16	0	0	0	0.84
23	0.12	0	0	0	0.88
24	0.08	0	0	0	0.92
25	0.04	0	0	0	0.96
26	0	0	0	0	1

4. Result of ROC for Logistic Regression (LR)

AUC = 0.767

The following section list detailed statistics for each threshold.

With each threshold, the following 2x2 contingency table is calculated

---

	Reality (reference image)	
Simulated by threshold	1	0
1	A (number of cells)	B (number of cells)
0	C	D

For the given reference image: A+C=19 B+D=800147

No.	Exp. Thrhlds(%)	Act. Thrhlds(%)	Act. raw cuts	A	True posi.(%)	B	False posi.(%)
1	0	0	0	0	0	0	0
2	4	4.0002	0.0001	8	42.1053	32000	3.9993
3	8	8.0001	0	11	57.8947	64003	7.9989
4	12	12.0001	0	11	57.8947	96010	11.999
5	16	16.0002	0	11	57.8947	128017	15.9992
6	20	20.0001	0	11	57.8947	160023	19.9992
7	24	24.0001	0	11	57.8947	192030	23.9993
8	28	28.0001	0	11	57.8947	224036	27.9994
9	32	32.0001	0	11	57.8947	256043	31.9995
10	36	36.0002	0	11	57.8947	288050	35.9996
11	40	40.0001	0	11	57.8947	320056	39.9996
12	44	44.0001	0	12	63.1579	352062	43.9997
13	48	48.0002	0	16	84.2105	384065	47.9993
14	52	52.0001	0	16	84.2105	416071	51.9993
15	56	56.0001	0	16	84.2105	448078	55.9995

16	60	60.0002	0	17	89.4737	480084	59.9995
17	64	64.0001	0	19	100	512088	63.9992
18	68	68.0001	0	19	100	544095	67.9994
19	72	72.0002	0	19	100	576102	71.9995
20	76	76.0001	0	19	100	608108	75.9995
21	80	80.0001	0	19	100	640115	79.9997
22	84	84.0001	0	19	100	672121	83.9997
23	88	88.0001	0	19	100	704128	87.9998
24	92	92.0002	0	19	100	736135	92
25	96	96.0001	0	19	100	768141	96
26	100	100	0	19	100	800147	100

** For the given reference image, the following seven statistics are the same for all thresholds. The unit of each statistic is the proportion correct attributable to a combination of information of location and quantity.

No info of location and no info of quantity: N(n) = 0.5000

Perfect info of location and perfect info of quantity: P(p) = 1.0000

Perfect info of location and no info of quantity: P(n) = 0.5000

No info of location and perfect info of quantity: N(p) = 1.0000

No info of location and no info of quantity: PerfectChance= 0.5000

No info of location and perfect info of quantity: PerfectQuantity= 0.5000

Perfect info of location given no info of quantity: PerfectLocation= 0.0000

No.	M(m)	N(m)	P(m)	M(p)	M(n)
1	1	1	1	1	0.5
2	0.96	0.96	0.96	1	0.5
3	0.92	0.92	0.92	1	0.5
4	0.88	0.88	0.88	1	0.5
5	0.84	0.84	0.84	1	0.5
6	0.8	0.8	0.8	1	0.5
7	0.76	0.76	0.76	1	0.5
8	0.72	0.72	0.72	1	0.5
9	0.68	0.68	0.68	1	0.5
10	0.64	0.64	0.64	1	0.5
11	0.6	0.6	0.6	1	0.5
12	0.56	0.56	0.56	1	0.5
13	0.52	0.52	0.52	1	0.5
14	0.48	0.48	0.48	1	0.5
15	0.44	0.44	0.44	1	0.5
16	0.4	0.4	0.4	1	0.5
17	0.36	0.36	0.36	1	0.5
18	0.32	0.32	0.32	1	0.5
19	0.28	0.28	0.28	1	0.5
20	0.24	0.24	0.24	1	0.5
21	0.2	0.2	0.2	1	0.5
22	0.16	0.16	0.16	1	0.5
23	0.12	0.12	0.12	1	0.5
24	0.08	0.08	0.08	1	0.5
25	0.04	0.04	0.04	1	0.5
26	0	0	0	1	0.5

No.	Kno	Klocation	Kquantity	Kstandard
1	1	0	1	0
2	0.92	0.397	0.92	0
3	0.84	0.542	0.84	0
4	0.76	0.521	0.76	0
5	0.68	0.499	0.68	0
6	0.6	0.474	0.6	0
7	0.52	0.446	0.52	0
8	0.44	0.415	0.44	0
9	0.36	0.381	0.36	0
10	0.28	0.342	0.28	0
11	0.2	0.298	0.2	0
12	0.12	0.343	0.12	0
13	0.4	0.696	0.4	0
14	-0.04	0.671	-0.04	0
15	-0.12	0.642	-0.12	0
16	-0.2	0.736	-0.2	0
17	-0.28	0.998	-0.28	0
18	-0.36	1	-0.36	0
19	-0.44	1	-0.44	0
20	-0.52	0.99	-0.52	0
21	-0.6	0	-0.6	0
22	-0.68	0	-0.68	0
23	-0.76	0	-0.76	0
24	-0.84	0	-0.84	0
25	-0.92	0	-0.92	0
26	-1	0	-1	0

No	Correct Chance	Correct Quantity	Correct Location	Error Location	Error Quantity
1	0.5	0.5	0	0	0
2	0.5	0.46	0	0	0.04
3	0.5	0.42	0	0	0.08
4	0.5	0.38	0	0	0.12
5	0.5	0.34	0	0	0.16
6	0.5	0.3	0	0	0.2
7	0.5	0.26	0	0	0.24
8	0.5	0.22	0	0	0.28
9	0.5	0.18	0	0	0.32
10	0.5	0.14	0	0	0.36
11	0.5	0.1	0	0	0.4
12	0.5	0.06	0	0	0.44
13	0.5	0.02	0	0	0.48
14	0.48	0	0	0	0.52
15	0.44	0	0	0	0.56
16	0.4	0	0	0	0.6
17	0.36	0	0	0	0.64
18	0.32	0	0	0	0.68
19	0.28	0	0	0	0.72
20	0.24	0	0	0	0.76
21	0.2	0	0	0	0.8
22	0.16	0	0	0	0.84
23	0.12	0	0	0	0.88
24	0.08	0	0	0	0.92
25	0.04	0	0	0	0.96
26	0	0	0	0	1

5. Result of ROC for Multiple Regressions (MR)

AUC = 0.967

The following section list detailed statistics for each threshold.

With each threshold, the following 2x2 contingency table is calculated

---

	Reality (reference image)	
Simulated by threshold	1	0
1	A (number of cells)	B (number of cells)
0	C	D

For the given reference image: A+C=19 B+D=800147

No.	Exp. Thrhlds(%)	Act. Thrhlds(%)	Act. Raw cuts	A	True posi(%)	B	False posi.(%)
1	0	0	0	0	0	0	0
2	4	4	0.0002	13	68.4211	31995	3.9986
3	8	8	0.0001	19	100	63995	7.9979
4	12	12	0.0001	19	100	96002	11.998
5	16	16	0.0001	19	100	128009	15.9982
6	20	20	0.0001	19	100	160015	19.9982
7	24	24	0.0001	19	100	192022	23.9983
8	28	28	0	19	100	224028	27.9984
9	32	32	0	19	100	256035	31.9985
10	36	36	0	19	100	288042	35.9986
11	40	40	0	19	100	320048	39.9986
12	44	44	0	19	100	352055	43.9988
13	48	48	0	19	100	384062	47.9989
14	52	52	0	19	100	416068	51.9989
15	56	56	0	19	100	448075	55.9991

16	60	60	0	19	100	480082	59.9992
17	64	64	0	19	100	512088	63.9992
18	68	68	0	19	100	544095	67.9994
19	72	72	0	19	100	576102	71.9995
20	76	76	0	19	100	608108	75.9995
21	80	80	0	19	100	640115	79.9997
22	84	84	0	19	100	672121	83.9997
23	88	88	0	19	100	704128	87.9998
24	92	92	-0.0001	19	100	736135	92
25	96	96	-0.0001	19	100	768141	96
26	100	100	-0.0002	19	100	800147	100

** For the given reference image, the following seven statistics are the same for all thresholds. The unit of each statistic is the proportion correct attributable to a combination of information of location and quantity.

No info of location and no info of quantity: N(n) = 0.5000

Perfect info of location and perfect info of quantity: P(p) = 1.0000

Perfect info of location and no info of quantity: P(n) = 0.5000

No info of location and perfect info of quantity: N(p) = 1.0000

No info of location and no info of quantity: PerfectChance= 0.5000

No info of location and perfect info of quantity: PerfectQuantity= 0.5000

Perfect info of location given no info of quantity: PerfectLocation= 0.0000

No.	M(m)	N(m)	P(m)	M(p)	M(n)
1	1	1	1	1	0.5
2	0.96	0.96	0.96	1	0.5
3	0.92	0.92	0.92	1	0.5
4	0.88	0.88	0.88	1	0.5
5	0.84	0.84	0.84	1	0.5
6	0.8	0.8	0.8	1	0.5
7	0.76	0.76	0.76	1	0.5
8	0.72	0.72	0.72	1	0.5
9	0.68	0.68	0.68	1	0.5
10	0.64	0.64	0.64	1	0.5
11	0.6	0.6	0.6	1	0.5
12	0.56	0.56	0.56	1	0.5
13	0.52	0.52	0.52	1	0.5
14	0.48	0.48	0.48	1	0.5
15	0.44	0.44	0.44	1	0.5
16	0.4	0.4	0.4	1	0.5
17	0.36	0.36	0.36	1	0.5
18	0.32	0.32	0.32	1	0.5
19	0.28	0.28	0.28	1	0.5
20	0.24	0.24	0.24	1	0.5
21	0.2	0.2	0.2	1	0.5
22	0.16	0.16	0.16	1	0.5
23	0.12	0.12	0.12	1	0.5
24	0.08	0.08	0.08	1	0.5
25	0.04	0.04	0.04	1	0.5
26	0	0	0	1	0.5

No.	Kno	Klocation	Kquantity	Kstandard
1	1	0	1	0
2	0.92	0.397	0.92	0
3	0.84	0.542	0.84	0
4	0.76	0.521	0.76	0
5	0.68	0.499	0.68	0
6	0.6	0.474	0.6	0
7	0.52	0.446	0.52	0
8	0.44	0.415	0.44	0
9	0.36	0.381	0.36	0
10	0.28	0.342	0.28	0
11	0.2	0.298	0.2	0
12	0.12	0.343	0.12	0
13	0.4	0.696	0.4	0
14	-0.04	0.671	-0.04	0
15	-0.12	0.642	-0.12	0
16	-0.2	0.736	-0.2	0
17	-0.28	0.998	-0.28	0
18	-0.36	1	-0.36	0
19	-0.44	1	-0.44	0
20	-0.52	0.99	-0.52	0
21	-0.6	0	-0.6	0
22	-0.68	0	-0.68	0
23	-0.76	0	-0.76	0
24	-0.84	0	-0.84	0
25	-0.92	0	-0.92	0
26	-1	0	-1	0

No	Correct Chance	Correct Quantity	Correct Location	Error Location	Error Quantity
1	0.5	0.5	0	0	0
2	0.5	0.46	0	0	0.04
3	0.5	0.42	0	0	0.08
4	0.5	0.38	0	0	0.12
5	0.5	0.34	0	0	0.16
6	0.5	0.3	0	0	0.2
7	0.5	0.26	0	0	0.24
8	0.5	0.22	0	0	0.28
9	0.5	0.18	0	0	0.32
10	0.5	0.14	0	0	0.36
11	0.5	0.1	0	0	0.4
12	0.5	0.06	0	0	0.44
13	0.5	0.02	0	0	0.48
14	0.48	0	0	0	0.52
15	0.44	0	0	0	0.56
16	0.4	0	0	0	0.6
17	0.36	0	0	0	0.64
18	0.32	0	0	0	0.68
19	0.28	0	0	0	0.72
20	0.24	0	0	0	0.76
21	0.2	0	0	0	0.8
22	0.16	0	0	0	0.84
23	0.12	0	0	0	0.88
24	0.08	0	0	0	0.92
25	0.04	0	0	0	0.96
26	0	0	0	0	1

Appendix-VII

ATTERBERG LIMIT TEST (SOIL CONSISTENCY TEST)

1. Soil Sample: **Motijharna**

Collection Date: 18 May 2013

Test Date: 28 May 2013

Tested by: Yiaser Arafat Rubel

Test Centre: Geotechnical Engineering Laboratory, BUET, Bangladesh

Liquid Limit Test					
No. of Blows	30	20	17	26	35
Container No.	607	773	154	853	74
Weight of Container, gm	6.9	6.9	7	6.8	6.5
Wt. container+ Wet soil, gm	16.9	20.6	18.6	18.3	17.3
Wt. container+ Dry Soil, gm	14.1	16.7	15.1	15.1	14.3
Weight of Water, W_w in gm	2.8	3.9	3.5	3.2	3
Weight of Dry Soil, $W_s$in gm	7.2	9.2	8.1	8.3	7.8
Water Content, W in %	38.88	39.79	43.21	38.55	38.46

Plastic Limit Test		
Container No.	828	4444
Weight of Container, gm	7.3	7.2
Wt. container+ Wet soil, gm	18.6	18.4
Wt. container+ Dry Soil, gm	16.8	16.7
Weight of Water, W_w in gm	1.8	1.7
Weight of Dry Soil, $W_s$in gm	9.5	9.5
Water Content, W in %	18.37	17.89

Liquid Limit, LL from graph=39.9085

Plastic Limit, PL=19.635

Shrinkage Limit, SL=30

Plasticity Index, PI=LL-PL=39.9-19.635=20.265

Liquidity Index, LI = w_n- w_p/PI =26-19.636/20.265=0.314

Flow Index from flow curve, FI= Slope of Flow Curve= (39.9-38.82)/log (30/25) =13.747

(for 25 blow w=39.9 and for 30 blows w=38.82)

Activity, Ac=PI/%of clay size particles (<0.002mm)

Toughness Index, TI= PI/FI=20.265/13.747=1.474

Linear Shrinkage, LS=(1-Final length/Initial Length)*100=(1-127/140)*100=9.2857

Plasticity Index, PI=2.13LS=2.13*9.2857=19.778

2. Soil Sample: **Foys Lake Hill**

Collection Date: 18 May 2013

Test Date: 29 May 2013

Tested by: Yiaser Arafat Rubel

Test Centre: Geotechnical Engineering Laboratory, BUET

Liquid Limit Test					
No. of Blows	29	34	21	23	26
Container No.	575	231	76	170	214
Weight of Container, gm	6.6	5.5	6.9	6.7	7
Wt. container+ Wet soil, gm	19.5	16.3	20	17.4	19.8
Wt. container+ Dry Soil, gm	15.7	13.3	16.9	14.7	16.5
Weight of Water, W_w in gm	3.8	3.0	3.1	2.7	3.3
Weight of Dry Soil, $W_s$in gm	9.1	7.7	10	8	9.5
Water Content, W in %	41.75	38.96	43.57	42.04	41.04

Plastic Limit Test		
Container No.	321	125
Weight of Container, gm	7.1	7.4
Wt. container+ Wet soil, gm	18.3	18.7
Wt. container+ Dry Soil, gm	16.6	16.8
Weight of Water, W_w in gm	1.7	1.9
Weight of Dry Soil, $W_s$in gm	9.5	9.4
Water Content, W in %	17.89	20.21

Plastic Limit, PL=19.85

Shrinkage Limit Test:

Dish No.:04

Weight of Dish: 22.4

Wt. dish+Wet soil: 49.7

Wt. Dish+ Dry Soil: 41.8

Wt. of Dry Soil Pat: 19.4

Wt. displaced mercury: 205.4 – 28.75

Volume of displaced mercury: 12.98cc

Volume of dish: 15.412 cc

Volume of dry soil pat: 12.98 cc

Shrinkage Limit: 28.7

Liquid Limit, LL=41.89

Shrinkage Limit, SL=28.7

Plasticity Index, PI=LL-PL=41.79-19.85=21.94

Liquidity Index, LI = w_n- w_p/PI =24.92-19.85/21.94=0.23

Flow Index from flow curve, FI= Slope of Flow Curve= (41.75-41.04)/log (29/26) =14.79

(for 26 blow w=41.04 and for 29 blows w=41.75)

Toughness Index, TI= PI/FI=21.94/14.79=1.483

Linear Shrinkage, LS= (1-Final length/Initial Length)*100= (1-121.5/135)*100=10.29

Plasticity Index, PI=2.13LS=2.13*10.29=21.917

Appendix-VIII

OUTREACH ACTIVITIES

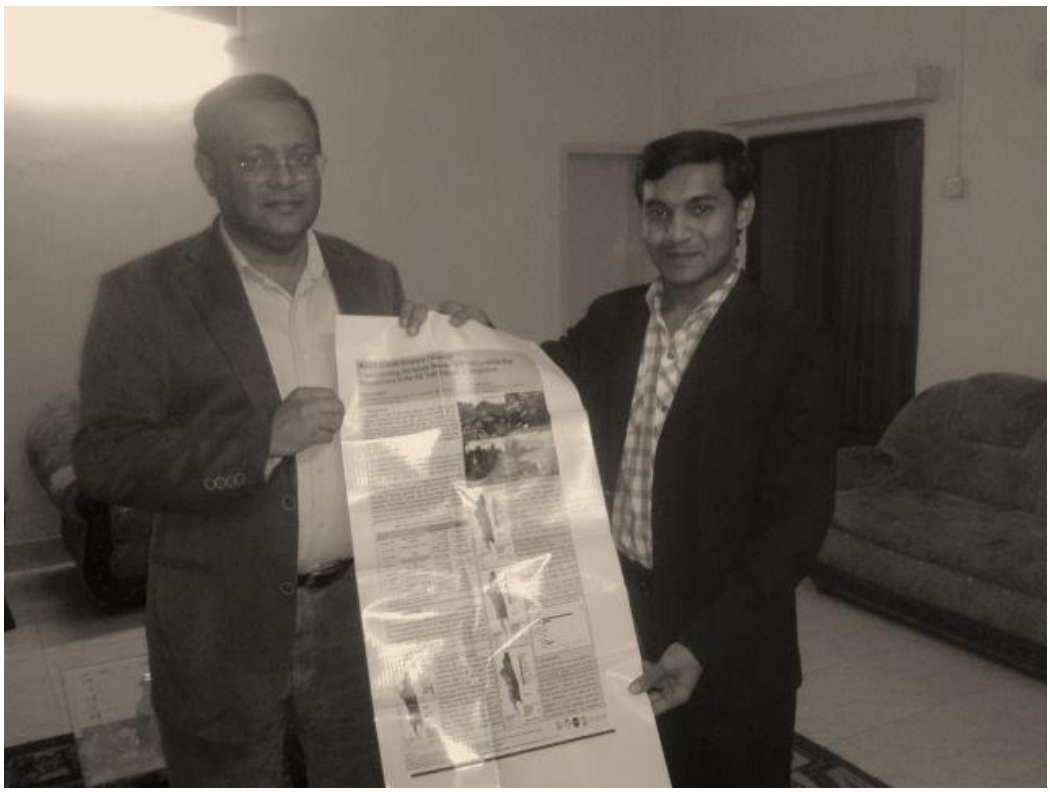

Mr. Yiaser Arafat Rubel (student fellow) was presenting this research outcome to the honorable Environment and Forest Minister of Bangladesh, Dr. Hasan Mahmud. He urged him to implement all the suggestions that were suggested in the research report for combating landslide risks in hilly regions like Chittagong Metropolitan Area (CMA). Dr. Hasan was consented to install early warning system in the areas lying in landslide prone zones in the way that was provided in this research work. Dr. Hasan thanked AAG, NASA and USAID for undertaking such a good initiative for the betterment of landslide vulnerable people.

Moreover, in near future, we will try to disseminate the outcome of this research in the following sectors to create awareness related to urban landslide disaster risk management:

a) Among the local people and communities that are vulnerable to landslide risks
b) Disaster Management & Relief Division and Ministry of Environment & Forest, Government of the People's Republic of Bangladesh
c) Bangladesh Institute of Planners (BIP) and Institute of Engineers, Bangladesh (IEB)
d) Chittagong Development Authority (CDA) and Chittagong City Corporation (CCC).

Thanks for Reading this Report!